HENNA NIEMELÄ-ANTTONEN
WETTABILITY AND ANTI-ICING PROPERTIES OF SLIPPERY
LIQUID INFUSED POROUS SURFACES

Master of Science Thesis

ABSTRACT

Nature has provided intriguing possibilities to tackle wetting and to some extent even icing. By capturing the unique and inventive structures, novel surfaces with low wettability and low adhesion to ice are being under research. After deliberate material selection, these surfaces would provide easement to many industries suffering from ice accretion. In the Arctic region, buildings, wind turbines, maritime vessels, aviation and other transportation operators could benefit surfaces with anti-ice or ice-repellent properties.

The aim of this master's thesis was to study slippery liquid infused porous surfaces, SLIPS, by selecting proper porous solid and water immiscible lubricant combinations. The focus was in finding a surface which would have low ice adhesion and good anti-wetting properties with low lubricant evaporation. Different lubricants and oils with altered viscosities, were used in the tests as they naturally repel water. As a porous solid material, polytetrafluoroethylene (PTFE) –membrane was used to impregnate the lubricant into. The membranes had altering pore sizes and were manufactured by two different companies. Since PTFE is also water-repellent, that is hydrophobic, the produced SLIPS surfaces functioned in wettability tests as expected.

From the fabricated SLIPS, the evaporation was examined as to its effects on wettability of the surface. The wettability was observed as a function of time as static contact angle, contact angle hysteresis and sliding angle tests were performed to the SLIPS. From the evaporation and wettability tests, the most promising and interesting SLIPS –samples were selected to the cyclic ice adhesion test. The cyclic ice adhesion test encompassed ice accretion in icing wind tunnel, ice adhesion measurement with centrifugal machinery and wettability tests afore next cycle.

It was noticed that different pore sizes in the membranes had effects on wettability, but more significantly on ice adhesion strength. Moreover, when the results of the work are reviewed, submicrometer pore sizes were superior to micrometer pore sizes, as the ice detached from them more easily. It was detected that different lubricants had altering evaporation rates but also differenced in wettability experiments. Altogether, more cyclic ice adhesion testing is needed to perform in order to gain better comprehension towards SLIPS lifespan in icing and de-icing cycles. In addition, more lubricant and porous solid pairs are needed to tests to yield good performance SLIPS with exceptionally low ice adhesion strength.

TIIVISTELMÄ

HENNA NIEMELÄ-ANTTONEN: Lubrikantti-impregnoitujen huokoisten pintojen kastuvuus- ja jäätymättömyysominaisuudet
Tampereen teknillinen yliopisto
Diplomityö, 102 sivua, 1 liitesivu
Marraskuu 2015
Materiaalitekniikan diplomi-insinöörin tutkinto-ohjelma
Pääaine: Polymeerit ja biomateriaalit
Tarkastajat: Prof. Petri Vuoristo, TkT Heli Koivuluoto TkT Hannu Teisala

Avainsanat: hydrofobinen, jääfobinen, lubrikantti-impregnoitu, kastuminen, kontaktikulma, biomimetiikka, jäätyminen, pinnoitteet

Luontoon pohjautuvia ideoita käyttäen on mahdollista valmistaa pintoja, jotka ovat vettähylkiviä ja jopa jään kerääntymistä estäviä. Tällä hetkellä tutkitut ja kiinnostuksen kohteena olevat uudenlaiset pinnoitteet ja materiaalit perustuvat luonnossa esiintyville rakenteille ja niiden avulla jään adheesion alentaminen on mahdollista. Onnistuessaan nämä vettä ja jäätä hylkivät pinnat tarjoaisivat uudenlaisia mahdollisuuksia useille eri teollisuuden aloille ja toimijoille, sillä erityisesti arktisilla alueilla jään kerääntyminen on haaste muun muassa rakennelmille, tuuliturbiineille, merialuksille, ilmailulle sekä myös muille kuljetusaloille.

Työn tavoitteena oli löytää vettähylkiviä öljyjä ja huokoisia materiaaleja yhdistelemällä optimaalisia, ns. SLIPS –pintoja, joilla olisi mahdollisimman alhainen jääadheesio. Lubrikantteina käytettiin eri viskositeetein öljyjä, sillä ne hylkivät luonnostaan vettä. Huokoisena materiaalina, jonka sisään lubrikantti imeytettiin, käytettiin kahden eri valmistajan polytetrafluoroetyleeni (PTFE) –membraaneja erilaisin huokoskoin. Sillä myös PTFE hylkii vettä – eli on hydrofobinen, aikaan saadut SLIPS -rakenteet toimivat kastuvuustesteissä odotetusti.

Valmistetuista SLIPS rakenteista tutkittiin lubrikantin haihtumista huokoisesta rakenteesta ja sen vaikutuksia pintojen kastuvuuteen. Kastuvuusmittauksia arvioitiin staattisen kontaktikulman avulla, mutta myös hystereesiä ja kaltevuuskulmaa seuraamalla ajan funktiona. Saatujen tietojen pohjalta valittiin alkuperäisestä näytematriisista kiinnostavimmat ja lupaavimmat SLIPS –näytteet syklisiin jäätesteihin. Sykliin kuului jään kerryttäminen tuulitunnelissa, jääadheesion mittaaminen sentrifugaalisella laitteistolla, sekä kastuvuusmittaukset ennen seuraavaa sykliä.

Eri huokoskokojen välillä huomattiin olevan eroja kastuvuudessa, mutta erityisesti jääadheesiossa. Työssä esitettyjen tulosten perusteella pienistä, alle mikromerin huokoskoon membraaneista jää irtosi pinnasta suurempia, usean mikrometrin huokoskoon rakenteita paremmin. Eri viskositeettisten lubrikanttien välillä huomattiin eroavaisuuksia etenkin haihtuvuudessa, mutta myös kastuvuudessa. Kuitenkin, lisää syklistä jäätestausta on tehtävä, jotta pidemmän aikavälin vaikutukset näkyvät jäätymis- ja sulamissyklien jälkeen. Myös enemmän lubrikantti – huokoinen matriisi –pareja tulisi testata, jotta saadaan parempi käsitys mahdollisimman monesta toimivasta, alhaisen jääadheesion omaavasta SLIPS –pinnasta.

PREFACE

This master's thesis was started in May 2015 and finished in November 2015 at the Department of Materials Science, Tampere University of Technology. The thesis was funded and a part of Roll-to-roll fabrication of advanced slippery liquid-infused porous surfaces for anti-icing applications (ROLLIPS) project under Tekes' Arktiset meret - program.

The work was supervised by Professor Petri Vuoristo, Dr. Heli Koivuluoto and Dr. Hannu Teisala. I would like to thank Professor Vuoristo for encouraging comments about the work and also for the great advises given. Another expression of gratitude goes for Dr. Koivuluoto for always having time for questions and support for me. Likewise, I wish to thank Dr. Teisala for inspiring conversations and valuable comments regarding the thesis. My greatest gratitude is with all of you. I am truly grateful for the project and my supervisors for giving me this abundant and yet so interesting topic. In addition, it was extremely rewarding and motivating to have such a freedom in the work as to having such a great team to help me.

For the assistant in icing tests and compassionate peer support, I am thanking M.Sc. Christian Stenroos. The icing tests could not be performed without your help. Moreover, I wish to thank all the staff of Department of Materials Science, it has been a pleasure working with you.

Finally, I want to thank my family and friends, especially my mother and grandmother, from whom I continuously gain strength and wisdom. And to end with, my gratitude goes for my dearest husband Antti, who always has faith in me and believes in me when I forgot to do so. Thank you.

Tampere, 25.11.2015

Henna Niemelä-Anttonen

CONTENTS

APPENDIX A: The contact angle hysteresis results for all the SLIPS samples

LIST OF SYMBOLS AND ABBREVIATIONS

Chemicals and Materials

AFP	Amplifying fluorescent polymer
AFP	Anti-freeze proteins
Ag	Silver
Al	Aluminum
Al_2O_3	Alumina
BMA-EDMA	Butyl methacrylate-ethylene dimethacrylate
C	Carbon
CeO_2	Cerium(IV) oxide, ceric oxide, ceria, cerium oxide
CHINF	Chitin nanofiber
CLE	Cellulose lauroyl ester
CO_2	Carbon dioxide
CS	Chitosan
DBP	Butyl phthalate
DBP	Dibutyl phthalate
F	Fluorine
FAS	Fluorinated alkyl silane
FD-POSS	Fluorinated-decyl polyhedral oligomeric silsesquioxane
GLP	General purpose lubricant
HEMA	Hydroxyethylmethacrylate
LDPE	Low-density polyethylene
LFS	Liquid flame spray
LIS	Lubricant impregnated surface
$MgAl_2O_4$	Magnesium aluminate
NaCl	Natrium chloride
NiTi	Nickel titanium, nitinol
O	Oxygen
OTS	Octadecyltrichlorosilane
PDA	Polydopamine
PDADMAC	Poly diallyldimethyl ammonium chloride
PDMS	Polydimethylsiloxane
PEG	Polyethylene glycol
PEI	Polyethyleneimine
PFAE	Perfluoroalkylether
PFDS	1H,1H,2H,2H-perfluorodecyltriethoxysilane
PFPAE	Perfluoropolyalkylether
PFPE	Perfluoropolyether
PNA	Peptide nucleic acid
PNIPAAm	Poly(N-isopropylacrylamide)
PP	Polypropylene
PSU	Polysulfone
PTFE	Polytetrafluoroethylene
PU	Polyurethane
PVDF	Polyvinylidene fluoride, or polyvinylidene difluoride
PVDF-HFP	Polyvinylidene fluoride-*co*-hexafluoropropylene
PVDMA	Polyvinyl-4,4-dimethylazlactone

PVPON	Polyvinylpyrrolidone
SiO_2	Silica
STST	Stainless steel
TAH/LS	Iron tetradecanoate / low alloy steel
TiO_2	Titanium dioxide, titanium(IV)oxide, titania
TMCTS	1,3,5,7-tetramethylcyclotetrasiloxane
Zn	Zinc
ZnO	Zinc oxide
([EMI][TFSI])	1-ethyl-3-methyl-imidazolium bis(trifluoromethylsulfonyl) imide

Greek and Latin symbols

γ	Interfacial tension
θ	Contact angle
φ	Fraction
τ	Maximum shear stress
ω	Angular velocity
A	Area
F	Force
m	Mass
r	Radius

Other abbreviations

ESEM	Environmental scanning electron microscope
LV	Liquid-vapor
ROLLIPS	Roll-to-roll fabrication of advanced slippery liquid-infused porous surfaces for anti-icing applications
RPM	Rotates per minute
SEM	Scanning electron microscope
SHS	Superhydrophobic surface
SL	Solid-liquid
SLIPS	Slippery liquid infused porous surface
SRB	Sulphate reducing bacteria
SV	Solid-vapor

1. INTRODUCTION

Classically, it is well known how effortlessly rain drops roll off from the leaves of certain plants. Many surfaces in nature, most notably the leaves of the lotus flower, are known to be superhydrophobic. These surfaces show distinct characteristics with respect to water-repellency, self-cleaning and anti-fouling. These desired features are in ambition of many researchers, as they are needed in several of industries and applications ranging from bioengineering to materials engineering. (Barthlott & Neinhuis, 1997a; Wong et al., 2011)

Practical applications for super liquid-repellent surfaces are abundant and versatile: if the characteristics are imparted to fabrics, water resistant garments can be made. When added on transparent surfaces, e.g. glass windows and wind shields, the surface could remove impacting and condensed water droplets from its surface and thus possess self-cleaning ability. In addition, outdoor optical devices, such as solar panels or satellites, have long craved for dirt and dust free surfaces to maintain their functionality. Moreover, mobility of liquids could be enhanced as the super liquid-repellent surfaces can lower the drag between the liquid and the surfaces of boat hulls or pipes. When applied on machinery in the artic conditions, the ice adhesion could be lowered or even prevented and the functionality and safety improved. Same applications and fundamentals could provide solutions from anti-fogging in tropics as to anti-ice in cold regions. (Kim, 2008; Shillingford et al., 2014; Wilson et al., 2013; Wong et al., 2011)

Especially in the Arctic region, surfaces tend to be prone to ice formation and accumulation. This affects and concerns many industries and operators, in particular, aviation, maritime logistics, buildings, wind turbines, heat exchangers, refrigerator units, power lines, meteorological instruments antennas, radars and traffic and warning signs. It is stated that there are yet no surface coatings or materials which could be identified as perfectly icephobic (Laforte & Beisswenger, 2005). Though, surface sciences and nanomaterial research have given encouraging results and reinitiated interest towards icephobic materials.

As stated, the demand for anti-ice or lowered ice adhesion surfaces truly exists as it hinders the industries and operators especially in Arctic conditions. Icing has been account for lethal accidents, major power losses, lost capital and other nuisances around the world. (Mara et al., 1999; National Transportation Safety Board, 1988, 1996) The techniques for dealing with accreted ice have so far being costly, laborious and somewhat challenging to perform and to maintain. For this, anti-ice or low-ice-adhesion surfaces have been developed. The engineered coatings would provide a passive method

in dealing with icing when compared to more active methods which are widely being utilized nowadays.

Ideal ice-repellent coatings rely on micro- or nanotextured surface roughness and carefully detailed surface chemistry. Earlier, their properties have been based on superhydrophobicity as to now a more novel idea has aroused the interest of many. Slippery liquid infused porous surfaces, SLIPS, exploit the textured benefits of superhydrophobicity with a porous solid material and are being impregnated with water immiscible lubricant oil. Therefore, the SLIPS show water-repellent features with high water contact angle but low contact angle hysteresis, as to showing promising results in ice adhesion tests. (Kim et al., 2012; Subramanyam et al., 2013; Wilson et al., 2013)

2. WATER AND SURFACE INTERACTION

Wetting as a phenomenon can be characterized as the contact angle that is the angle between a solid surface and a liquid drop. Many factors influence the contact angle, including surface geometry or roughness, surface energy and cleanliness of the surface. (Chau et al., 2009; Michael & Bhushan, 2007; Nosonovsky & Bhushan, 2008)

The surface can be stated as wetted if the contact angle' value of water is from 0° to 90°– that is a hydrophilic surface. On the contrast, a hydrophobic surface obtains the contact angle value larger than 90° and therefore, the surface remains non-wetted by water. Surfaces having a contact angle value greater than 150° are considered as superhydrophobic, since the drop seems to be almost spherical on the surface, as illustrated in Figure 1. (Oberli et al., 2014) For almost any given material, the surface energy can be modified chemically, for example by using fluorination to enhance the hydrophobicity. (He et al., 2003) Likewise, the hydrophobicity or hydrophilicity can be altered by engineering the surface roughness (Nosonovsky & Bhushan, 2008). The aforementioned wetting states are illustrated in Figure 1 with given contact angles.
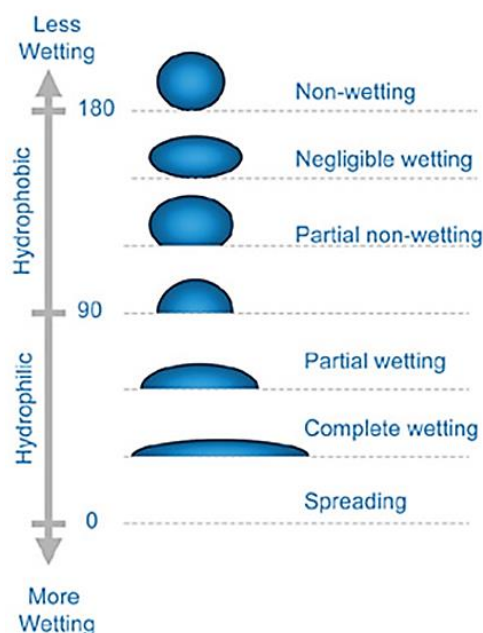
Figure 1. *Wetting and hydrophobic and hydrophilic states.* (Ketelson et al., 2011)

Sliding behavior of the water droplet also defines surfaces/materials superhydrophobic nature. Surface tension and the gravity both affect the droplets sliding behavior on the surface. (Kim, 2008) Submitting the mass conservation principle, the drop starts to have

asymmetric shape on a tilted surface, depicted in Figure 2. The contact angle of the lower side, advancing contact angle, becomes greater and the upper side, receding contact angle, gets reduced. The so called hysteresis, the difference of the two contact angles, has its peak value as the liquid droplet starts to move down the tilted plane as the sliding angle, the inclination angle of the surface, is reached. It can be seen from the literature that a liquid droplet will roll off easily from the surface when the contact angle is greater than 150° and the hysteresis smaller than 5° (Quéré, 2005). This can be explained by the solid-liquid contact reduction, which leads to the self-cleaning possibility: rolling droplets can trap dirt and dust from the surface and so clean the surface.
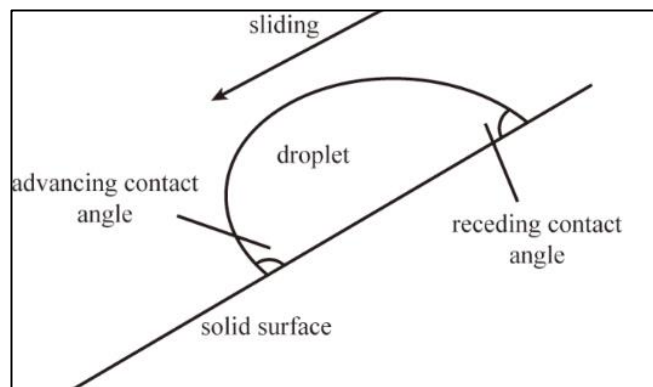
Figure 2.   *Droplet on a tilted plane with advancing and receding contact angles. Contact angle hysteresis is equivalent to the difference of advancing and receding contact angle.* (Pan et al., 2014)

2.1 Factors affecting surfaces

As the factors influencing to most solid surfaces range from physical to chemical, the main features are considered to be heterogeneity, roughness of the surface and shape and size of surface structures, e.g. particles (Chau et al., 2009). In contact angle measurements, the roughness of the surface is known to influence the hysteresis. However, the exact relationship of contact angle hysteresis and surface roughness may not be obvious as to the wetting model equations validity can be questioned. There are some research papers challenging the reliability of the wetting models as they excessively idealize the real solid surfaces to be homogeneous and uniform whilst other results still rely on the recognized models. (Bartell & Shepard, 1953; Chau et al., 2009; Gao & McCarthy, 2007; Kwon et al., 2010; McHale, 2007)

Additionally, the asperities in the surface, as to their shape and size, make every point in the surface unique, i.e. the surface truly is non-uniform when it comes to roughness. In consequence, the apparent contact angle varies within the surface. (Chau et al., 2009) Spori et al., have demonstrated the importance of topological influence, hence contact angles cannot be foretold only by roughness factors (Spori et al., 2008). Also the

influence of the surface roughness on the wettability has been debated within the research community. (Starov et al., 2007; Veeramasuneni et al., 1997)

Variations in roughness are also caused by the heterogeneous characteristics, impurities and contaminants on the surface. Heterogeneity is caused by the composition of different constituents on the surface which have altering surface properties. Dissolution of functional groups and material anisotropy have an influence on the contact angles of droplets, on the surface that is. Deliberately considered sample preparation and surface cleaning techniques are essential when dealing with accuracy and delicate surfaces. (Chau et al., 2009) The preparation conditions of surface particles have also stated to have effects on the contact angles. In the research made by Prestidge and Ralston 1995, the particle size of prepared galena particles was irrelevant when compared to preparation process. Moreover, there are studies which outline the importance of the particle size as not so relevant (Prestidge & Ralston, 1996; Subrahmanyam et al, 1996).

Texturing and particle shape on the surface are fundamental aspects for hydrophobicity as many studies discuss the effects of particle shape, morphology and the microfabricated textures (Ebert & Bhushan, 2012; Khorasani et al., 2005; Patankar, 2004; Spori et al., 2008; Ulusoy & Yekeler, 2005). Hydrophobic surface designs can be made with numerous of methods as the final structure can have various of shapes as seen in Figure 3. Callies et al. used forests of micro-pillars to trap air in the surface structure and to control the degree of superhydrophobicity by altering the density and height of the pillars. The silicon wafers were patterned via conventional photolithography techniques and deposited on aluminum substrate which after deep reactive etching was performed to gain high aspect ratios. (Callies et al., 2005) Other researchers have studied the effects of the pillar shape and height even further and found interdependence on environmental resistance, effortless droplet rolling and pressure stability (Kim et al., 2012; Roach et al., 2008; Zheng et al., 2010).
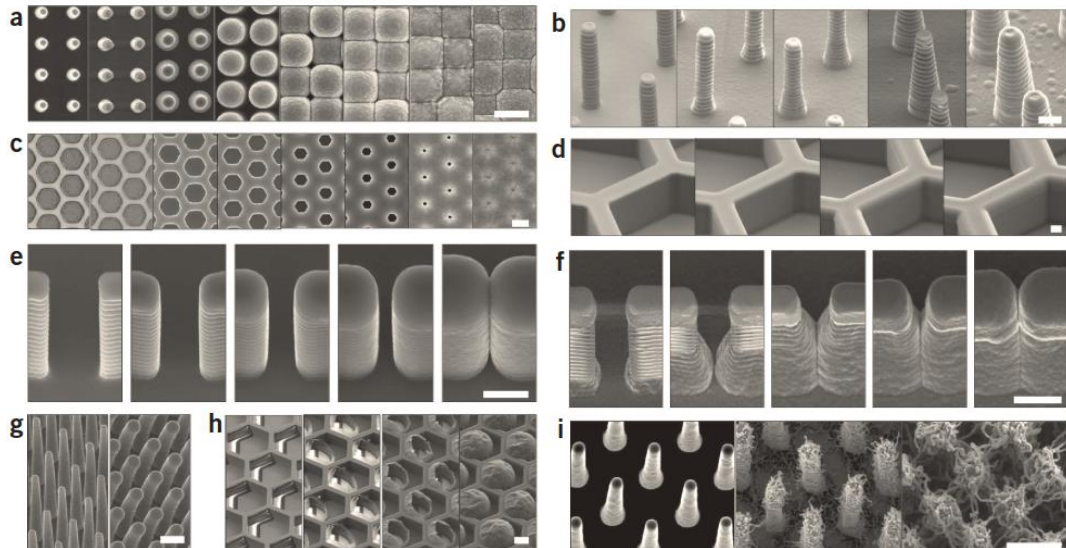
Figure 3. *Possible textured micro- and nanostructures for future hydrophobic surfaces. The surface texture can be constituted to resemble pillars, columns or even honeycomb structure as seen in (a) to (i). Scale bars in (a)-(g) and (i) are 2 µm and in (h) 10 µm. Adapted from (Kim, et al., 2012)*

Randomly distributed particles on surface can also yield altering wetting states. Surface roughness and wettability of some industrial minerals were examined by Ulusoy and Yekeler. They ground the samples, namely, calcite, barite and quartz, in different mills and showed that the degree of hydrophobicity increase with decreasing surface roughness. The particles which had rougher surfaces led to greater wettability regardless of the milling type. The range of the surface roughness values were between 0.55 to 4.49 µm. (Ulusoy & Yekeler, 2005)

In terms of hydrophobicity, adhesion of water is often unfavorable force within/on the surface. The term can be characterized by a several types of attractive forces affecting between the solid surface and the liquid droplets. These factors can be electrostatic, van der Waals, chemical or capillary forces. (Bhushan, 2009; Burton & Bhushan, 2006). For a liquid drop, the forces determining its shape include the interfacial tensions between solid, liquid and air and the gravitational force. The surface tension of liquid tends to minimize the surface area that is, making the drop shape spherical. The gravitational force, which affects only to larger drops than the capillary length of 2.7 mm, tries to flatten the spherical droplet. That is, when the droplet is smaller than this, the effect of gravity is insignificant and is often ignored. (Kim, 2008)

Commonly, surface area of the interface is determined by imaging. In consequence, the roughness ratio is impacted by the scan size and the resolution from the imaging system. It is alleged, that there may not be truly accurate method to canvass the true average roughness ratio for microscopically rough surface. As to the instruments used in imaging have limitations: discrete information collection of the wanted topography.

Atomic force microscopy, on the other hand, might reveal more detailed characteristics with higher resolution and accuracy. (Chau et al., 2009; Lai & Irene, 1999)

2.2 Wetting models

One way to measure hydrophobicity is using the contact angle value. The hydrophobicity or hydrophilicity can be evaluated in terms of contact angle which is developed amongst three phases with liquid, solid and gas phases. (Chau, 2009) Parameters controlling the formation of contact angle vary essentially (Kumar & Prabhu, 2007). Hence it can be challenging to find reproducible contact angles in systems. That is, many of contact angle equations and situations have been constructed to demonstrate various of states. The foremost models, respectively, are the Young's equation, Wenzel's equation and the Cassie-Baxter equation. Young's equation describes wetting on a smooth surface whereas Wenzel's and the Cassie-Baxter equation can be used to describe rough surfaces. In Figure 4 the models are presented altogether – the surface roughness has been taken into consideration in Wenzel's and in Cassie-Baxter's equations.
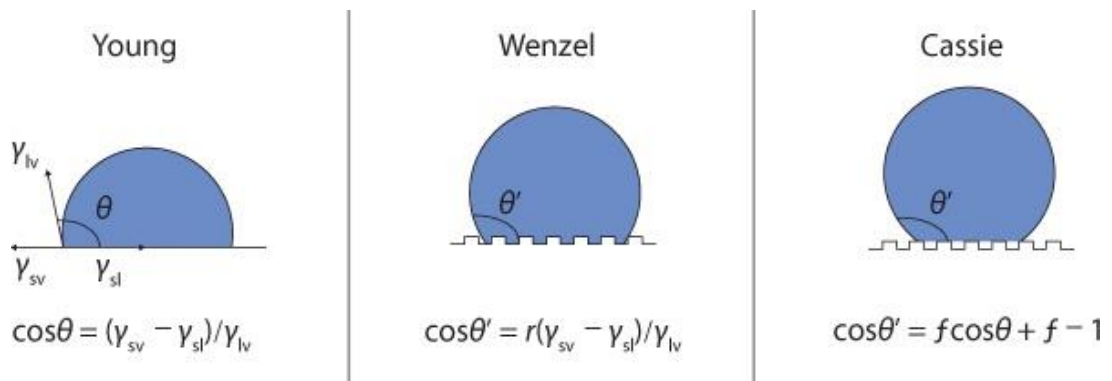
Figure 4. *The wetting models of Young, Wenzel and Cassie-Baxter.* (Nakajima, 2011)

Ideal surfaces are thought to be chemically and topographically homogeneous. Young reported in his work in 1805 a correlation between contact angle and surface tension on an ideal surface. By his work, it can be stated that there are three interfacial free energies affecting the contact angle. (Young, 1805) As the droplet sits on a plane, three interfaces are linked in equilibrium contact angle of liquid: solid-liquid (SL), liquid-vapor (LV) and solid-vapor (SV), presented in Figure 5. As these interfacial tensions are balanced on tangential direction of non-deformable solid surface, Young's equation is constructed as in Equation 1:

$$\gamma SL + \gamma LV \cos \theta y = \gamma SV \tag{1}$$
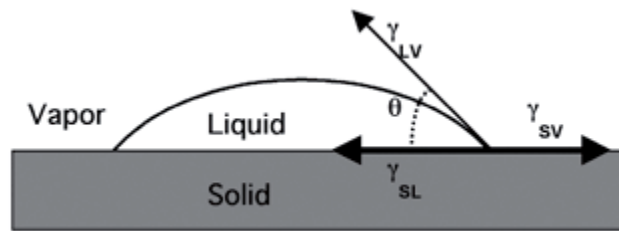
Figure 5. *Presentation of a liquid droplet on a solid surface. The contact angle (θ) is due to three interphases (γ): solid-liquid (SL), liquid-vapor (LV) and solid-vapor (SV). (Della-Bona, 2005)*

Young's contact angle θ_y is balanced by the surface tension forces as to the Young's equation describes the balance of surface forces. The surface hydrophobicity increases with decreasing the surface free energy of the γ_{SV} (solid air interphase), as to conclusion of the equations. Regarding the surface ideality, wettability of the surface can be considered mainly to be determined by the chemical composition. Due to this, such a surface might be hard to be engineered, but also the contact angle measurements require considerable care. (Chau, 2009; Kwok et al., 1998)

Wenzel (1936) examined the effects of surface roughness on the static contact angle. He proposed that the surface geometry outcomes the effect of chemistry on the static contact angle and observed that the surface roughness made hydrophobic solid to behave even more hydrophobic - surface textures enhances the hydrophobic nature of the material. The effective surface area enlarges as the surface becomes rough. Therefore, liquid will be likely to spread less on a rough hydrophobic substrate to decline the contact area to solid. By this discovery, a dimensionless roughness factor was created, thus, it describes the ratio of the actual surface area over its apparent surface area. It was assumed by Wenzel that water conformably fills the cavities on the surface, hence, the equilibrium condition, for the rough surface, was derived. (Wenzel, 1936)

According to the Wenzel Equation 2, the apparent contact angle is the related to the ideal contact angle, when the surface is rough. This adaptation is needed when the droplet size is adequately large compared with the roughness scale and if the liquid entirely fills the pores of the surface.

$$cos\theta_w = r\, cos\theta_y \tag{2}$$

where θ_w is the Wenzel contact angle on a rough surface. θ_y is the ideal Young contact angle on a smooth surface and r is the average roughness ratio. Since the roughening

increases r (>1), water contact angle on a smooth surface can be increased by texturing. If the surface in flat the Wenzel formula actually gives the Yong's equation (r = 1). The fundamental notion of this model states, that liquid drop is in complete contact with the solid surface – called the Wenzel state.

Cassie (1944) modified equation for contact angle changes, for two component surfaces in Equation 3. The apparent contact angle is related to the ideal contact angle by the Cassie equation, on a heterogeneous surface that is. (Cassie, 1944)

$$cos\theta_c = f_1\ cos\theta_1 + f_2\ cos\theta_2 \qquad (3)$$

where f_1 is the fractional area of the surface with θ_2 , θ_c is the Cassie contact angle. The equation can be reduced into Cassie-Baxter equation, Equation 4, for porous surfaces:

$$cos\theta_c = f_1\ cos\theta_1 - f_2 \qquad (4)$$

Here f_2 is the fraction of air space (open area), that makes $cos\theta_2$ = -1, as θ = 180° as to a non-wetting state. In the Cassie state, air is trapped between the water droplet and the rough surface. In this state water is in contact with the solid surface and air, hence, it forms so called fakir droplets which sit on the surface, on the trapped air. The Cassie-Baxter equation describes the apparent a contact angle in this phenomenon, as in Equation 5:

$$cos\theta_{rough} = \varphi_S cos\theta_{flat} + \varphi_V cos\theta_{LV} = \varphi_S cos\theta_{flat} - (1 - \varphi_S) \qquad (5)$$

φ_S and φ_V are the fractions of solid and air contacting the water (φ_S + φ_V = 1). Because the contact angle of water on θ_{LV} air is 180° ($cos\theta_{LV}$ = -1), air under the droplet significantly enhances the apparent surface hydrophobicity. In the Cassie-Baxter equation, monotonic decline of φ_S results in an increase of θ_{rough} and finally turns to a superhydrophobic state.

In most cases, droplets on minor roughness hydrophobic surfaces follow Wenzel state behavior whereas on greater roughness surfaces droplets are likely to obey Cassie-Baxter behavior. As understood, Wenzel's equation can describe relations in homogeneous solid-liquid interphase whereas Cassie-Baxter equation can be applied for heterogeneous surfaces. It is also relevant to realize that on the surface the Wenzel as

the Cassie-Baxter states both can coexist in droplets (Quéré, 2008). In Cassie's and Baxter's proposal the uneven surface is composed of two fractions: fractional area f_1 with contact angle θ_1, and other area f_2 with θ_2, whereas $f_1 + f_2 = 1$.

By appreciating the pioneering work of Wenzel, Cassie and Baxter, it is clear that two requirements are needed to fulfill to gain superhydrophobicity – elevated contact angle value and minute contact angle hysteresis. This combination yields for well-engineered surface chemistry and well fabricated surface roughness. It can be seen that obtaining reproducible values for contact angles may be challenging as the measurements and yielded results are vulnerable to many factors. The usage and reliance of Young's, Wenzel's and Cassie-Baxter's equations has to also be taken into consideration as to surfaces are not as uniform as the formulas consider them to be.

3. SUPERHYDROPHOBICITY

3.1 Bioinspired engineering

Water repellent surfaces are found in several places in the nature - from plants (Barthlott & Neinhuis, 1997a; Bohn & Federle, 2004) to insects (Gao & Jiang, 2004; Parker & Lawrence, 2001) and even to bird feathers (Liu et al., 2008). These surfaces and structures have served as an inspiration for super liquid-repellent surfaces. Especially, the lotus effect, known as a self-cleaning effect, possess excellent water repellent properties by which rain drops are rolled off from the leave thus carrying dirt from the surface. The lotus, in Figure 6, tries to keep its leaves dry to inhibit pathogen attraction (Barthlott & Neinhuis, 1997a), similarly, fungi and bacteria free surfaces are a great interest to several applications to engineers as to water and ice repellency.
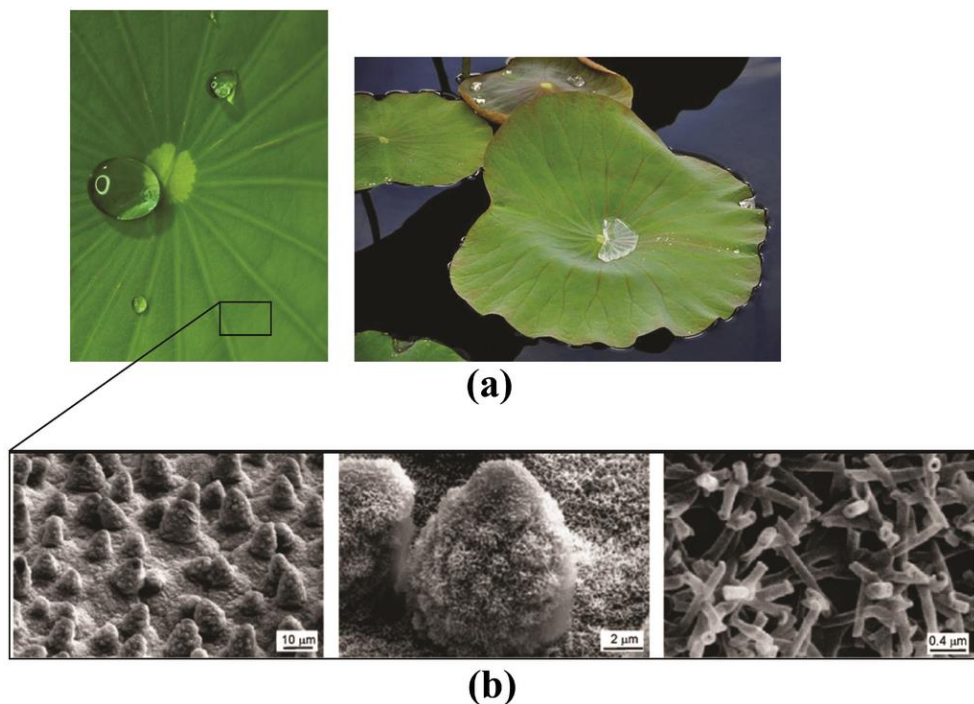
Figure 6. *The surface of the Lotus leaf is hydrophobic resulting in rolling off droplets. (a) The Lotus leaf. (b) The microtexture of the Lotus leaf with nature's own roughness factor.* (Koch et al., 2009)

Barthlott & Neinhuis (1997) studied hundreds of water repellent plants and demonstrated that epidermal cells form papillae onto the leaf, from which the microstructural roughness is gained from. The papillae and wax crystals have

hydrophobic properties resulting in reduced contact area between water and the leaf surface. (Barthlott & Neinhuis, 1997a).

By the use of high resolution scanning electron microscope (SEM) it was revealed that nature's own superhydrophobic surfaces have micrometer papillae and also bumps with nanoscale structure, demonstrated in Figure 7 (a). With these studies it was learned that micro and nanoscale hierarchical structures amplify the superhydrophobicity with the epicuticular wax film on the leaf surface, as seen in Figure 7 (b). The lotus leaf has water contact angle around 150-160° and critical sliding angle as small as 2°. This makes the effortless self-cleaning possible for the plant to gain as much sunlight as possible. (Barthlott & Neinhuis, 1997a, 1997b) Also the SEM images of the water strider legs revealed micro hairs or setae with nanoscale grooves which help the insect to stay on water. (Gao & Jiang, 2004)
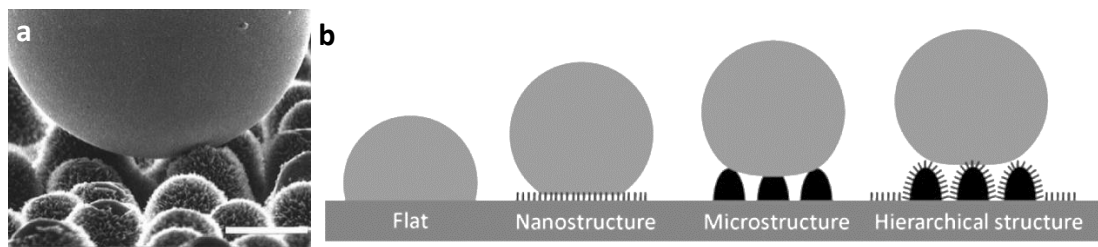
Figure 7.   Wetting is different depending on the surface and its roughness. (a) A droplet of mercury on a plant surface. It can be seen that air is trapped under the droplet inducing a water-repellent surface. Bar 20 µm. Adapted from (Barthlott & Neinhuis, 1997b) *(b) Surfaces with different structures on them resulting in altering roughness.* (Bhushan et al., 2009a)

Consequently, nature's applications rely on dual-scale roughness via surface texture and micro- or nanoscale hierarchical structures, which are required for high contact angle and low sliding angles (Gao & McCarthy, 2006). These structured surfaces are presented in Figure 7, where a droplet is illustrated on a plant's surface and in schematic illustration on various surfaces. In the Figure 7, it is shown that by combining nanostructure onto microtexture, hydrophobicity could be enhanced. Understanding and mimicking these principles, many synthetic approaches can be engineered as hydrophobic chemistry and geometric effects are combined.

3.2 Superhydrophobic surfaces

Superhydrophobic surfaces repel water and their surfaces are remarkably difficult to get wet. In the nature, many biological surfaces can be found that are known for their superhydrophobic or self-cleaning features. Superhydrophobicity, or solid-air composite surface, refers to a state where air is trapped under a water droplet, between the bumps of the surface texture. (Cassie, 1944; Nosonovsky & Bhushan, 2005) It can be easily

observed from the literature that the micro or nanostructure is the heart of the matter in nature's own inspirational hydrophobic surfaces. Great efforts have been done to reveal nature's secrets in exceptional and complex surface structures. Abundant inspiration for superhydrophobicity has come from the lotus leaves (Barthlott & Neinhuis, 1997a, 1997b) but also from the anti-reflective eyes of moths (Genzer & Efimenko, 2006), water strider's legs (Gao & Jiang, 2004), shark skin (Bechert et a., 2000) and also from duck feathers (Liu et al., 2008).

Apart from the microstructure, the composite-like nature of the hydrophobic surfaces in nature, are known to have, depending on the surface that is, different waxes and fibrils, papillae or microsetae (Barthlott & Neinhuis, 1997a; Koch et al., 2009a; Koch et al., 2009b). The epicuticular wax layer has usually low surface energy which makes the superhydrophobicity possible for the biological surfaces (Tuteja et al., 2007).

On any surface there are chemical bonds between the molecules and certain amount of energy is needed to break these molecular bonds. If the molecules do not have bonds, they possess greater potential energy than the bond forming molecules at the surface. The surface molecules do not form bonds at the site of the surface hence therefore they have higher energy, which is called the surface free energy. As well known, any system tries to accomplish a state which corresponds to a minimum energy, thus, droplets and bubbles have a spherical shape on the surface. (Nosonovsky & Bhushan, 2008)

As elements of altering characteristic lengths are structured in a certain routine, a hierarchical surface is fabricated and as a result the organization leads to a certain functionality (Nosonovsky & Bhushan, 2008). It is stated that the hierarchical structure of the nature's own surface is responsible for the superhydrophobicity and that hierarchic structures enhance the superhydrophobic activity. The droplets of water are recorded to sit effortlessly on the nanostructure as the bubbles of air fill the cavities beneath the droplets in the porous structure. (Burton & Bhushan, 2006; Jung & Bhushan, 2006; Liu et al., 2008) The trapped air in the structure prevents the water droplet from entirely touching the surface, hence, superhydrophobicity is possible. The self-cleaning phenomenon, presented in Figure 8, is also based on chemical interactions: the van der Waals forces between the biological surface, such as the lotus leaf, and dirt particles are weaker than the capillary forces of the water droplet and the dirt. (Koch et al., 2009c) Dirt and dust are captivated into the droplets and rolled off as seen in the Figure 8.
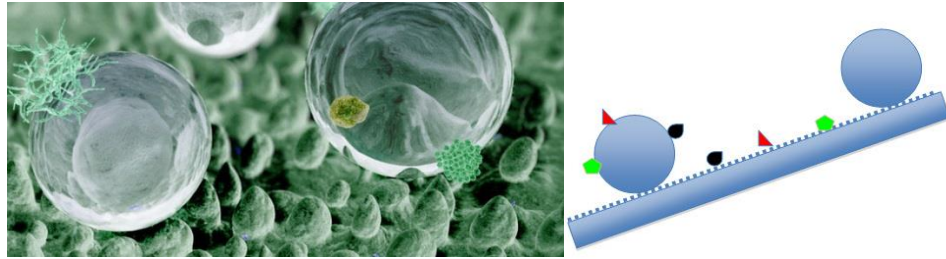
Figure 8. *The self-cleaning effect, or so called Lotus effect: certain dirt particles are trapped onto water droplet as it rolls off from the uneven surface.* (Rolith Inc., 2015; Meyers, 2008)

The artificial superhydrophobic coatings usually suffer from poor durability against physical forces thus hindering their application fields. Decomposition from sunlight, scratching by wind and dirt may lead to permanent damage of superhydrophobic surfaces. Redeposition, in general, is needed to mend low-surface materials' superhydrophobicity which can be seen as expensive or intractable for the application. (Kim, 2008)

Plants can maintain their superhydrophobic nature and characteristics by reproducing their epicuticular wax layer after external stress (Koch et al., 2009; Neinhuis et al., 2001). The same self-healing mechanism has also been fabricated by scientist in materials and coatings for example by chemical self-healing. Yet challenges still remain in producing widely functioning self-healing super liquid-repellent surface (Cordier et al., 2008; Wang et al., 2011; White et al., 2001).

Li et al. constructed a superhydrophobic coating fashioned by chemical vapor deposition of a fluoroalkyl silane on a layer-by-layer assembled porous surface. The self-healing mechanism was gained by the reacted fluoroalkyl silane implanted in the rigidly flexible coating layer. (Li et al., 2010) Another self-healing super-liquid repellent surface with abrasion, ultraviolet light and acid resistance was synthetized by Wang et al. The fabric was coated with a hydrolysis product from fluorinated-decyl polyhedral oligomeric silsesquioxane (FD-POSS) and a fluorinated alkyl silane (FAS) to gain the self-healing superhydrophobic surface. (Wang et al., 2011) Self-healing as damage reparation has been used in smart materials in consumer products from smartphones to even in diesel truck engines (LG Electronics Inc., 2015; Nosonovsky & Rohatgi, 2011) From an engineer's point of view, self-healing surface should perform the healing mechanism without an active human operator.

3.2.1 Challenges of solid-air composite surfaces

The superhydrophobicity of a surface is based on plastron layer, in which air is trapped in the roughness between the solid substrate and the liquid, as described by Cassie.

Consequently, the air and the porous solid material together constitute a composite-like structure. Surfaces generated by using this phenomenon are considered to have promising repellent properties as a result of their low contact area between the solid and the liquid. (Bird et al., 2013; Chen et al., 2013) In the laboratory scale, applications relying on the air layer have shown promising results. Yet, regardless of these encouraging outcomes, there are records of several superhydrophobic surfaces that fail in further testing. This might be caused by fragility in the structure and the insufficient capability to withstand condensation, dirt contamination or impacted high-velocity droplets. (Kim et al., 2012)

The potential applications are abundant, promising and intriguing, albeit there are only a small number of actual products with water-repellent surface technology. The limitations are account for the challenges of superhydrophobic surfaces – mostly their fragility and contamination. The solid-air composite surfaces and especially their microtextures are delicate and frail due to their minute size. Some of these textures can be demolished with a slight amount of force, easily created by a wind or other external force. Depending on the application, it may be a challenge to introduce desired characteristics to a superhydrophobic surface or to combine significant features to one coating. (Callies & Quéré, 2005)

Conventionally, the bulk material used to construct topographic and textured surfaces are hydrophilic, as a certain hydrophobic coating is created to gain superhydrophobicity of the exterior. As a consequence of wear, the hydrophilic material is exposed and the water-repellency is lost due to revealed hydrophilic sites on the surface as illustrated in Figure 9. In general, also mechanical wear leads to sticking of water droplets on the surfaces, even if material is hydrophobic by its nature. (Verho et al., 2011; Xiu et al., 2010) By using dual scale roughness, the problem of fragility may be overcome. This could ensure the Cassie state permanence even if some structures might get worn away. Self-healing or self-repairing texture is ought to be needed to sustain non-wettability over time. (Verho et al., 2011)
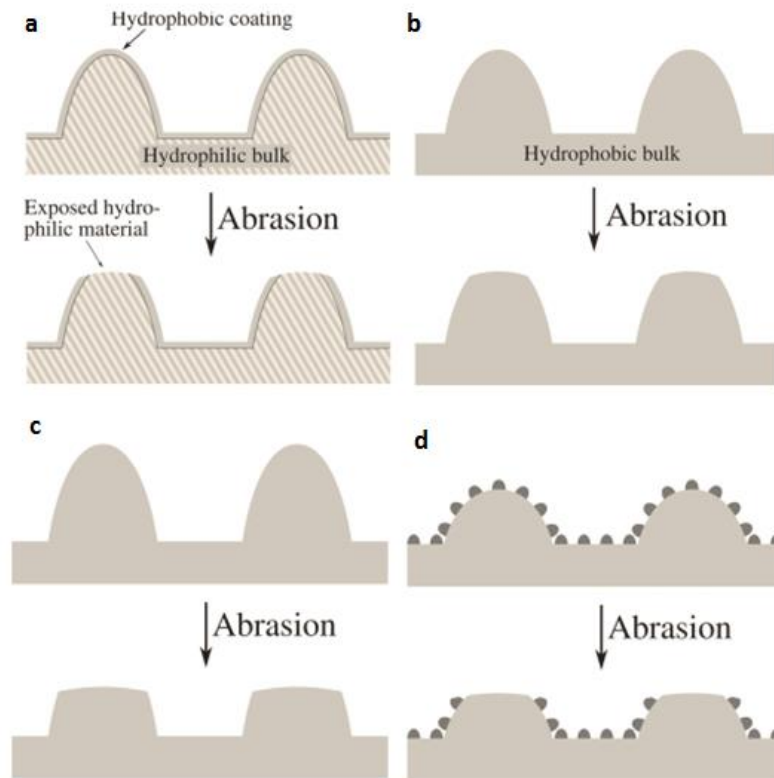
Figure 9. *Wearing effects on different superhydrophobic surfaces. (a) If only microtexture is used, wearing may results in losing hydrophobic Cassie-Baxter –state. (b) If dualscale roughness is used, even after wear the Cassie-Baxter –state can be maintained. (c) The wear of the surfaces can cause hydrophobic properties of the coating to shift into hydrophilic as the bulk material is revealed. (d) If using only hydrophobic material is used, no hydrophilicity occurs. Adapted from* (Verho et al., 2011).

In addition to brittleness, contamination of superhydrophobic materials is another issue limiting the usage of the surfaces. In spite of these surfaces are considered to possess the lotus effect, as to clean themselves, the texture is expected to adsorb oily substances that will migrate throughout the surfaces. This can lead to oil inflation of the air cavities, resulting in diminishing of the repellent properties. (Callies & Quéré, 2005) As shown by Bhushan et al. certain dirt can be rolled off from the surface with moving droplets (Bhushan et al., 2009). Albeit, not all contaminants are washed away from the textured surfaces with the help of rolling off droplets. Zimmermann et al. studied the loss of water-repellency over a 12 months period of a silicone nanofilament coating. The study showed that particularly organic impurities can be considered as a foremost degradation cause of the superhydrophobicity. (Zimmermann et al., 2007)

3.3 Hydrophobic materials

One of the earliest patents made in field of superhydrophobic materials was claimed by F. J. Norton in 1945. Norton had developed a waterproofing treatment for textile materials by dipping fabrics into a solution made of toluene and methylsilicone. After drying in 100°C the textile samples became water-repellent. (Norton, 1945) After few decades, in 1964, Johnson and Dettre made pioneering studies on the effects of roughness with receding and advancing water contact angles. The studied samples consisted of glass substrates with sprayed waxes on them. It was shown that as the surface roughness increases, the advancing water contact angle also increases. The receding contact angle reduces until the roughness of the surface gains its critical point where the receding contact angle shifts to a value near the advancing angle. Subsequently, these findings can be explained by a change from the Wenzel state to a Cassie-Baxter state. (Johnson & Dettre, 1964)

Further discoveries were made by a group of Japanese scientists who investigated fractal surfaces and their water-repellency when the surface was composed of hydrophobic materials. The results gained from the experiments were prominent – a surface made with alkylketenedimer yielded a water contact angle of 174°. (Onda et al., 1996) The researchers from Kao Corporation continued their work by studying the relationship of a flat surface and a fractal surface to proof the prominence of the fractal concept. (Shibuichi et al., 1997)

3.3.1 Hydrophobic polymers

Fluorinated polymers inherently possess low surface energy. Due to this, they exhibit pronounced hydrophobicity. For example the noted and versatile poly(tetrafluoroethylene), PTFE, is shown to have water contact angle approximately 112° – 120° (McKeen, 2006; Zhang et al., 2004). PTFE can be considered as one of the most well-known fluoropolymers. Its brand name Teflon® is DuPont's trade name for the polymer developed in the late 1930's. Teflon® fluoroplastic coatings, films and resins are widely been used in various industries due to the polymer's extreme resistance towards elevated temperatures, corrosion, stress cracking and chemical reactions. The polymer is linear and the bonds between carbon-carbon and carbon-fluorine atoms are exceptionally strong resulting in extreme properties. (DuPont, 2015; McKeen, 2006)

Superhydrophobicity can be achieved by roughening of surfaces, plasma etching being one of the foremost techniques for fluorinated polymers. The water contact angle can be increased to around 170° by etching the surface with high-energy oxygen species generated by plasma. (Morra et al., 1989; Shiu et al., 2004) Moreover, hydrocarbon polymers such as polypropylene, (PP), also benefit plasma etching process by the

creation of surface roughness to attain superhydrophobicity. (Youngblood & McCarthy, 1999)

Roughening of PTFE on the surface can also be done by stretching (Zhang et al., 2004). If the PTFE film is stretched more than 100% of the original length, the surface of the polymer consist of fibrous microcrystals which have a great fraction of voids space in the surface. Alternatively, fluorinated block polymers with microphase separation can be prepared. By this way it is possible to generate a number of nanoscale features to gain superhydrophobicity. (Kim, 2008) As stated, stretching can result in hydrophobicity in PTFE as demonstrated by Zhang et al. It was concluded by the research team that formed void spaces and the presence of fibrous crystals were due to the achievement. The results showed water contact angle improvement from 118° to 165° after stretching. (Zhang et al., 2004)

A copolymer of methyl methacrylate and fluorinated acrylate monomers can develop hexagonally packed nanopores at the cast film surface whilst drying in humid conditions. Optical transparency could be achieved by controlling film deposition parameters as the pore size under the wavelength can be produced. (Yabu & Shimomura, 2005) Likewise, poly(dimethylsiloxane), PDMS, is a hydrophobic polymer which surface can also be effortlessly altered to increase roughness and texture. Micro- and nanoscale textures can be utilized by a laser ablation technique. When treated with laser ablation, PDMS surfaces can reach to a contact angle 160° with water sliding angle under 5°. (Jin et al., 2005; Khorasani et al., 2005)

PDMS is a silicone elastomer and can be considered as chemically inert, thermally stable, transparent and non-toxic. In consequence, the elastomer is been used as a biomaterial in implants but also in microfluidic devices. The mechanical properties of PDMS can be altered without variations in surface chemistry, which gives more possibilities for the material to be used in harsh environment. (Franssila, 2010; Mata & Fleischman, 2005) Khorasani et al. treated the surface of PDMS with CO_2 –pulsed laser to attach peroxide groups initiating 2-hydroxyethyl methacrylate (HEMA) onto the surface of PDMS. This yielded the water contact angle around 175° from the virgin PDMS's 105°. (Khorasani et al., 2005)

Hydrocarbon polymers can also be modified towards superhydrophobicity. In the experiments made by Lu et al. porous surface was fabricated onto low density polyethylene (LDPE) by adjusting nucleation rate of crystallization and time. By controlling the crystallization behavior of the LDPE, water contact angle arose from native LDPE's 101° to around 173°. (Lu et al., 2004)

3.3.2 Inorganic hydrophobic coatings

Commonly, metals and ceramics are likely to have hydrophilic nature since their surface have a great amount of polar sites due to coordinative unsaturation. For instance, in

aluminum surface the atoms suffer deficiency of electrons since they have six electrons in their three sp^2 –hybrid orbitals. Thus, the atoms form a hydrogen bond with possible interfacial water molecules to achieve a full octet. Contrary to aluminum, the atoms in rare-earth oxides compose dissimilar electron structure. The incomplete 4f orbitals are prevented from interactions with the immediate environment because of the full octet of electrons in the $5s^2p^6$ outer shells. Rare-earth oxides have been used to accomplish superhydrophobic surfaces and films as the hydrophobicity is sustained after extreme conditions, such as 1000°C, and rough wear treatments. The application possibilities for inorganic hydrophobic surfaces are abundant, ranging from industry to another, for example many components in auto industry can benefit these robust coatings as seen in Figure 10. (Aytug et al., 2014; Azimi et al., 2013)

Figure 10. *By examining and studying different coating solutions, even frost-free windshields are made possible. A coating of indium tin oxide has been applied on glass by Volkswagen.* (Tokic, 2015)

Cerium dioxide, CeO_2, a rare-earth material, is considered fairly inexpensive and furthermore, exceptionally versatile in gas sensors, electrolyte and polishing materials. CeO_2 film can be fabricated to have hierarchical structure for trapping air in the surface within micro- and nanotextures. Hence, the air-liquid interface is increased by the air: droplets cannot reach the shallows of the surface. (Ishizaki & Saito, 2010) Corrosion resistant properties of CeO_2 on aluminum substrate have been studied by Liang et al. Their CeO_2 film was proven to maintain high water contact angle (152°) after 21 days of sodium chloride aqueous solution. CeO_2 surface had good chemical stability and maintained durable in corrosive solution. (Liang et al., 2013) High chemical stability was also reported by Ishizaki and Saito, who investigated the stability of the surface in pH ranging from 1 to 14 with respectable results. (Ishizaki & Saito, 2010)

Titanium dioxide, TiO_2, can be used as a hydrophobic and self-cleaning surface film when robustness for the surface and material is desired. Especially crystalline TiO_2 layers are suitable for rapid decompositions of organic compounds in vapor and liquid states under UV-light. The photocatalytic phenomenon can be improved with the crystallinity of TiO_2, surface roughness and pore size alterations. Thus, the reactive surface area can be achieved by fabricating large number of pores on a textured surface to gain the light-harvesting and organic complex degrade capacity. There has been

advantageous studies with self-cleaning, antifouling and easy reparability of the TiO_2 surface which disclose optical photosensitivity to be entailed with hydrophobicity by the surface roughness. (Hsieh et al., 2009; Zhang et al., 2013)

Feng et al. reported controllable wettability of aligned zinc oxide, ZnO, nanorod films. In the experiment, water contact angle shifted from 160° to near 0° as the wettability was reversibly altered by ultraviolet irradiation and storing samples in dark. Superhydrophilicity was achieved with ultraviolet illumination whereas superhydrophobicity was gained after dark storage. (Feng et al., 2004) In another experiment, it was concluded by Hou et al. that high surface roughness and low surface free energy effect crucially on surfaces hydrophobic nature. By studying ZnO film on a Zn substrate, the water contact angle was shown to be only 40° whereas *n*-octadecyl thiol monolayer treated ZnO film had noteworthy 153°. (Hou et al., 2007)

In the research of Li et al. metal oxide monoliths were treated with novel technique with inorganic precursor route to achieve significant improvement in water contact angle – increase from 8° to 150° by the process. The macroporous complex metal oxide monoliths, such as $MgAl_2O_4$, were prepared with inorganic precursor route by selective leaching of self-generated magnesium oxide sacrificial template from the sintered two phase composites. It was demonstrated by the discovery that monolithic materials microstructure and properties can be altered by changing the compositions and sintering temperatures of used precursors. (Li et al., 2007)

3.3.3 Polymer-inorganic composite coatings

To top it off, a numerous of composite coatings made from inorganic particles and polymers exist showing hydrophobicity. The main idea is to present wanted roughness or texture with the inorganic particles as the polymer binds the particles as a composite structure. By using polymers that are naturally hydrophobic, hydrophobic materials and surfaces are fabricated relatively easily by using spray coating and dip coating methods. (Cao et al., 2009; Sellinger et al., 1998) As a inorganic component for these coatings, silica, titania and ceria particles have widely been used (Bharathidasan et al., 2014; Cao et al., 2009; Farhadi et al., 2011; Hu et al., 2014; Kulinich & Farzaneh, 2011; Sellinger et al., 1998)

In was observed by Cao et al., that the inorganic particle size plays important role on the properties of composite structure in wettability as to in anti-icing capability. The particle size in the composite structure needs to be right in order to prevent ice formation on the coating. They used radical polymerization of styrene, butyl methacrylate and glycidyl methacrylate in toluene to yield acrylic polymer resin. As the inorganic particles, organosilane –modified silane was used in different particles sizes ranging from 20 nm to 20 μm in diameter. The mixtures of polymer binder and silica particles were sprayed on Al substrate, and during curing, the reactive glycidyl groups

on the acrylic polymers crosslinked with silicone resin. Supercooled water was poured on the surfaces and ice attachment was observed by operator. It was reported that particles over 50 nm increased the icing probability as to 20 nm diameter particle samples did not form ice. (Cao et al., 2009)

Moreover, some studies record polymer-inorganic composite coatings to be rapid and simple method in producing robust superhydrophobic coatings. Zhou et al. used PDMS and fluorinated alkyl silane combinations to gain a surface that was durable against acids, alkali, boiling water and abrasion. They stated the composite material to last 500 machines washes after applied on fabrics. The silica was prepared by co-hydrolysis and co-condensation of silicate with fluorinated alkyl silane. The silica nanoparticles were dispersed into PDMS solution, after which dip coating could be performed to the fabric substrate. (Zhou et al., 2012) Moreover, Sellinger et al. constructed a nanocomposite material that mimicked natural structure of abalone shell. By dip coating, they combined silica, surfactant and organic monomers for nanolaminated coating. The polymerization completed the assembly process of nanocomposites, as it locked the nanotexture and bonded covalently the inorganic-organic interphase to the structure. The coating method could be used rapidly for finishes and hard coatings hence it was said to be optically transparent. (Sellinger et al., 1998)

4. SLIPPERY LIQUID INFUSED POROUS SURFACES - SLIPS

One potential approach to fabricate super liquid-repellent surfaces is a solid-liquid composite surface with pores infused with a liquid instead of air as in superhydrophobic surfaces. Introductory work to the subject was given by David Quéré in 2005, presenting the idea of liquid impregnated texture. It was assumed, that depositing a drop of immiscible liquid onto the impregnated surface, the drop would be non-sticking and float on the surface. Quéré prefigured these kinds of composite surfaces to have self-cleaning properties and also contemplated the characteristics of the ideal surface texture and its optimal size and shape. (Quéré, 2005)

The actual slippery liquid infused surfaces, SLIPS, were introduced by Wong et al. who reported a bioinspired self-repairing slippery surface with pressure-stable omniphobicity in 2011. The gained surface was described as self-healed material which could be made transparent and resist pressure. (Wong et al., 2011) Yet another advantages of SLIPS are dropwise condensation (Glavan et al., 2014; Lalia et al. 2013), repellency to ice and frost (Kim et al., 2012; Rykaczewski et al., 2013a; Subramanyam et al., 2013; Wong et al., 2011), stain repellency (Epstein et al., 2012; Lafuma & Quéré, 2011), repellency to insects (Wong et al., 2011), repellency against biofilm growth (Epstein et al., 2012; Li et al., 2013) and corrose inhibition (Qiu et al., 2014; Wang et al., 2015). The illustration of the porous solid material infused with a lubricating liquid is shown in Figure 11.
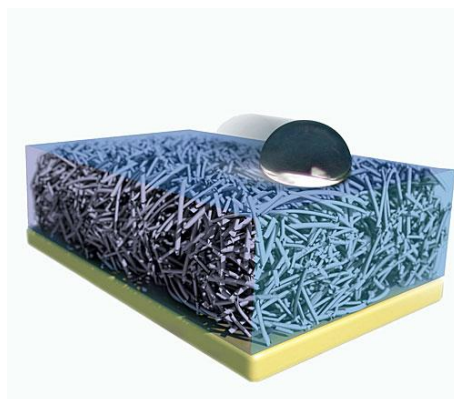
Figure 11. *Slippery liquid infused porous surface – SLIPS, consists of a porous membrane where a lubricating agent is impregnated to gain omniphobic characteristics.* (Rutter, 2011)

Three criteria for SLIPS have been stated by Wong et al. Firstly, the lubricating liquid must wick into, wet and stably adhere within the substrate, meaning micro or

nanotextured rough substrate with chemical affinity for the lubricant oil. Also, the solid must be preferentially wetted by the lubricating liquid rather than by the liquid one wants to repel. And finally, the lubricating and impinging test liquids must be immiscible. (Wong et al., 2011)

4.1 Solid-liquid composite surfaces

Inspired by the nature and *Nepenthes* pitcher plant, lubricant liquids were used to generate a repellant surface in the work made by Wong et al. Thus, the oily liquid was introduced to the textured porous surface leading in formation of continuous lubricant film on the surface. The liquid is captured between the uneven cavities and bumps in the topography but also throughout the microporous matrix, provided by the substrate. In the research, it was shown that the fabricated SLIPS eliminated pinning of the droplets, was able to self-heal, withstand mechanical stress and held the possibility to be manufactured optically transparent. (Wong et al., 2011)

It has been stated that solid-air composite structure has limitations which can be overcome by using the solid-liquid composite structure. In the foregoing, the trapped air can be seen as inadequate defense towards low surface tension liquids – such as organic liquids and mixtures – especially when countered under pressure, for example in windy conditions. Moreover, the fragility of synthetized texture in solid-air structures remains as a challenge. (Wong et al., 2011)

When the porous substrate material is infused with lubricant oil, the gained solid-liquid structure repels the water droplet as seen in Figure 12. The lubricant is held by its place by the texture and features in the substrate, that is, the topology itself does not enable the water-repellency of the structure. In the Cassie-Baxter state, the droplet of water lies on the air cavities whereas when compared to the Wenzel model, there are no air cavities under the droplet. The trapped air under the droplet decreases the contact of the surface and water, thus, texture being regular and right in size, the surface can be stated as non-wetted. (Nosonovsky, 2011; Wong et al., 2011)
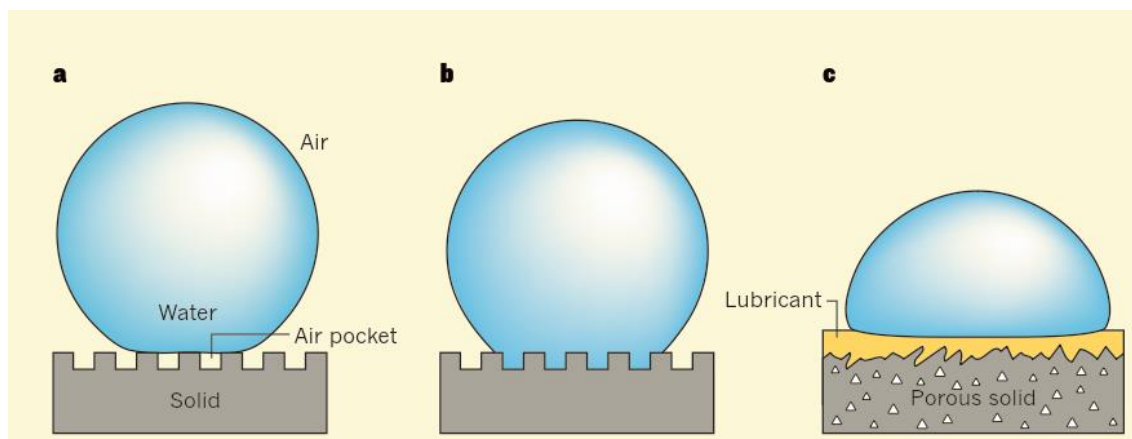
Figure 12. *Surface wetting in solid-liquid and in solid-air composite structures. (a) In Cassie-Baxter state, droplet sits on air cavities resulting in hydrophobicity. (b) Wenzel state has no air beneath the droplet, hence the surface in contact with water. (c) In slippery liquid infused porous surfaces, a thin film of water immiscible lubricant repels water. (*Nosonovsky*, 2011*)

4.2 Tailoring lubricant impregnated surfaces

SLIPS have been tailored in several ways by using various lubricants and even wider spectrum of porous solids. There are few commercial substrates tested by researchers but even more studies have been made with tailored substrates. Since SLIPS are multifunctional and held a potential to revolutionize many industries, there are several of properties needed to fulfill. Depending on the final application, SLIPS may have to endure sea water, bacteria, abrasion, corrosion and so on. These kinds of applications can be tailored in many ways, from 3D printing to molding methods. Mostly the used lubricants have been perfluoropolyethers, (PFPE) and silicone oils, although, some experiments have been carried out by using vegetable oils, such as olive and almond oils. PFPE is also referred as perfluoroalkylether (PFAE) and perfluoropolyalkylether (PFPAE) (DuPont, 2011) The used porous solid material varies heavily on the application and desired properties. In Tables 1 and 2 there are some preparation materials and methods used in creating lubricant impregnated surfaces.

Table 1. *Some recorded methods and other details for tailoring lubricant impregnated surfaces.*

Properties	Materials: solid + liquid	Fabrication method(s)	Pore size / roughness / sphere diameter	Reference
Liquid-repellent, ice-repellent, pressure stable, transparent	Sterlitech Teflon membranes ; Krytox oils	Replica moulding	$\geq$ 200 nm pore size	(Wong et al., 2011)
Omniphobic for low-surface-tension liquids at 200°C	UV-cured and fluorinated PU, Teflon membrane; Krytox 100, 103,105	Replication technique	ca. 200 µm pore size	(Daniel et al., 2013)
Liquid repellency, anti-icing, and transparency	Nanoporous CLE -films ; perfluoropolyether	Nanoprecipitation, spray coating	30 to 1060 nm	(Chen et al., 2014)
Liquid repellency, transparent, mechanically robust	SiO_2 nanoparticles, polyelectrolytes and fluorinated silanes ; Krytox 100	Layer-by-layer deposition	-	(Sunny et al., 2014)
Corrosion protective	TAH/LS ; perfluorinated lubricant	Electrolysis, infusion	Surface asperities ca. 70 µm	(Yang et al., 2015)
Water, organic fluids and blood repellent, foldable	Whatman chromatography papers ; Krytox 105	Vapor-phase silanization	Pore sizes: 2.7 to 11 µm	(Glavan et al., 2014)
Ice-repellent, condensation-repellent, frost-free	Al substrate, Ppy ; Krytox 100	PPy electrodeposition on Al substrate	Diameters from submicrometer to ca. 2µm	(Kim et al., 2012)
Fog-harvesting capability	PVDF-HFP ; polymerquartz oil, Krytox 1506	Electrospinning	Fibers diameter 100 to 500 nm, roughness 2,4 µm	(Lalia et al., 2013)
Highly transparent, biocompatible, anti-fouling, biodegradable	CS/PVPON/alginate -film ; almond oil	Layer-by-layer self-assembly	-	(Manabe et al., 2015)
Transparent, antireflective	CHINF, SiO_2 nanoparticles ; PFPE lubricant	Layer-by-layer self-assembly	RMS surface roughness 54,45 nm	(Manabe et al., 2014)
Slippery surface coating	PVDMA, PEI ; silicone oil, canola oil, coconut oil, olive oil	Layer-by-layer assembly	Micro to nanoscale pores	(Manna & Lynn, 2015)

Table 2. *Recorded methods and other details for tailoring lubricant impregnated surfaces continue.*

Properties	Materials: solid + liquid	Fabrication method(s)	Pore size / roughness / sphere diameter	Reference
Physical and chemical stability	TMCTS ; ([EMI][TFSI])	Chemical vapor deposition	Microspheres with diameters of 0.5 - 3.0 μm	(Miranda et al., 2014)
Transparent, self-standable	(PVDF-HFP)/DBP ; Krytox 103	Non-solvent-induced phase separation	ca. 450 to 850 nm pore size	(Okada & Shiratori, 2014)
Transparent, mechanically robust	PDADMAC, SiO_2 nanoparticles, substrate Al, PMMA, STST, PP, PSu ; Krytox 100, 103	Layer-by-layer deposition	Nanoscale	(Sunny et al., 2014)
Solvent-repellent	PDA-coated, TiO_2-coated, fluorinated and silicified surfaces ; Fluorinert FC-70	Micro-omnifluidic (μ-OF) system assembly	Micro to nanoscale, roughness	(You et al., 2014)
Microbiological corrosion protective	PFDS on Al substrate ; Perfluoropolyether (PFPE) Nascent™ FX-5200	Anodization, modification with fluorocarbon	Nanoscale	(Wang et al., 2015)
Corrosion protective	Hydrophobic TAH/LS ; perfluorinated lubricant (Nascent FX 6200)	Dissolution–deposition	Micrometer scale cavities and protrusions	(Yang et al., 2015)
Ice-adhesion reductive	Nanotextured silicone ; OTS (octadecyltri-chlorosilane)	Standard photolithograph	Micropost spacing 5 to 50 μm, depth 10 μm	(Subramanyam et al., 2013)
Frost-repellent, self-healability	Al2O3 -nano-particles, silicon nanowires, microstructured SHS based on silicon microposts ; octadecyltrichlorosilane (OTS from Sigma-Aldrich)	Vapor-phase-deposition	Si-nanowires' diameters 50 to 200 nm, height ca. 2.5 μm, 10-μm-tall square silicon microposts with 10 μm width and 5,10, and 25 μm interpillar spacings	(Rykaczewski et al., 2013b)
Self-healability	Smooth and textured silicon wafers functionalized with fluorosilane coatings ; Krytox-1506	Vapor phase reaction, spray coating, photolithography	Microposts ca. 10μm	(Rykaczewski et al., 2014)
Ice-phobicity	PDMS with SiO_2 -reinforced coating layer ; silicon oil	Polymerization	-	(Zhu et al., 2013)

As seen from the Tables 1 and 2, for many experiments the most used lubricant has been fluorinated oils (Kim et al., 2012; Manabe et al., 2014; Rykaczewski et al., 2013; Wong et al., 2011). The suitability of these oils is definite as to the fact that they are clear, colorless, nonreactive, nonflammable and to some extend long-lasting. The polymer chain of perfluoropolyether is entirely saturated, containing carbon, fluorine and oxygen atoms, as seen from the chemical structure in Table 3, with weight basis of 22% of C, 69% of F and 9% of O. (DuPont, 2011)

Recently, perfluorinated compounds have been under distress and assessments, hence they might have effects to human health as to environment. It is know that the compounds are persistent in nature and may be toxic towards organisms. Reduction of the usage of perfluorinated compounds seems to be in process worldwide. Forth, it is needed to consider the suitable lubricating liquid used in applications ranging from any field of industries. (Lindstrom et al., 2011; Zaggia & Ameduri, 2012; Zushi et al., 2011)

Likewise, silicone oils with various viscosities are used in making lubricant impregnated surfaces. The polydimethylsiloxanes are mainly categorized according to their average chain length – that is their viscosity. The chemical structure backbone is constructed by silicon and oxygen atoms with methyl groups chained from the silicon atoms, as seen in Table 3. Silicone fluids work respectable well in liquid infused surfaces since they are strongly hydrophobic, physiologically inert, lubricating by their nature and possess excellent release properties. (Moretto et al., 2000) When choosing the lubricant, it must be immiscible towards repelled liquid – for example to water. Yet other desired properties are complete spreading and high affinity towards the porous matrix in comparison with water. (Wang et al., 2015; Wong et al., 2011)

Table 3. *Generally used lubricants for liquid impregnated surfaces preparation, Perfluorinated lubricants and silicone oils.*

Lubricant	Chemical name	Chemical structure
Perfluorinated oil	Perfluoropolyether, PFPE	$F-(CF-CF_2-O)_n-CF_2CF_3$ $\|$ CF_3
Silicone oil	Poly(dimethylsiloxane), PDMS	$\left[\begin{array}{c} CH_3 \\ \| \\ -Si-O- \\ \| \\ CH_3 \end{array} \right]_n$

4.2.1 Antibiofilm and antifouling

Different bacteria and micro-organisms tend to form vast colonies, or biofilms, abundantly on almost any possible surface. Biofilms are ubiquitous and they tend to be resistant towards many different cleaning treatments. In consequence, as posing pathogenic threats or hindering processes from maritime to cell culturing, bacteria and micro-organism free surfaces are in aspiration of medical technology but also to more robust maritime technology, hence pathogenic bacteria and maritime biofouling both are caused by organisms submerging and colonizing the surface. Inhibitive effect of SLIPS towards micro-organisms is suggested to be due to the slippery properties of the surface (Epstein et al., 2012b; Wang et al., 2015). For instance, bacteria cannot anchor onto the surface through cellular mechanisms, since the interface is mobile contrary to most solid

surfaces. Moreover, the lubricating liquid in the structure can be seen as immiscible towards aqueous bacteria/micro-organism medium and the surface tension impedes organisms' adhesion to the surface. (Epstein et al., 2012b; Wang et al., 2015) The so-called biofouling, micro-organism growth on a surface, is been demonstrated in Figure 13.

Figure 13. *Classical examples of biofouling in structures having somewhat continuous water contact. Adapted from* (Callow & Callow, 2011)

Howell et al., 2014 documented molding and direct embedding methods for 3D printed vascular systems into polydimethylsiloxane (PDMS). The structure was filled with silicone oil, to gain a nontoxic oil-infused material. These experiments showed a major reduction in biofilm adhesion when compared to plain PDMS and glass controls. After 12 days incubation with microalga, lubricant impregnated PDMS had biofilm coverage of 7% as opposite to plain glass' 95%. (Howell et al., 2014) Nontoxic material with low biofilm adhesion could have many targets of applications. Also Epstein et al. reported a SLIPS-based antibiofilm surfaces that worked under extreme pH, salinity and in UV environment. After the incubation tests, the SLIPS showed better performance than PEG-functionalized surfaces, nowadays majorly used for protein and cell-absorption resistant surfaces especially in bioreactors. Their SLIPS prevented more than 99% of *Pseudomonas aeruginosa*, 97% of *Staphylococcus aureus* and 96% of *Escherichia coli* biofilm attachment after a week incubation time, whereas polytetrafluoroethylene gained biofilm after hours. (Epstein et al., 2012)

Xiao et al., 2013 stated that by using microporous butyl methacrylate-ethylene dimethacrylate (BMA-EDMA) surfaces, cured with UV-initiation, it is possible to achieve potential concept of fouling resistant marine coating. The samples held their water-repellent nature even after a month of incubating in sea water. Slippery BMA-EDMA can also be used for antibacterial applications reported by Li et al., 2013. Their studies suggest that in high nutrient medium, biofilm formation can be more dependent on the bacteria strain than physiological conditions. (Li et al., 2013; Xiao et al., 2013)

4.2.2 Anticorrosion

As viewed from operational and economical point of view, corrosion of metals and alloys is a severe problem affecting various of engineering systems from automobiles, to naval vessels to pipelines and so on, as depicted in Figure 14. Corrosion may occur in many materials by chemical and/or physical pathways. It is present everywhere and causes hindrance to many industrial applications. Especially in structures existing near ocean environment, it can be considered as the main factor of degradation. Water-repellent surfaces generate vast opportunities to inhibit or hinder corrosion as protecting the metal surfaces from oxidation (Borenstein, 1994; Qiu et al., 2014; Wang et al., 2015). Moreover, as discussed in chapter 4.2.1, the lubricant impregnated surfaces can protect the surface from micro-organism attachment, a considerable characteristic tackling against yet another cause of corrosion – microbiologically influenced corrosion.


Figure 14. *Various structures suffering from corrosion: anchor, vessel and painted surface.* (Vincentz Network GmbH & Co. KG, 2011)

Wang et al. reported SLIPS that had high resistance towards sulfate reducing bacteria (SRB) - known for causing bio-corrosion failures. SLIPS were constructed for sea water environment by constructing a rough aluminum oxide layer with fluorinating and infusing it by using fluorosiloxane derivate lubricant. After a 7-days period, their SLIPS had only few colonies, as to bare aluminum samples were abundant with vast colonies SRB. Another approach combating against corrosion was introduced by Qiu et al. A universal protocol for metals was developed in which electrochemically gained metal structure was covered with carbon fiber and a lubricant working as a barrier to inhibit corrosion. Method is suitable for copper, copper/aluminum alloy, aluminum/magnesium alloy and for low alloy steel, in addition, showing SLIPS acting as a tough barrier for corrosion. (Qiu et al., 2014; Wang et al., 2015)

To tackle mineral fouling, calcium carbonate and barium sulphate build-up in heat transfers and in oil production facilities, Charpentier et al., demonstrated SLIPS to reduce mineral scale deposition in potentiodynamic mode. Microporous poly(pyrrole) (PPy) were generated onto substrates from stainless steel by using electrodeposition. They recorded noteworthy results: calcium carbonate deposition reduced by 18 times when compared to plain stainless steel. (Charpentier et al., 2015) These new-age SLIPS

coating are ought to be promising candidates for low-active metal as to active metal protection in marine and industrial environments.

Porous PPy microtexture
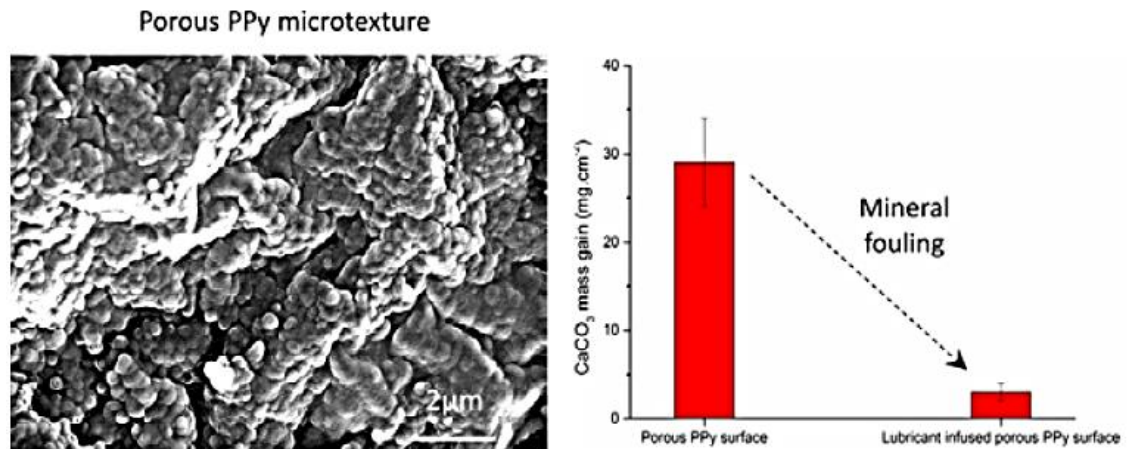
Figure 15. *Charpentier et al. generated a SLIPS via electrodeposition onto stainless steel substrate. The PPy surface reduced significantly mineral fouling.* (Charpentier et al., 2015)

4.2.3 Anti-icing

Anti-ice and ice ice-repellent coatings would have substantial impact on energy and economic savings but also major step in improving safety and reinsuring functionality of processes and systems. Previous anti-ice surfaces relying in superhydrophobic surface technology have shown promising results although fully functioning, long-lasting and low-cost applications have not been developed. (Kim et al., 2012) Heavy accretion of ice is known to impact detrimentally in many industries and especially on maritime logistics, as in Figure 16.

Figure 16. *A cargo ship covered in exceptionally heavy layer of ice. 450 tons of ice was removed from the ship.* (Ocean, 2012)

In the promising study of Wong et al. commercial materials were combined to achieve multifunctional SLIPS with omniphobicity. Porous Teflon membrane was used as solid material and low-surface-tension perfluorinated liquid was used to have lubricating film to SLIPS. It was illustrated for the first time that SLIPS can be developed to function as omniphobic material, in addition, to repel ice as shown in the study. (Wong et al., 2011)

Kim et al. described ice-repellent material based on SLIPS –technology, as portrayed in Figure 17. They were able to maintain smooth and low-hysteresis lubricant overlayer by infusing water-immiscible liquid into nanosurface. Liquid and the surface had high affinity towards each other as to the liquid was locked into the structure. The method was developed to industrially relevant metals and showed that SLIPS –coated metals surfaces suppressed ice accretion and had relatively low ice adhesion strengths. In the study, polypyrrole was electrodeposited on Al substrates, fluorinated and impregnated with lubricant. Texture diameters in the PPy were ca. 2 µm and the lubricating agent was Krytox 100. From SLIPS-Al surface, the cooled droplets sled away as to in untreated Al droplets froze before sliding away. In the study, the ice was formed to columns and pulled or pushed with a constant rate to define the ice adhesion force. The SLIPS-Al had ice adhesion strength of 15.6 +/- 3.6 kPa as to bare Al the values were 1360 +/- 210 kPa at -10 °C. (Kim, et al., 2012)
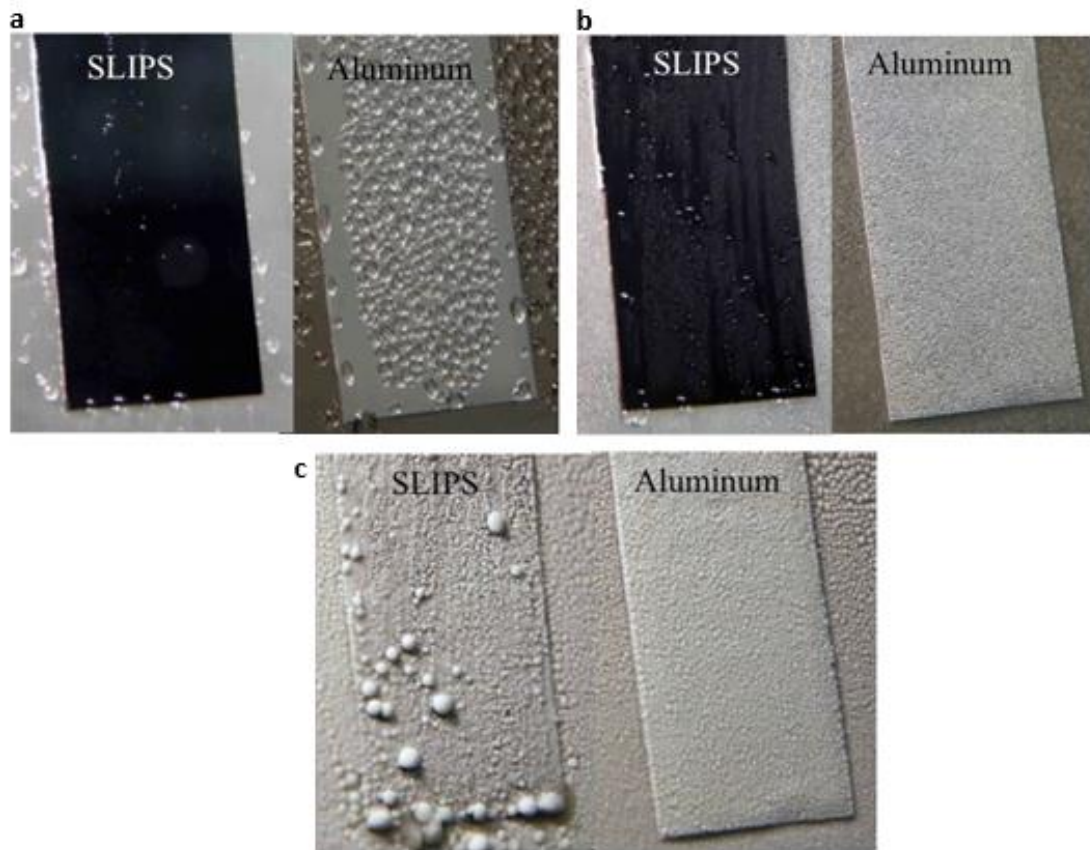
Figure 17. *Comparing the wettability and ice-repellency of SLIPS to Al –samples. (a) Melting water is not pinned on SLIPS –surface as they can slide off as the temperature increases. (b) After formation of condensate, the formed water drops slide off from SLIPS –sample. (c) If water droplets are frozen onto SLIPS, they tend to isolate – not to form continuous ice layer. Adapted from* (Kim et al., 2011)

Subramanyam et al. performed systematic ice-adhesion measurements and observed, by their work with SEM imaging, that ice-adhesion strength can be assumed to be dependent on the surface texture and to decline with increasing texture density. Their surfaces were tailored by using photolithography to gain square silicon microposts and coated with OTS by liquid deposition. In the experiments water was frozen into cuvettes and a probe of force transductor was used to apply a shear force to the cuvettes – the force required to fracture the ice-substrate interface was then recorded. (Subramanyam et al., 2013)

By testing samples with frosting and defrosting cycles, Rykaczewski et al. detected that lubricant infused surfaces, LIS, with perfluorinated oil were vulnerable to permanent impairment and were prone to losing their self-healing mechanism. The findings suggested the damages were due to lubricant migration from the wetting ridge and the texture to frozen droplets. In their experiments, they condensed frost to the studied surfaces and viewed the surface interactions by using ESEM microscope. Their LIS samples were fabricated by using vapor-phase-deposited alumina nanoparticles, silicon

nanowires and microstructured superhydrophobic surfaces based on silicon microposts. Microposts were 10 µm tall, 10 µm in widths and had different interpillar spacings: 5, 10 and 25 um, as seen in Figure 18. The oil depletion was observed from all the LIS samples with perfluorinated oil as discussed more in the chapter 4.3. (Rykaczewski et al., 2013)
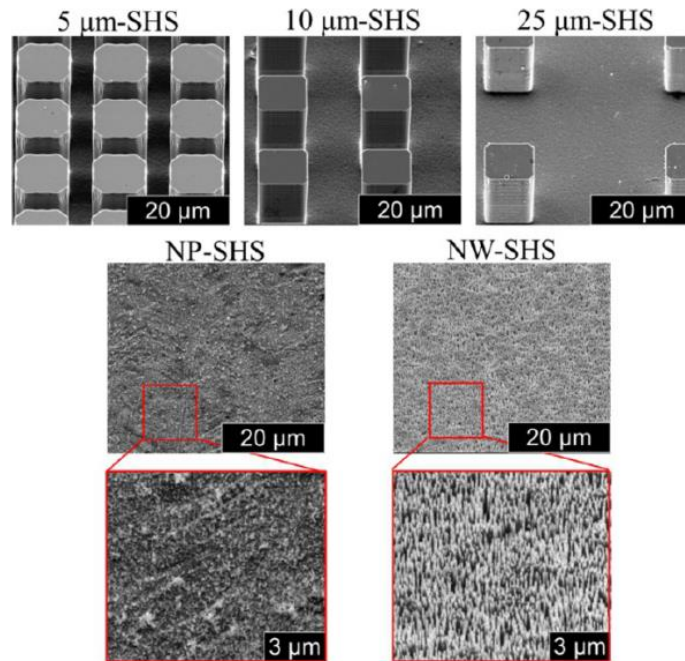
Figure 18. *The ESEM images of structured samples of Rykaczewski et al. SHS refers to superhydrophobic surface, NP alumina nanoparticles and NW silicon nanowires.* (Rykaczewski et al., 2013)

4.3 Current challenges and promising future applications

Slippery liquid infused porous surfaces can possess the key to become a next generation anti-icing solution for many industries (Wong et al., 2011). Additionally, SLIPS have proven to have potential properties and characteristics in self-healing (Wong et al., 2011), anti-sticking (Richard & Quéré, 2007), anti-fouling (Barthlott & Neinhuis, 1997a) and self-cleaning (Blossey & Scientifique, 2003; Akira Nakajima et al., 2000). Significant properties, in which these characteristics could be advantageous, are anti-snow adhesion (Kako et al., 2004), anti-ice adhesion (Saito & Takai, 1997; Saito et al., 1997) and cleaning-surfaces (Quéré, 2005; Zielecka & Bujnowska, 2006) to name a few. It is easy to imagine, that these properties would enable easy emptying of containers, anti-graffiti walls, frictionless and anti-fouling liquid transportation in tubes and so to contribute to energy and cost savings.

Advantageous properties are not only limited to hydrophobicity, but also include omniphobicity, pressure stability, self-healing ability, optical transparency and salt water endurance. It is also needed to state that construction of SLIPS may not be

dependent on special and expensive materials or equipment since the surface properties are insensitive to the precise geometry of the underlying substrate. There are studied commercial materials, porous solids and lubricants, which make fabricating of SLIPS potentially a realistic prospect to resolve liquid-repellence and icing problems among other issues. (Wong et al., 2011)

Optically transparent surfaces have, as stated, multiple desired application fields when added to other desired properties of the SLIPS. Even if prolonged for, optical transparency in visible or even near infrared wavelength can be challenging to achieve as the size of underlying texture should be smaller than the wavelength of visible light 400 nm. Yet, SLIPS have proven to have optical transparency hence SLIPS rely on nanoscale surface structures as dimensions being under the sub-diffraction limit (even under 100 nm). Because there is a great difference in refractive index in the interfaces of solid and air of the textured surfaces, it results in significant scattering of light which reduces the transmission of light. This means that in SLIPS, optical transparency can be achieved by choosing right lubricant and porous membrane pairs. (Nakajima et al., 1999; Wong et al., 2011) As a porous solid material, Teflon membranes have been used in SLIPS to demonstrate the transparency properties, as in Figure 19 (Wong et al., 2011).
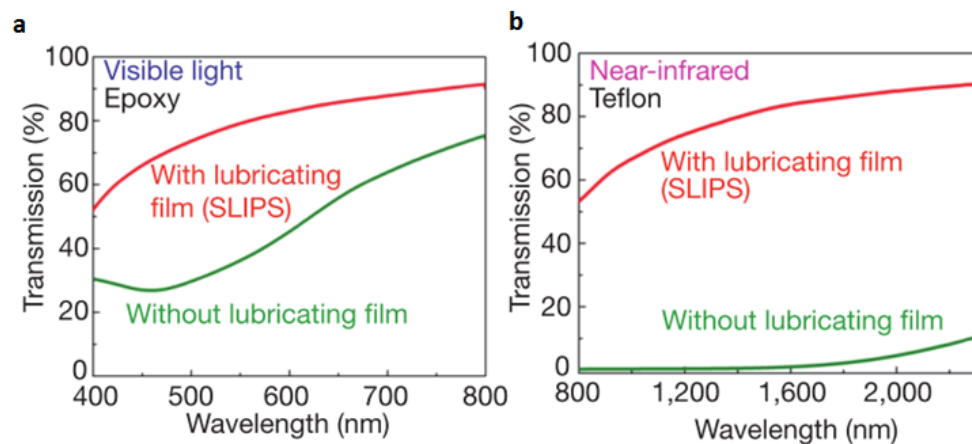

Figure 19. *Aizenber's team optical transmission measurements for different SLIPS. (a) An epoxy-resin based SLIPS in the visible light range (400-750 nm). (b) A Teflon based SLIPS in near infrared range (800-2,300 nm).Adapted from* (Wong et al., 2011)

In addition to Teflon membrane, also SLIPS from cellulose lauroyl ester (CLE) and poly(vinylidene fluoride-*co*-hexafluoropropyle (PVDF-HFP) as a porous solid can be made transparent with PFPE lubricant (Chen et al., 2014; Okada & Shiratori, 2014). Liquid repellent surfaces with transparency would be of interest in broad range of applications including solar cells, windows and windscreens.

Based on liquid infused surfaces, many applications are being explored and further developed in a variety of industries. Enhancing condensation heat transfer (Anand et al,

2012; Xiao et al., 2013), self-cleaning (Akira Nakajima et al., 2000; Wong et al., 2011), fog harvesting (Lalia et al., 2013), omniphobic textiles (Shillingford et al., 2014), minimizing ice nucleation (Kim et al., 2012; Wilson et al., 2013), decreasing ice adhesion (Subramanyam et al., 2013; Zhu et al., 2013) and biofouling prevention (Epstein et al., 2012; Xiao et al., 2013) are some examples where the engineering of SLIPS might go in the future. Under these applications, there are many other possibilities to refine the urges, for example, in self-cleaning solar panels or harvesting condensate water for irrigation purposes. Albeit, to attain the possibilities, the existent of technical difficulties needs to be overcome. The problems of superhydrophobic and liquid infused surfaces both are being addressed by many researchers. (Emelyanenko et al., 2013; Jianyong et al., 2014; Samaha et al., 2012; Yao et al., 2011) Problems include wetting ring formation, cloaking, mechanical endurance of the micro- and nanoscale textures and lubricant depletion.

In the experiment of Anand et al., enhanced condensation was achieved by designing proper texture geometry and chemistry whilst added lubricant. It was observed that cloaking inhibits droplet growth in the case of condensation, however, there are differences between lubricant liquids. As the water droplet starts to form on the liquid infused surface, the lubricant induces an annual sphere around the condensed drop, called the wetting ridge. Depending on the interfacial tensions of the oil and the drop, oil encapsulation, or cloaking, of the droplet may also occur by the impregnated oil. Some of these problems are illustrated in Figure 20. Cloaking can be considered as an undesirable effect since it can deter the growth of condensate, contaminate the forming droplets and accelerate the oil depletion from the porous material. The effect itself can limit the usage of liquid lubricant infused surfaces in the field of fog-harvesting or condensate water harvesting as to colloid water droplets can exhibit noncoalescence. (Anand et al., 2012; Boreyko et al., 2014)
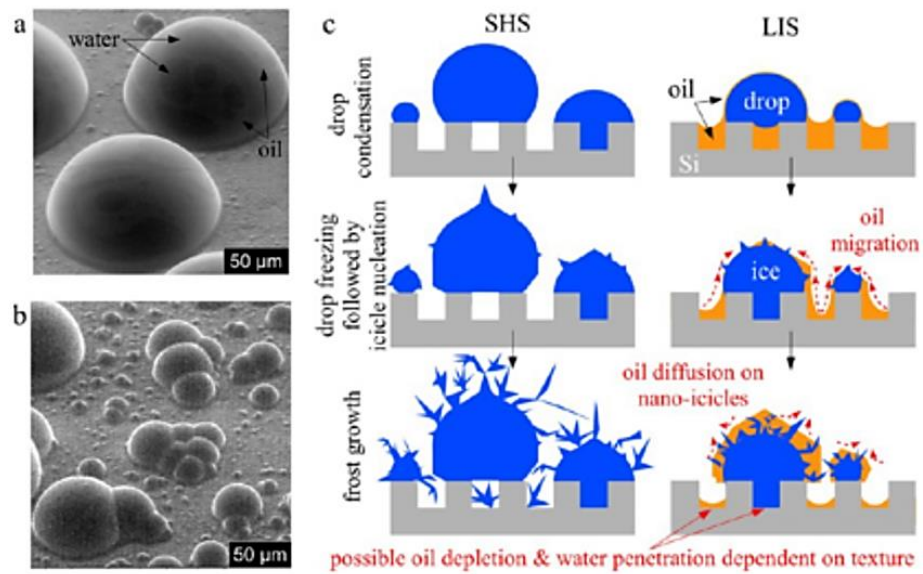
Figure 20. *Possible problems of SLIPS. (a) Lubricant swirls onto droplets. (b) Condensed compound droplets. (c) Frost growing by condensate and probable oil depletion of the structure. SHS stands for superhydrophobic surfaces and LIS lubricant impregnated surfaces. Adapted from* (Rykaczewski et al., 2013)

Rykaczewski et al., 2013, showed that irreversible damage had occurred in the porous surface impregnated with perfluorinated oil. They recorded oil depletion from the wetting ridge as to the lubricant drained from the vicinity of the drop but also underneath the drop. This caused a loss of self-healing properties within tested frosting and defrosting cycles. The decrease in characteristics was seen as a result of oil mitigation from the wetting ridge onto frozen drops and the oil mitigation seemed to be driven by capillary forces arising from nanoicicle nucleation. Cryo-SEM images of recorded droplets and micro-crystal ice are presented in Figure 21. (Rykaczewski et al., 2013)
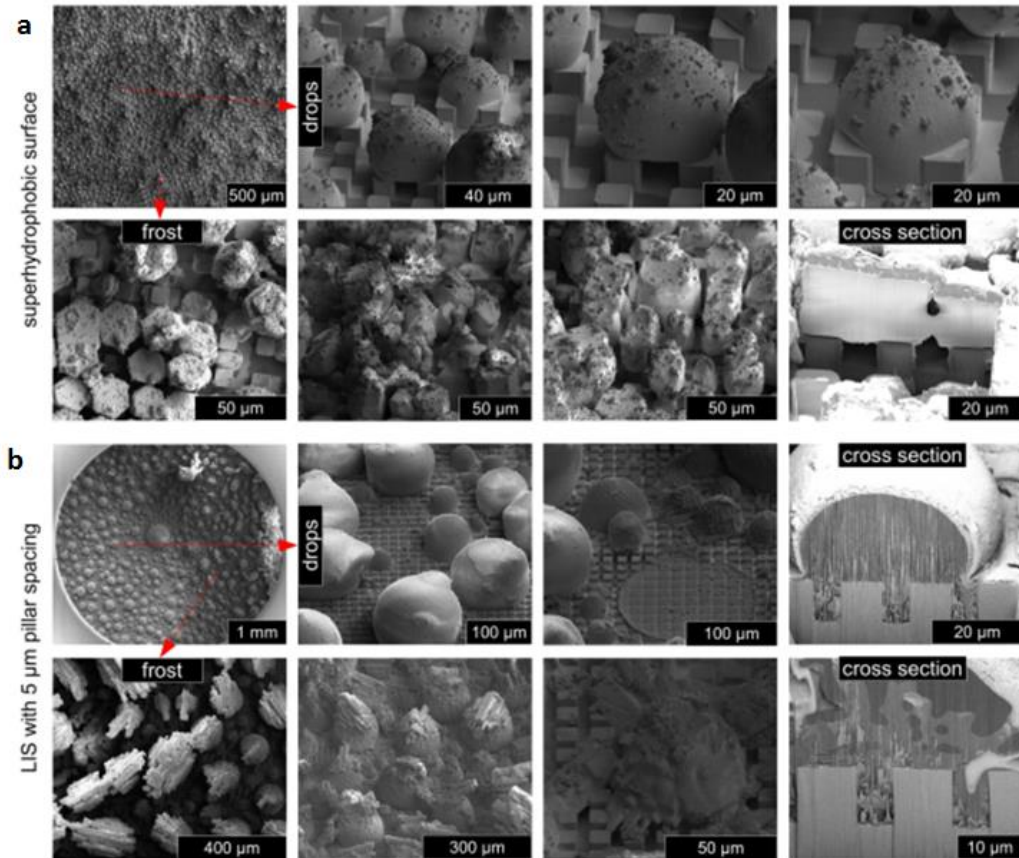
Figure 21. *Cryo-SEM images of droplets freezing on (a) superhydrophobic surfaces and (b) lubricant impregnated surfaces (LIS). Adapted from* (Rykaczewski et al., 2013)

Kim et al. showed that lubricant impregnated nanotextured surfaces had better shear-tolerant, liquid-repellent features that superhydrophobic surfaces. Sandblasted Al substrate samples with boehmite nanostructure formation, fluorofunctionalizing treatment and lubricant application were prepared. They observed that under high acceleration conditions the lubricant was lost from the larger cavities of the texture. (Kim et al., 2008) The stability of the impregnated liquid-porous solid interface is crucial. The lubricant can be lost from the textured structure for various reasons, such as cloaking, solubility, evaporation and body forces. Hence, it would seem suitable to use and to examine low-vapor-pressure lubricants for further applications but also to develop lubricant reservoir to the structures to maintain the slippery effect (Subramanyam et al., 2013)

4.3.1 Multilayer liquid infused structure

In SLIPS, porous surface membrane structure is impregnated with lubricating fluid resulting in robustness to condensation and impinging droplets. SLIPS have also

presented similar properties as superhydrophobic surfaces, including self-healing, self-cleaning and anti-ice properties to name a few. (Kim et al., 2012; Wong et al., 2011) As seen from the literature, lubricant depletion can be seen as a major challenge for SLIPS. To prepare for evaporation and lubricant lost by droplets, a reservoir layer is ought to be developed beneath the porous membrane, as depicted in Figure 22. Self-lubricating surfaces should have a continuous and to some extent permanent lubrication system built-in. They can have the ability to shift minute volumes of lubricant onto the outmost layer and surface. It would be advantageous to the application to maintain the continuous lubricant transfer throughout the operational life on the application. (Wong et al., 2011)
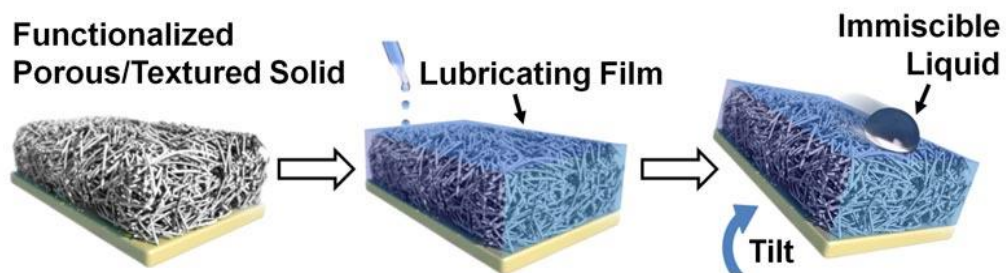
Figure 22. *Impregnation of SLIPS structure and droplet mobility after tilting the surface. Under the surface membrane, another layer could be constructed to maintain SLIPS characteristic. The ideal multilayer structure would have a slippery liquid-infused porous topmost layer as an outmost surface. Adapted from* (Wong et al., 2011)

The surface-energy-driven capillary actions ease the lubricating fluid's movement to the porous outmost layer (Wong et al., 2011). To get the lubricant releasing from the reservoir layer towards the top layer, surface energy gradient should be used to gain the movement. Explicitly, chemistry of the solid needs to be thought carefully to obtain ascending affinity with the lubricating fluid from the bottom to the top of the porous layer. Since the dimensions of the pores are under the capillary length of the lubricating fluids to be used, gravity is expected to have no effect on the lubricant movement in the porous structure. Some commercial materials have the portrayed characteristics. (Kim et al., 2012; Wong et al., 2011)

Depending on the final application surface, fabricating super liquid-repellent surfaces would be costly to manufacture in site. However, manufacturing these surfaces in advance by a cost-effective method would bring significant savings. Furthermore, optical transparency could be achieved by infiltrating the porous surface layer of the construction by a lubricating fluid which would reduce light scattering in the structure (Wong et al., 2011). Therefore, end-use applications could grow considerably as to anti-ice, self-cleaning, anti-fouling and transparent warning signs would be possible to prepare. This could be possible by choosing the used materials and components with great care.

5. ICEPHOBICITY

5.1 Icing behavior

Icing can be considered as a state when supercooled water drops collide and freeze on a solid surface, which happens when sufficient moisture exists and the surface temperature is below zero degrees of Celsius (Antonini, 2011). Icing causes problems, inefficiencies and costs for a variety of industries. Atmospheric icing is known to hinder aeronautics (Heinrich et al., 1991), off-shore platforms (Ryerson, 2008), wind turbines (Dalili et al., 2009), maritime industry (Ryerson, 2011) and power lines (Laforte et al., 1998). Consequently, there are documentations of lost lives, injuries and detriments due to accretion of ice in critical points (Mara et al., 1999; National Transportation Safety Board, 1988, 1996). Fortunately, in general icing tends to work as a decelerator and to be an annoyance more than a severe risk, nevertheless, it is clear, that controlling and preventing ice formation is utmost important. (Antonini, 2011; Ryerson, 2011)

Operators working in the Arctic region are familiar with harsh conditions ranging from cold and windy to high humidity. Especially, sea spray and atmospheric icing can affect functions, such as productivity, safety, reliability and operational tempo. Moreover, ring stability in vessels and oil ships and disabilities in antennas, cranes, equipment, hatches, valves and cargo can be reduced by variety forms of icing, demonstrated in Figure 23. Consequently, frost and ice free surfaces are truly desired in many industries as to ice accretion effects on several segments in operations and processes. Icing can cause detrimental measurement errors up to 60% in wind turbines under icing events (Parent & Ilinca, 2011). Also aircraft sensors and probes can suffer of erroneous data, such as inaccurate airspeed indication, because of icing problems. Furthermore, substantial power losses have been recorded hence accreted ice changes wind turbines' shape and roughness. Mechanical failures have been documented frequently in the literature since accumulated ice increases loads on accumulated surface. This can cause resonance, vibration and imbalance in processes and lead to overheating. In aircrafts, ice contamination reduces maximum lift and increases profile drag and especially during take-offs, serious stability and control problems may occur. Different safety hazards are also due to icing buildup as falling off ice from upper surfaces and slippery planes pose threats machinery and to operators. Icing also impedes cables by locking them into continuous ice, risking power, information and load transferring. (Parent & Ilinca, 2011; Perkins, 1978; Ryerson, 2011)

Figure 23. *Different icing problems caused by ice accretion on different systems from cables and airplanes to maritime vessels.* (DNV GL AS, 2015; Mastenbroek Aeroskill, 2015; SWZ Maritime, 2014; Yinhe Wind Power Co. Ltd., 2012)

Activity in the Arctic region is expected to grow, as several industries continue to increase their operations. This involves maritime, off-shore, extractive and tourism industries at the very least. Furthermore, climate change pushes the limits of cross-scientific engineering, as it is extremely important to ensure secured activities and also green choices for the environment when it comes to tackling icing. (Finland's Prime Minister's Office, 2013)
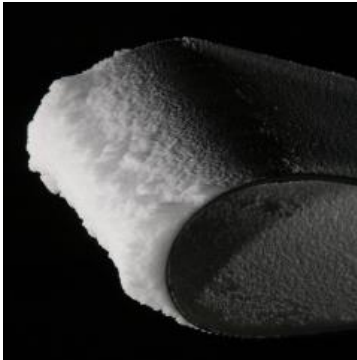
5.1.1 Ice accretion and adhesion

The gathered ice and accretion rate is influenced by aerodynamic and meteorological conditions, such as temperature, liquid water content, water droplet diameter and so on. Liquid water content can be characterized as the total mass of liquid water enclosed in a given unit in cloud. When liquid water content is high, number of supercooled drops striking on a surface is also high and below zero degrees of Celsius the liquid water content is at its highest. As said, temperature effects on liquid water content as to the ice forming type, since glace ice is generated near zero and rime in lower temperatures. Droplet diameter is generally given in the medium volume drop diameter where half of the drops are smaller and half larger than the given size. Collection efficiency of the ice accumulation is directly influenced by drop size. (Antonini, 2011)

Ice formation onto surface can have different mechanisms depending on the dominant conditions. In many cases, in-cloud icing or precipitation icing are the main liable

mechanisms but condensation can also accumulate ice particularly in heat exchangers. Apart from condensation icing, liquid state water droplets in sub-zero temperature catch the surface whilst freezing immediately upon contact or after a while. Dispersive, mechanical and chemical adhesion mechanisms affect the adhesion on the surface as the ice nucleates by heterogeneous nucleation. Especially northern countries, such as Canada, Iceland, Finland, Norway, Japan and Russia, suffer from atmospheric icing, explicated in Table 4, and its effects on manmade structures. On high grounds, the structures are haunted by rime ice, whereas in other areas, in lower altitudes, freezing rain or wet snow are nuisance of substructures. Subsequently, aircrafts, power lines, wind turbines and ski lifts are needed to withstand icing and its accretion on them. (Farzaneh, 2008)

Table 4.   *Atmospheric icing types and their ice accretion on aerodynamic profile.*

Icing type	Distinctive type of ice	Picture
Precipitation icing	Glace	
In-cloud icing	Rime	

Atmospheric icing as a term refers to all types of accretion of frozen water and two categories can be listed below: in-cloud icing and precipitation icing. Precipitation icing can produce wet snow, dry snow and glace ice, depending on temperature variations in hundreds meters above the ground and near the ground, with freezing temperatures, precipitation can cause freezing rain, famously known to impact in North America, as in 1998 snow storm (Mara et al., 1999). In glace ice formation, the impacted drops tend not to freeze right after surface contact. Hence, the ice is clear, smooth and also denser

and harder than rime. As the icing continues and droplets slide on the surface, glace ice can have altering shapes, reaching off the edges of the surface. (Antonini, 2011) (Farzaneh, 2008 pp.1-30) Both of the icing types are being demonstrated in Figure 24 and in Table 4.
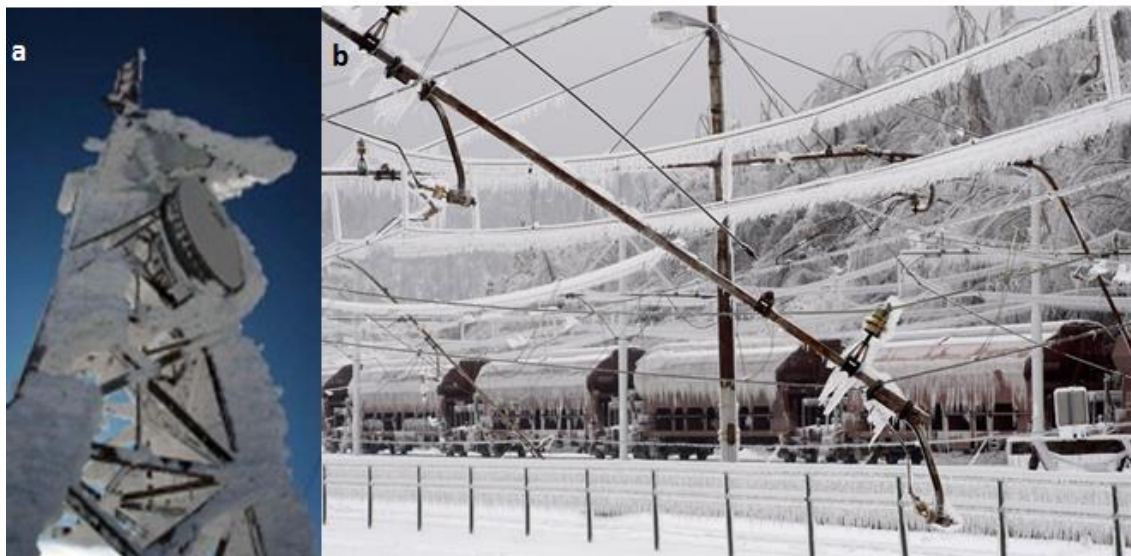
Figure 24.   *Different atmospheric icing types. (a) Rime ice accreted on antennae. (b) Glace ice covered electric lines and railroad car.* (Kourounis, 2007; Sim, 2014)

Depending on the freezing layer, temperatures and other parameters, the precipitation can reach ground as rain, slush, refrozen snow or snow. For precipitation icing the key parameters are precipitation rate, surface air temperature and liquid water content. (Farzaneh, 2008 pp.1-30)

When the temperature is below zero and yet droplets retain in liquid state, in-cloud icing occurs within clouds consisting of supercooled droplets. Water drops can change into crystals of ice as the temperature in the cloud reaches the freezing temperature. However, these in cloud drops can stay in the liquid state even within temperature range of -40 to 0°C, consequently, these droplets are called supercooled. Unfreezing is due to molecular disorientation: the drops cannot turn their structure into ice crystals but can freeze rapidly upon impacting on a surface. (Antonini, 2011)

Rime ice development is dependent on the size of cloud droplets, wind speed and temperature. It forms when tiny supercooled drops impact on solid surface and in general, it occurs in low temperatures, -15°C and below with low liquid water content, and can be characterized as opaque, milky and rough. Rime ice tends to occur near exposed mountain summits, upper towers and ski lifts hence the icing appears only above the cloud base. For in-cloud icing the most important parameters are liquid water content in the cloud, droplet size, air temperature and wind speed. Between

temperatures -15 and -5°C, so called mixed ice ban be observed which has both, rime and glace characteristics. (Antonini, 2011; Farzaneh, 2008 pp.1-30)

The pressure in developing ice-repellent surfaces and materials has only been increasing as shipping, cargo and travelling activities increase in northern areas as in everywhere else in the world. This has opened new routes, generated new infrastructures and pushed the limits of anti-icing engineering (Arclio, 2015). As said, different areas are prone to different icing types; nevertheless, wind direction, wind speed and temperature are the most noteworthy parameters in ice formation.

5.1.2 Anti-icing and de-icing

In aircrafts, maritime vessels and trains ice can be accumulated on route or in downtime and in airplanes, usually formats in wings but also stabilizers, engine inlets and rotors (Andersson & Torikian, 2000; Antonini, 2011; Dehghani-Sanij et al., 2015). Examples of structures suffering from accreted ice are shown in Figure 25. Present day ice removal methods tend to be unsustainable, reapplication dependent and dysfunctional for all the applications. These methods can be divided into anti-icing and de-icing methods, which include mechanical removal of ice, heating the application or treating it with chemicals. Needless to say, these methods may not be cost efficient or green choices as they consume energy and other resources. Hazardous methods may affect not only to environment but also to personnel and machinery itself. Hence the research and development for the passive anti-icing surfaces are truly needed to address the issue. As more sustainable and effective approach, passive anti-icing surfaces could be used to prevent the formation and adhesion of different ices by minimizing the interaction between the surface and incoming droplets. They could also hinder the nucleation of ice by reducing the accreted ice adhesion. (Antonini, 2011)

Figure 25. *Possible anti-icing or de-icing objects suffering from icing. (a) Powerlines. (b) Airplane under de-icing treatment.* (IWAIS, 2009; Met Office, 2015)

Anti-icing prevents ice to accrete on the surfaces, as de-icing removes the ice layer from the object. In both of these approaches, passive and active methods occur: passive approach utilizes physical properties of the surface to eliminate or prevent ice whereas active methods include chemical, thermal or pneumatic systems and energy (Parent & Ilinca, 2011) De-icing in general works occasionally, eliminating accreted ice; whereas anti-icing methods are developed to entirely avoiding ice accumulation by working somewhat continuously. (Antonini, 2011)

Anti-icing methods are essential in more critical areas – especially in aviation in wings, where it is critical to avoid droplets from impinging and freezing on the edge. In aircrafts, typical anti-icing system supplies thermal energy to the desired area – for example inlets or wings by hot air. Another type of heating element is a heating pad consisting of electrically conductive material. Chemical are also used as anti-icing approach. For example, alcohols reduce the adhesion of ice on the surface but also depress the freezing point of impacted cooled water. Chemical treatments can be performed on the ground or in flight but they are costly and in flight necessity needs to be sufficient. (Antonini, 2011)

De-icing methods are implemented as systems where some amount of ice can be tolerated without endangering safety or controllability of the systems (Antonini, 2011). These methods are used in order to accelerate the shedding process of accreted ice from the surface by using thermal melting or mechanical breaking methods. Thermal methods cause the melting of ice, therefore ice sheds from the surface. In mechanical methods the ice is broken from the accreted substrate. It has been stated that thermal methods need ca. 100 times more energy than mechanical methods in order to shed the ice. Although, in some cases thermal methods require a smaller amount of manpower than laborious mechanical methods. As a de-icing method in aircrafts, pneumatic boots can be installed to crack the accumulated ice on wings. The system is inflated with pressurized fluid, but requires maintenance and brings additional weight to the airplane. Other approaches could be shape memory alloys, like NiTi –alloy, which change dimensionally with temperature change as to the shape change smashes the gathered ice on the surface. (Antonini, 2011; Farzaneh, 2008 pp.229-268)

Mechanically, ice can be scraped off or energy releasement can be utilized with vibration or by shock waves. In power lines, scarping methods such as cutters or rollers are used by a maintenance worker or in some cases automated machinery is used. For the same purpose a cable twisting device has been developed, twisting the wire around its longitudal axis. These kinds of methods require complex processes, trained operators, continuous maintenance and electrical motors and power. Moreover, they are not applicable from industry to another. (Farzaneh, 2008 pp.229-268; Laforte et al., 2005)

Because of the need of continuous supply of these materials and methods, new approaches are in interest. Icephobic coatings, which have low adhesion on ice and reduce the shear force to remove the ice from the surface, are being developed. They

also take advantages of external forces, like gravity and aerodynamic or wind forces to shed the ice. At this time, the available anti-icing coatings are based on water repellency by relieving lubricant or melting point depressants thus ablation of ice. Recently, there has been ongoing studies involving phase change materials (Kenisarin & Mahkamov, 2007) and also anti-freeze proteins (Congdon et al., 2013; Duman, 2001). Quite a few anti-ice mechanisms seem to have promising prospect in dimishing ice accretion and adhesion. Nonetheless, more anti-ice derivatives are needed to meet the various kinds of application requirements.

5.2 Correlation between hydrophobicity and icephobicity

Icephobicity refers to ice-repellency characteristics of a surface or material. Analogously to hydrophobicity or oleophobicity, the surface repels and also possesses low adhesion towards the definite substance or compound. The novelty of the term can be seen from the fact that it has been used repeatedly in the early 2000's as it was used to describe a property of monolayer coatings in scientific article but also in industrial reports and in NASA publications (Ferrick et al., 2008; Kulinich & Farzaneh, 2004; Sivas et al., 2013). Even though being a great research theme of the decade, the Oxford English Dictionary yet not recognizes the term.

In the 2010s there has been some debate whether the mechanisms of ice and water are similar when constructing superhydrophobic surfaces into icephobic. The assumption lies that by low surface energy and high water contact angle icephobicity can be achieved. On the other hand, the mechanisms of surface adhesion of water and ice differ from each other as to water cannot support shear stress but can withstand pressure or tensile compression. In order to gain understanding on superhydrophobic surfaces and their icephobic characteristics, it is essential to comprehend mechanical forces affecting on ice and liquid drops. Subsequently, if there are no adequately proper voids at the surface, some superhydrophobic surfaces can have strong adhesion to ice. (Nosonovsky & Hejazi, 2012)

In the article of Menini and Farzaneh, 2009, it was noted that the measurement of hydrophobicity is a good indicator for materials icephobicity (Menini & Farzaneh, 2009). Recently, this claim has been proven to be incorrect as a number of papers have been published to state that superhydrophobic surfaces may not always be icephobic or even the preeminent choice for icephobic applications. (Jung et al., 2011; Kulinich et al., 2011; Nosonovsky & Hejazi, 2012) As compared by Hejazi et al., 2013, it can be observed that water and ice do have some features and properties in common. Their bouncing-off behavior towards incoming droplets seems to be similar. Also, both, the hydrophobic interactions and icephobicity behavior can be seen as entropic effects hence the formation of ice and hydrophobic interactions are driven by the minimization of the Gibbs' surface energy. Likewise, their effects in new structure assembly, as

snowflakes or complex molecules like protein folding, can be seen as a similarity, theoretically. (Hejazi et al., 2013)

5.3 Icephobic surfaces

Modern-day techniques for ice removal can be seen as sufficient but they involve continuous electrical power, chemicals or hot air. Icephobic coatings are considered as a new, potential possibility to tackle icing issues. They may not replace the old anti-icing and de-icing methods, but would still provide substantial savings as they could be used alongside the old systems reducing labor, capital and/or energy consumption. (Antonini, 2011)

Depressing ice adhesion strength of a surface and preventing incoming droplet freezing can have different approaches. Accretion of ice by supercooled droplets can be prevented upon impact on the surface. The ice formation can be prohibited altogether as in some methods a thin layer of water on the surface is generated by which ice could be shed by external forces for example by wind and gravity. A film of water between formatted ice and the surface could be achieved by freezing point depressed liquids which would have the capability to lower the freezing point of supercooled droplets. In aviation, these commercial liquids have been used – although there are same problems exist in depressant liquids than in low-surface energy lubricants – replicability, as they are non-permanent in most structures. (Farzaneh, 2008 pp.229-268)

Ice accretion prevention could be done by a detailed surfaces or engineered coatings relying in weakening mechanical and physio-chemical interfaces between accumulated ice and surface. Generally, the main polymeric approach towards icephobic surfaces and material seems to be PTFE and in some cases PDMS – both possessing low-surface energies. PTFE –tapes have been used in transmission lines to demonstrate the reduction of wet snow accretion. (Farzaneh, 2008 pp.229-268; Nakagami, 2007)

Also more marginal methods have been tested, such as lithium grease and other industrial lubricants. With these, the usual problem lies within the cost, safety regulations and environmental issues. (Farzaneh, 2008 pp.229-268; Laforte & Beisswenger, 2005)

5.3.1 Ice adhesion of superhydrophobic surfaces

Currently the focus has been on developing and designing of superhydrophobic surfaces in which the external components synergistically reduce ice nucleation and formation. Ice-repellent coatings would provide vast savings in energy, capital and labor as to substantial impact in environmental issues for industries ranging from transportation to infrastructure to cooling systems. Multiple papers have been published where repellency

towards ice and frost have been examined, nevertheless, fully functional and commercially producible ice-free surfaces or coatings yet remain to be developed. (Bird et al., 2013; Chen et al., 2013; Kulinich & Farzaneh, 2011; Peng et al., 2012; Saito & Takai, 1997)

Different polymeric coatings and superhydrophobic surfaces have gained good results in the literature. The properties of aluminum alloy 6061 were refined by Menini and Farzaneh by deposition of adherent PTFE –coating. The generated coating implemented high hydrophobicity even when compared to flat Teflon ® - ice adhesion was decreased by 2.5 times even after some ice shedding cycles. By using a centrifugal ice adhesion test method, they obtained shear stress values for plane Al 6061 –alloy to be 505 kPa (deviation 65 kPa) and for PTFE -coated samples 209.6 kPa (standard deviation 79,6). Water contact angle for PTFE –coatings were hydrophobic and around 130-140°. (Menini & Farzaneh, 2009) By studying wetting behavior, Kulinich and Farzaneh reported to find correlation in between low wetting hysteresis and ice adhesion strength but found no correlation between water contact angle and ice adhesion (Kulinich & Farzaneh, 2009a).

Peng et al., (2012) solved poly(vinyldiene) fluoride (PVDF) into N,N-dimethylformamide and coated a wind turbine blade with the mixture. The study records a rough porous surface with pores ranging from 1 to 5 micrometers, into which the air could be trapped theoretically. Anti-icing tests were performed in the climatic chamber with sprayed supercooled water droplets with the coated blades and showed excellent anti-ice properties in their studies. In their samples, the highest water contact angle was ca. 156° and sliding angle only 2°, likewise, the recorded anti-icing properties, were described as excellent: supercooled droplets rolled off from the surface and no ice crystals appeared to the surface of PVDF coating after spraying 60 minutes of supercooled water. With the same principle of air trapping into the porous surface, Wang et al., (2012) treated copper samples with nitric derivative of perfluorpoluoxyalkyl carbonate to obtain a nano-fluorocarbon film which was stated to be less than 10 nm thick. The results of icing test, made in the climate chamber with injected water droplets, yielded a good anti-icing performance and illustration on how droplets freeze on plain copper and fluorocarbon surfaces, as depicted in Figure 26. (Peng et al., 2012; Wang et al., 2012)
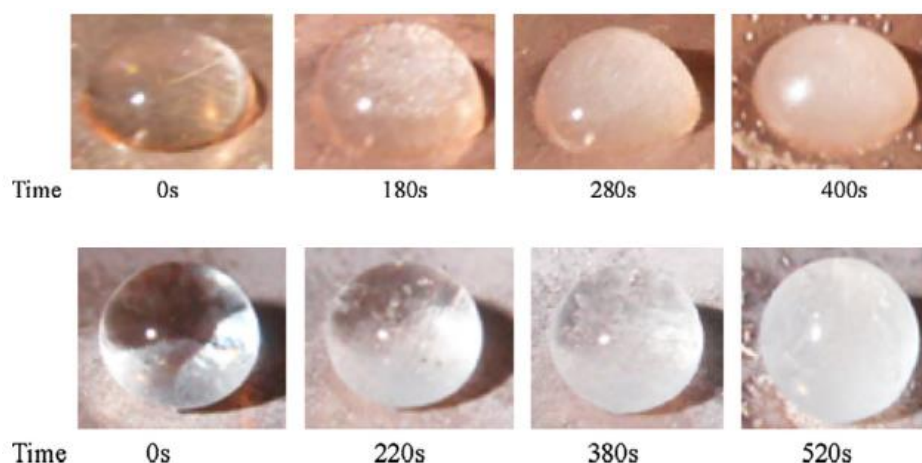
Figure 26. *Iced water droplets on plain copper surface (above) and iced drops on a nanofluorocarbon coated surface (beneath). Adapted from* (Wang et al., 2012)

Even though many researches and studies show very promising and optimistic forward-looking results, there are some proven limitations when it comes to nano-structured surfaces and humidity. Farhadi et al., (2011) investigated four different samples, consisting of aluminum alloy plates with various coating methods and materials. Perfluoroalkyl methacrylic copolymer and CeO_2 nanopowder with spincoating was used to gain the first studied surface. Second surface was fabricated by dip-coating aluminum with 1H,1H,2H,2H-perfluoro-octyltriethoxysilane, as the third aluminum plate was spin coated with a methanol/ethyleneglycol suspension of Ag nanoparticles. The final sample was prepared via spin coating with a silicone rubber and TiO_2 particles. For all the fabricated coatings, the water contact angles were relatively high, 150 to 156°, showing superhydrophobicity. The samples were iced in icing tunnel and shear stress was measured after centrifugal spun test as five to 11 icing cycles were performed. For uncoated, mirror-polished aluminum, the shear stress value was ca. 362 kPa +/- 26 kPa as to the prepared samples the values were between 55 to 110 kPa in the first cycle. The results showed doubts about the wide usage of superhydrophobic coating with nano-structures as the anti-ice performance of the samples degraded significantly during the icing cycles since the shear stress of ice detachment increased from ~90 kPa to ~190 kPa within twenty icing / deicing cycles. Especially humid and wet environments showed that the ice-repellency of the surface can be easily lost. (Farhadi et al., 2011)

Chen et al. stated that superhydrophobic surfaces cannot be used as ice-repellent or ice-reductive surfaces. By examining superhydrophobic and superhydrophilic surfaces it was observed that both of the surfaces had almost the same ice adhesion strength – for superhydrophobic surface they measured ice adhesion strength of 807 kPa (deviation 149 kPa) and for superhydrophilic for 913 kPa (deviation 138 kPa). Their testing was based on thirteen different silicon wafer samples ranging from superhydrophilic to superhydrophobic. The water was frozen into cuvettes and adhesion force was measured

by using force transductor. It was observed that textured surfaces had higher ice adhesion strength than smooth surfaces because of mechanical interlocking between ice and texture, proposed model in the Figure 27. The adhesive strength between ice and substrate as also the cohesive strength, are needed to overcome for the ice to detach from the surface. (Chen et al., 2012)
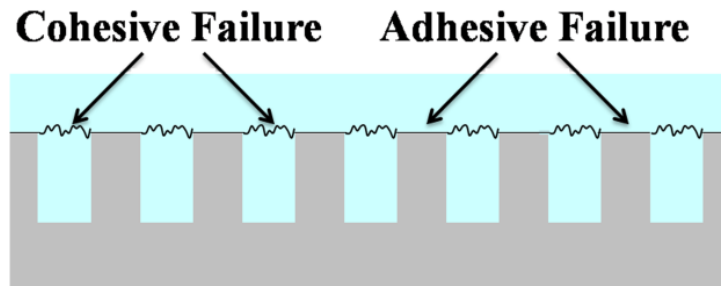
Figure 27. *A Model for ice adhesion failure mechanism. Ice adhesion from the texture has to overcome both, the adhesive strength and the cohesive strength.* (Chen et al., 2012)

In another set of experiments, it was found that ice-repellent properties of superhydrophobic surfaces deteriorated whilst icing cycles. SEM –images revealed that the surface asperities' tips damaged during the cycling, which is demonstrated in Figure 28. Elevated icing strength was believed to be due to an anchoring effect, where water condensates into the rough surface and then freezes. Kulinich et al. concluded that in some cases superhydrophobic surfaces have low abrasion resistance and they cannot withstand all climate conditions, as a result, their ice-repellency can be questioned. (Kulinich et al., 2011) Formation and effects of frost on superhydrophobic surfaces was also recognized and examined by Boreyko and Collier (Boreyko & Collier, 2013). Also studies conducted by Varanasi et al. indicated that on superhydrophobic surfaces, frost formation significantly compromises alleged icephobic properties and therefore, sets limitations on superhydrophobic surfaces usage as icephobic surfaces. (Varanasi et al., 2010)
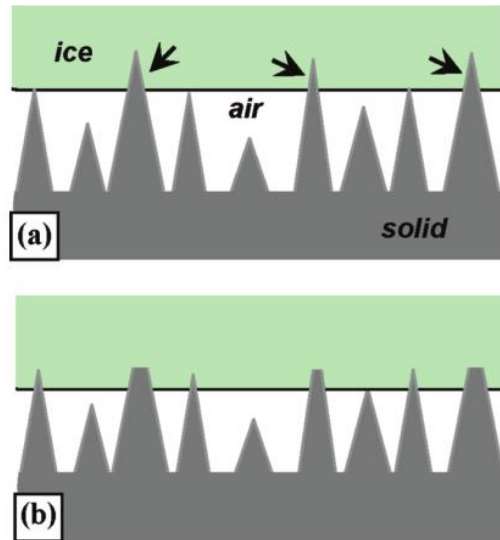
Figure 28. *Superhydrophobic surfaces with ice. (a) Ice accreted on a superhydrophobic surface and the surface asperities are shown to be on the ice. (b)The asperities are damaged during icing or ice accretion resulting in surface deterioration.*

In reference to previous studies, the correlation between superhydrophobic surfaces and ice-repellent behavior is being under debate, as there are some recorded results for superhydrophobic surfaces to have some icephobic features – on the other hand, other studies state to find no correlation in between.

5.3.2 Other approaches

Supercooled aqueous solutions can be lethal for living organisms in biological systems if they nucleate to ice. Due to this, strategies to combat the icing risk occur in the nature. So called anti-freeze proteins (AFPs) consist many families of proteins which can be found in several organisms ranging from insects to fish. In living organisms, AFPs lower the freezing temperature of the blood by mounting up onto the surface of ice to inhibit its further growth, in consequence, these proteins can prevent ice growth, as illustrated in Figure 29. (Duman, 2001; Meister et al., 2013)
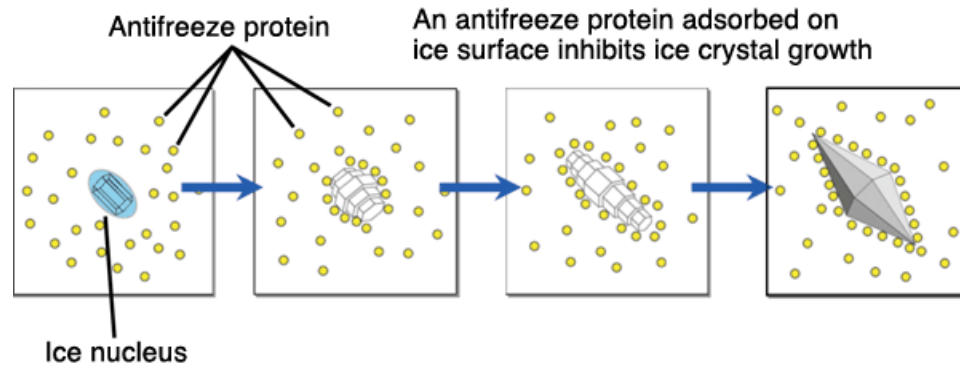
Figure 29. Ice crystal growth is inhibited due to antifreeze protein absorbent. (Kondo, 2012)

It is illustrated by Esser-Kahn et al., that AFPs have successfully been incorporated with polymer chains to make a thin film castable and inexpensive coating material. This novel approach can slower ice growth and also inhibit ice formation. (Esser-Kahn et al., 2010) Albeit, it is stated that the use of AFPs may not provide groundbreaking results for the industries dealing with ice accumulation (Charpentier et al., 2013). Their studying will continue providing more comprehensive understanding of the mechanisms of ice nucleation.

To gain synthetic materials mimicking proteins, AFPs can be imitated by poly(vinyl alcohol) as a means of inhibition of ice-recrystallization. The problem in the authentic AFPs lies in their separation and purification processes, additionally, AFPs have proved to be somewhat challenging to synthetize. (Congdon, et al., 2013; Peltier et al., 2010) Another study showed that ice nucleation process could be decelerated or inhibited by altering poly(vinylalcohol) molecular weight. Congdon et al. employed detailed polymerization process by which polymers structure can be used as a technique to moderate the activity of ice nucleation. In their tests, shortest polymers decreased ice nucleation by 2°C as to longest polymers almost 10°C. (Congdon et al., 2015)

Smart polymers and temperature sensitive polymers could provide an alternative research view for future anti-ice applications. Even though, the morphology change take place in rather high temperatures (25 to 40°C) when compared to freezing, it is prefigure that smart polymers might be developed towards anti-icing characteristics (Lv et al., 2014) Especially, interest has been in poly(N-isopropylacrylamide) polymer (PNIPAAm) which can change the surface morphology at certain temperatures as a result of reversible conformational polymer chain change. (Fu et al., 2004; Sun & Qing, 2011) Additionally, heat storage materials and phase change materials based on alkaline solutions or salt hydrates can release stored latent heat when their phase changes. This idea has also originated from nature, as some plants have ice nucleating agents in their extracellular fluids. Exploiting these phase change materials and their derivatives may be limited to high cost at the time. (Kenisarin & Mahkamov, 2007; Krog et al., 1979)

After investigating these potential future anti-ice materials and methods, anti-freeze-protein based or polymer-based, it is clear that more research is needed to be carried out for developing fully and precisely functioning anti-ice applications based on these.

6. AIM OF THE STUDY

The project scheme was to found, to design and to manufacture advanced liquid-infused surfaces. These surfaces could be attached to almost any solid surface to prevent the formation of ice and its adhesion to the applications and machines. This is thought to improve safety and to guarantee continuous industrial operation as to ensure flowing logistics in the global Arctic areas.

The main goal is to gain surfaces to tackle ice formation and adhesion but SLIPS could possibly be used in a broad range of applications in many fields of engineering, as said especially in self-cleaning, anti-fouling and low friction demands.

As stated by The Finnish Arctic strategy: 'Finland is an active player, capable of sustainable co-ordination of the constraints set by the Arctic conditions' (Finland's Prime Minister's Office, 2013). Consequently, this research is in the line with the strategy as the main objective is to design and develop high-performance SLIPS to prevent unwanted icing.

This thesis is a part of Roll-to-roll fabrication of advanced slippery liquid-infused porous surfaces for anti-icing applications (ROLLIPS) project under TEKES' Arktiset meret -program. Academic research partners consist of Tampere University of Technology's Laboratory of Paper Converting and Packaging Technology in Department of Materials Science, Laboratory of Surface Engineering in Department of Materials Science and Aerosol Physics Laboratory in Department of Physics. In addition, SP Technical Research Institute of Sweden's Department of Chemistry, Materials and Surfaces is collaborating in the program.

7. EXPERIMENTAL PROCEDURES

Before any testing could be performed, it was needed to fabricate the desired SLIPS - structures from obtained materials. After careful sample preparation, the testing was conducted by first observing the evaporation and wetting of the SLIPS -samples as a function of time. After these experiments, further investigations were performed in icing conditions by conducting cyclic ice adhesion testing. By mimicking natural outdoor ice accretion, as to spraying supercooled water droplets onto surface, the technique is expected to be the most reliable method when evaluating the adhesion between ice and solid. (Kulinich & Farzaneh, 2009b)

As to icing wind tunnel and sprayed supercooled drops, important information on the meteorological effects and input parameters on laboratory scale have been carried out by Stenroos (2015) and Ruohomaa (2014) as to these kinds of freezing information have had relatively less efforts (Farzaneh, 2008 pp.1-30) By their work, the parameters for the icing tests were set to fit the tests conducted in this thesis. Besides of the evaporation, wetting and ice adhesion measurements, the optical transparency of the SLIPS was recorded.

7.1 Methods and materials

PTFE –membranes used in this study to fabricate slippery liquid infused porous surfaces were acquired from two different suppliers, M1 and M2. The membranes were chosen by their pore size to match each other, though, the membranes were different by their thickness and by their supporting material as gathered in Table 5. Supplier M1's membranes were made completely from PTFE without any supporting material or structures, whereas supplier M2's membranes had a supporting texture behind the PTFE film. The membranes' size was 47 mm in diameter in every case.

Table 5. *Comparison of the membranes used in the experiments, their type, thickness and pore sizes.*

Membrane	Membrane type	Thickness (µm)	Pore sizes (µm)
M1	Full PTFE	25 – 250	0.2, 1.0, 5.0
M2	PTFE with supporting material	150	0.2, 1.0, 3.0

Two different liquid lubricant types were used in impregnation of the porous solid and were obtained from two different suppliers, L1 and L2. The viscosities varied between the lubricants, as shown in the Table 6, from low to high viscosity. However, there are minute differences in viscosity between the two most viscosius oils. Advisely, it was needed to gain information on both type of lubricants used in the experiments.

Table 6. *The lubricants used in the experiments and their viscosity.*

Lubricant	Viscosity
L1	low medium high
L2	low medium high

7.1.1 Preparation of slippery liquid infused porous surface samples

All the glassware used in the experiments were acid washed in 10% NaCl in order to eliminate impurities interfering the test. At any point, the membranes were handled with tweezers, to sustain their purity before impregnation and measurements.

For the impregnation process, five Whatman chromatography papers No 1 were placed into glass petri dish. On to the papers ca. 5 ml of appropriate lubricant was pipetted and the filter papers were let to soak into the lubricant for 24 hours. After complete infiltration of the filter papers, the PTFE membrane was placed onto the moist filter paper and was let to impregnate for ca. 5 minutes. In this time, the membrane attracted as much the lubricant as the structure was able to retain. The lubricant impregnated porous membranes were ready to be placed onto either metal substrate or glass substrate depending on the further examination.

7.1.2 Evaporation tests

The infiltrated membranes were placed onto glass substrate, VWR Microscope slides, for evaporation tests. The loss of lubricant from the surface by evaporation was observed in a conditioned room with ambient temperature +23°C and relative humidity of 50%. For evaporation tests three parallel samples were prepared for each lubricant/porous solid combination. The evaporation test was carried out for three months, whilst recording the changes of contact angle, hysteresis and sliding angle of the evaporation test samples.

7.1.3 Contact angle, hysteresis and sliding angle measurements

Water contact angle, hysteresis and sliding angle measurements were executed by using KSV CAM200 equipment supplied by KSV Instruments Oy, Finland. All the measurements were performed in a conditioned room with ambient conditions of 23°C as relative humidity was 50%. Grade of water used in the experiments was ultrapure from MilliQ -system.

For contact angle measurements, three seconds was awaited after placing 5 µl droplet onto the examined surface to gain steadiness of the water droplet. At least five parallel samples were recorded from each studied surface. Hysteresis was measured from the same parallel samples as in sliding angle measurements. Sliding angle was determined from three different droplets of 10 µl, from which three recordings were taken from the same drop. Droplets were placed on a levelled plane which after the plane was slowly and gradually tilted manually. The recordings were made with a camera taking pictures as the droplet started to slide off from the tilted plane. Pictures of the taken wettability tests are shown in Figure 30.
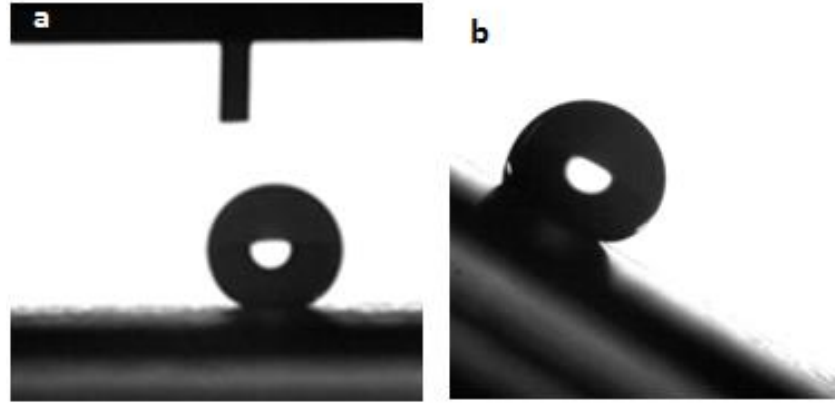
Figure 30. *Illustrations of wettability testing. (a) Static water contact angle and the injection needle above the droplet. The tested surface is from supplier M2 with 3.0 μm pore size and the water contact angle is 158°. (b) Sliding angle measurement on a tilted plane. Tested membrane was obtained from supplier M1 with 5.0 μm pore size and the sliding angle is around 30.5°.*

## 7.1.4 Accretion of ice and ice adhesion measurements

For ice accretion and ice adhesion measurements, tested samples were masked into 30 mm x 30 mm area on metallic substrate, seen in Figure 31. The substrate with tested surface is attached in composite blade and the blades are fastened under the icing wind tunnel. Tested surfaces were held at the climate room from 30 to 60 minutes before accreting ice on them in order to cool the specimen entirely to the climate room's temperature.

Figure 31. *The unmasked SLIPS samples on a metallic substrate ready for masking and cyclic icing test.*

The icing wind tunnel used in the experiments, has been described in the most detailed way elsewhere (Ruohomaa, 2014). The system, depicted in Figure 32, is established in climatic room in order to maintain desired icing conditions as temperature conditions as low as -40°C can be achieved. By altering icing parameters, glaze, rime and mixed ice

can be accreted onto samples, however, mixed ice was used in the tests as it is commonly used in TUT's icing laboratory as standard ice (Stenroos, 2015).
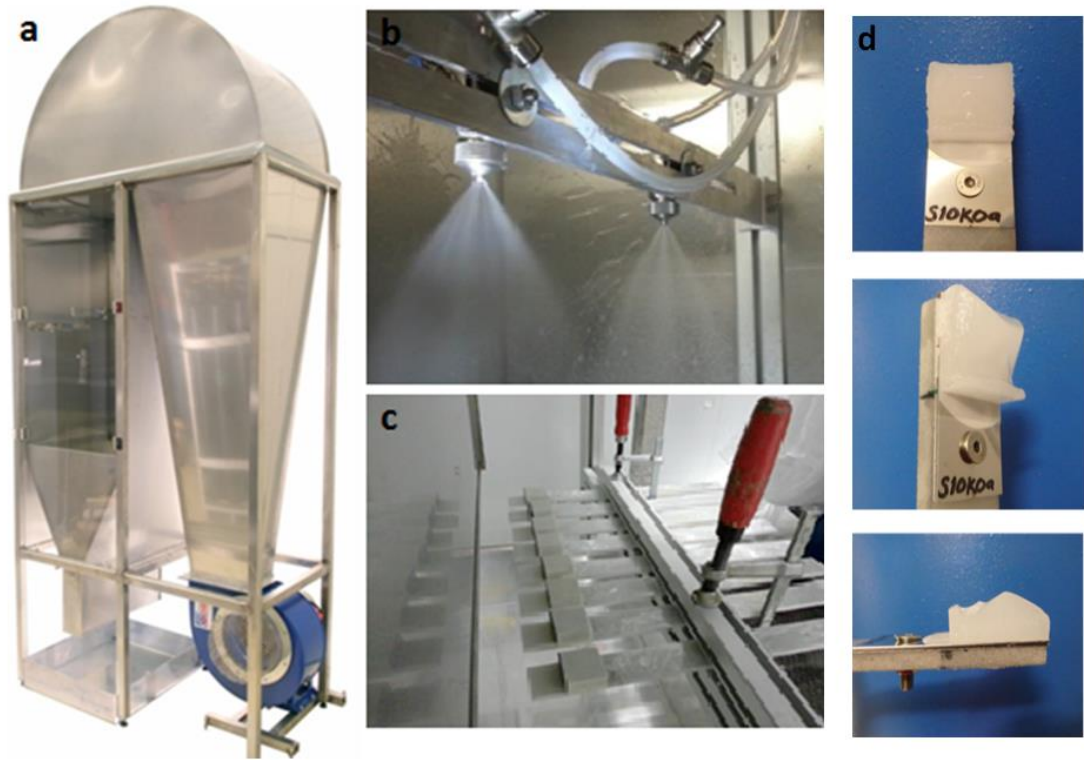
Figure 32. *The icing wind tunnel and ice accretion. (a) The wind tunnel. (b) The spray nozzles. (c) Masked samples on composite blades. (d) Accreted ice on a tested surface after mask removal.*

The airflow is generated by centrifugal fan (Suomen Imurikeskus) and directed past a nozzle spray system (Spray Systems ¼ J+SU12) which after the supercooled water drops can impact on a given substrate. Ultrapure water was used to generate the accreted ice. Other ice accretion parameters are shown in Table 7. Within the icing laboratory of TUT, mixed ice has commonly been used in the ice adhesion tests even though, pure glace and rime ice can be produced in the wind icing tunnel. Disciplined testing on icing conditions has been examined earlier (Stenroos, 2015) by which the parameters have been enabled.

Table 7.   *Ice accretion test parameters used in the studies.*

Parameter	Value
Wind speed	ca. 25 m/s
Water temperature	5.8 to 6.7°C
Room temperature	-9.0 to -11.0°C
Relative humidity	70 to 80%
Water pressure	3.0 to 3.4 bar
Average droplet size	ca. 30 – 31 µm

After ice accretion, the iced samples were let to ice in climate room for ca. 16 hours (+/-2 hours) before ice adhesion testing. In this time the ice accreted onto the surface was frozen and ready to be tested. After every icing / ice adhesion measurement cycle, the surfaces' wetting properties were tested by measuring the static contact angle, contact angle hysteresis and sliding angle in the same way as described earlier.

Ice adhesion testing based on centrifugal force (Laforte & Beisswenger, 2005; Ruohomaa, 2014) was carried out after samples were iced and stabilized in climate room. The ice accreted, and weight balanced, samples on a blade were attached into the machine one by one as they were rotated with increasing acceleration until ice adhesion was observed by acceleration sensor. The centrifugal force accelerator is seen in Figure 33.

Figure 33.   *The centrifugal ice adhesion test machine with a sample to be tested inside.*

Within the test, four parallel samples were tested and from them the ice adhesion strength was calculated within every four icing cycles. As a reference sample Teflon tape from 3M was used. The samples on the blade were weighted before and after the ice adhesion in order to gain the mass of the ice on the surface. The RPM value is given at the moment of ice releasement from the surface as a result angular velocity is been

calculated. The rotation's radius (17 cm) stays constant within the test, but exact value for ice detachment is calculated, ca. 300 mm x 300 mm, after the rotation. Consequently, the maximum adhesive shear stress is calculated as the area of ice adhesion and the release point's rotation speed are recorded. Thus, by using Equations 6 and 7 the shear stress for the ice attachment can be calculated: in Equation 6 the centrifugal force F is composed as:

$$F = mr\omega^2 \tag{6}$$

where m is the mass, r the radius of rotation and ω angular velocity. After solving the centrifugal force F, it is possible to calculate the shear stress τ by Equation 7:

$$\tau = \frac{F}{A} \tag{7}$$

in which the centrifugal force F is divided by the area of detached ice A.

8. RESULTS AND DISCUSSION

The evaluation of fabricated SLIPS was based on not only gravimetric analysis and wettability measurements, such as static contact angle, hysteresis and sliding angle, but also examining the ice adhesion of the surfaces in cyclic ice adhesion tests. It was needed to examine, whether the SLIPS fabricated from commercial materials, could function as anti-ice or ice-repellent surfaces.

It was recognized that PTFE –membranes were indeed wetted by both of the studied lubricants. However, in the preliminary tests, it was discovered that paraffin oil did not penetrate to the PTFE -membrane but stayed as a droplet onto the membranes. After fabricating the SLIPS, as introducing the lubricant into the porous membrane, the properties of the SLIPS were studied in a series of experiments. First, it was relevant to figure out how quickly the lubricant would be evaporated from the membrane, in another words, how long-lasting the SLIPS would be in the room temperature. As the vaporization was tested, the wetting behavior was also recorded in the same time points. The evaporation and wettability studies for this thesis lasted for 95 days, as the weight loss of the lubricant from the membrane was examined with the wetting behavior. After gathering the data about lubricant vaporization and its effects on SLIPS wetting, cyclic ice testing was performed to the most interesting surfaces. The icing tests were performed in four cycles and after every cycle the wetting behavior was examined by measuring the static contact angle, contact angle hysteresis and sliding angle from the tested surfaces.

8.1 Evaporation and wetting behavior

All the lubricant and membrane combinations, SLIPS, are presented in Table 8 consisting of 21 different samples. Moreover, the plain PTFE –membranes without any lubricant, were also tested to gain information on the effects of lubricant impregnated to the membrane.

Table 8. *The tested membrane (M) and lubricant (L) combinations for evaporation and wetting behavior tests. The pore size of the membrane is depicted after the supplier code as are the viscosities of the lubricants.*

	No oil	L1-low	L1-med	L1-high	L2-low	L2-low	L2-high
M1-0.2	x	x	x	x	x	x	x
M1-1.0	x	x	x	x	x	x	x
M1-5.0	x	x	x	x	x	x	x
M2-0.2	x		x				
M2-1.0	x		x				
M2-3.0	x		x				

All the data collected within 95 days is presented in Figure 34 where the percentual weight loss is given in vertical axis. The samples' 100% lubricant rate was weighted 10 minutes after sample preparation, hence the lubricant amount being full 100%. In general, it is noteworthy to observe that a great number of samples hold the lubricant within them after the three months of period. In a majority of SLIPS, the lubricant evaporation is under 10% as seen from the Figure 34. As hypothesized, the lubricants having low viscosity did vaporize from the membranes more rapidly than more viscous lubricants.
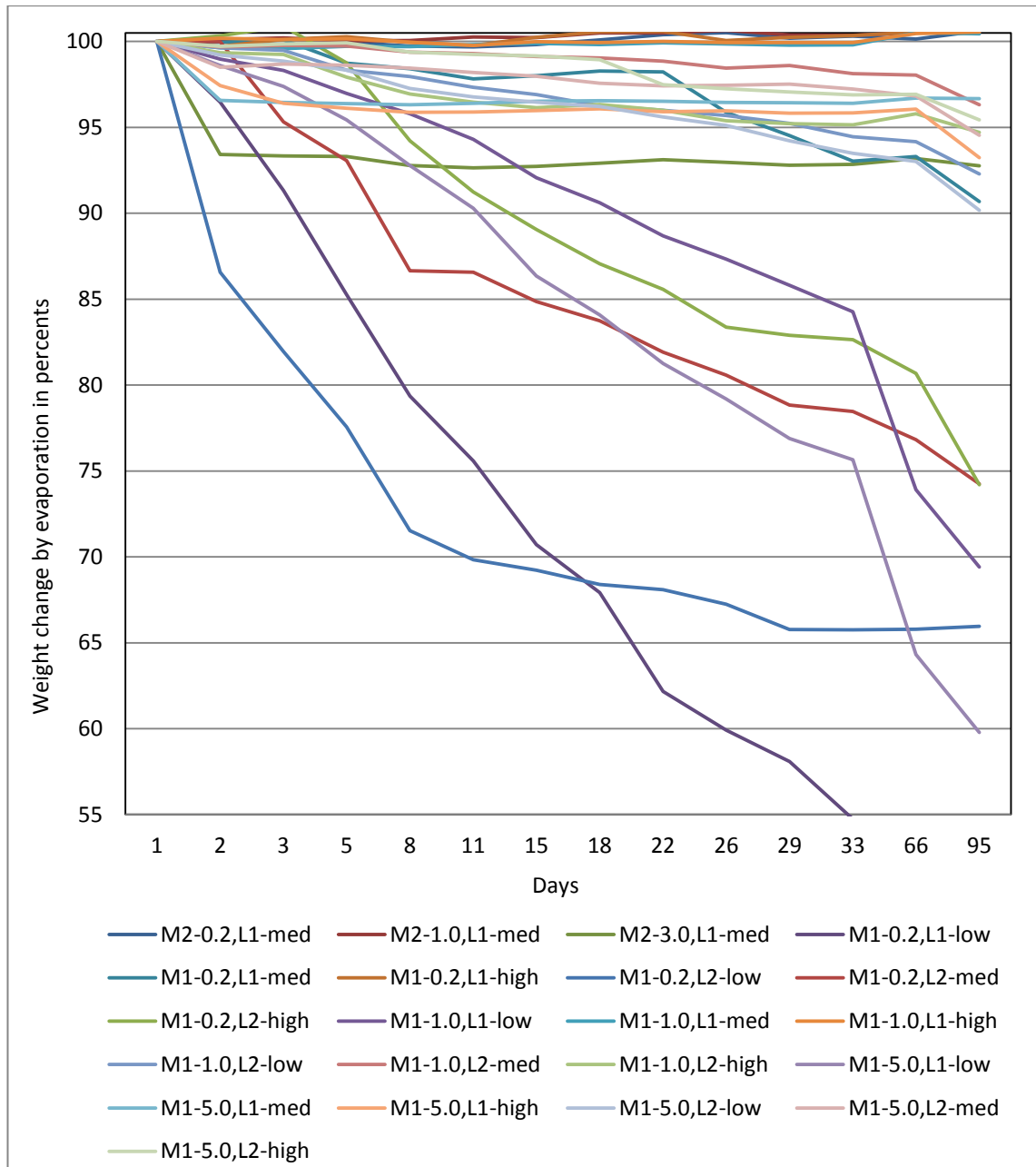
Figure 34. *Lubricant evaporation rates, from two different PTFE –membranes (M1 and M2), in percents as a function of time, 95 days.*

In some of the cases, the sudden decline after the first day can be explained by the fact that in a few lubricant/membrane combinations, or SLIPS, the lubricant did not have as good affinity as in other combinations. Some amount of lubricant was leaked from the PTFE –membrane after first days. It is assumed, that this is due to poorer affinity, but also the possibility of excess lubricant absorption to the membrane has to be taken into consideration. Especially when examining the six most reclining samples, it is seen that three of them are M1-0.2 membranes with supplier L2's oils and the other three L1-low lubricants with M1's membranes. Since the viscosity of L1-low lubricant was the lowest of any lubricants tested here, it can be concluded that the steady and somewhat linear

decrease in lubricant amount in the structure is due to vaporization. Moreover, it was observed with the naked eye that these membranes lost their transparency as the lubricant loss was observed. This would support the hypothesis that the lubricant was indeed mainly evaporated from any of the microporous structures of M1's 0.2, 1.0 or 5.0 µm pore size membranes. As seen from the Figure 34, the M1's pore size 0.2 µm with L1-high lubricant was one of the SLIPS combinations to lose the least amount of lubricant since the curve stays constantly around 100%.

The reasoning why M1-0.2 membranes lost such a great amount of L2's lubricant in the test period is not as obvious. These membranes had the smallest pores is the structure but also were the thinnest of the tested membranes – only 25 µm in thickness. The affinity factor is likely to be part of the mystery, since from the same membranes the L1 lubricants did not vaporize at the same rate than the L2 oils. More testing is needed to perform in order to reveal the properties of L2 oils' and PTFE –membranes' interchemistry.

The water contact angles for unimpregnated PTFE –membranes are shown in Table 9. All of the membranes express extreme hydrophobic nature and almost all of them could be classified as superhydrophobic, as the water contact angle is above 150°. In M2's membranes, the contact angle seems to enhance as the pore size grows, however, the same linear increase cannot be seen in M1's membranes.

Table 9.   *The static contact angles of plain PTFE –membranes in degrees.The pore size is given after the supplier code M1 or M2.*

	Static contact angle in degrees
M2-0.2	146,1
M2-1.0	153,4
M2-3.0	158,0
M1-0.2	150,2
M1-1.0	154,2
M1-5.0	147,7

In static contact angles, it is clear from the Figure 35 that L2's oils do have a lower static water contact angle than L1's lubricants. From the first days' results it can be seen that L2's oils water contact angle seems to be around 103 to 108°, depending on the viscosity, as in L1's oils the static contact angle varies more, from 114° to 121°. In L2's oils, the static contact angle stayed steady from the first days towards three months' time. There are some variations in the contact angle results but still the variations tend to stay within 5 degrees in the L2 oil impregnated SLIPS -samples.
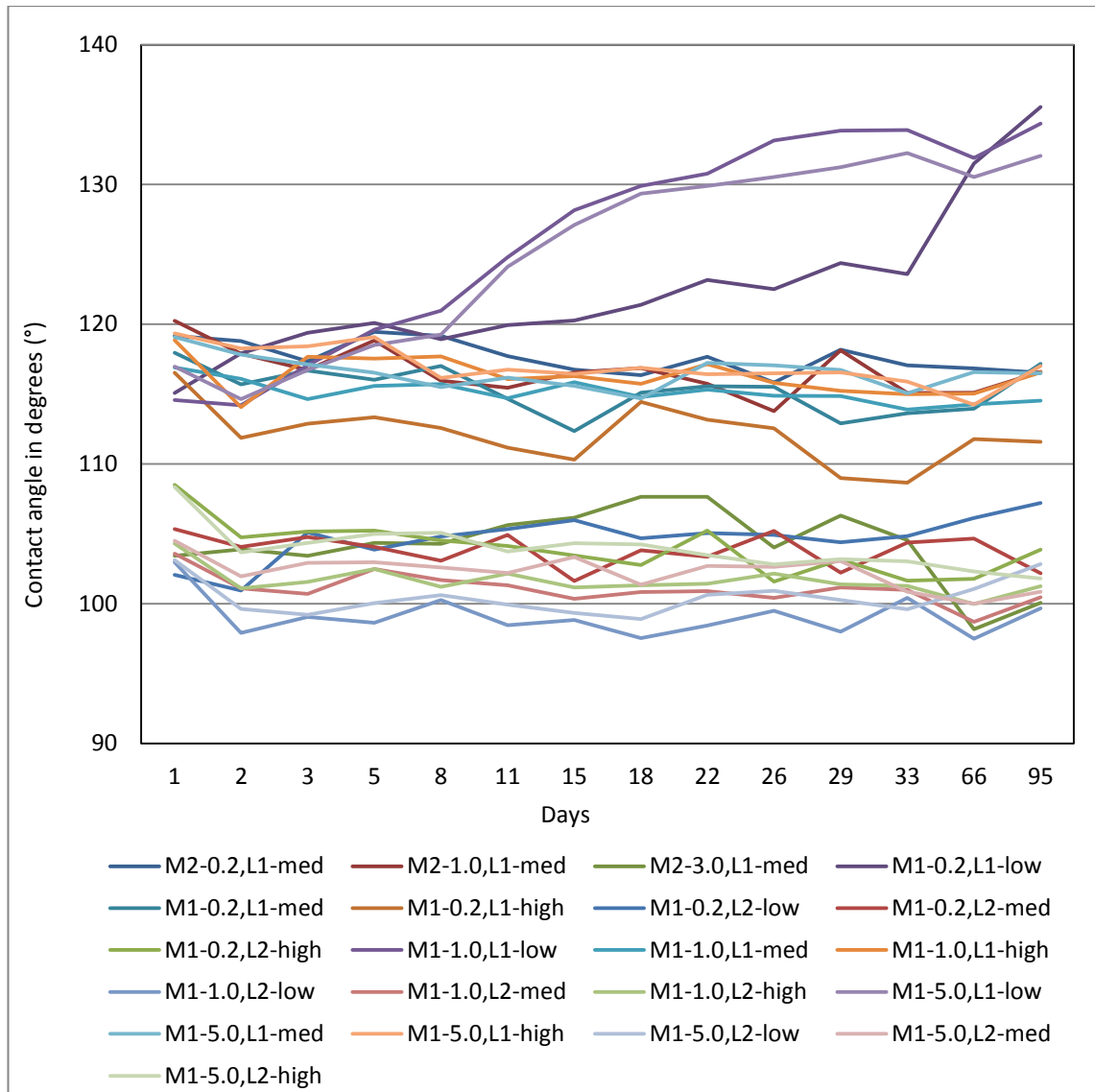
Figure 35. *Water contact angle results of all the tested samples as a function of time, 95 days.*

In L1's oils, it would seem that the static contact angle depresses as time passes. In most cases the L1's oils had few degrees higher contact angle in the first days than after three months. Though, there are three exceptions. In the case of L1-low lubricant, the vaporization from the porous solid made the contact angle to increase. It is likely that the contact angle of these samples would rise as elevated as in dry reference samples where no lubricant was introduced.

As said, L1-low lubricant impregnated samples with membranes of M1's 0.2, 1.0 and 5.0 μm pore sizes have ascending curve due to vaporization of more viscous lubricant. Other L1's oil impregnated membranes had more constant contact angle behavior through the tested period, as Figure 36 shows. More close examination of the L1 impregnated SLIPS shows that water contact angle stays relatively even within the test,

excluding L1-low saturated samples. This shows that the affinity between the lubricant and the membrane stays constant throughout the test and that the hydrophobic properties of the gained SLIPS do not deteoriate within three months in room temperature, that is, the surface maintains its water-repellent features.
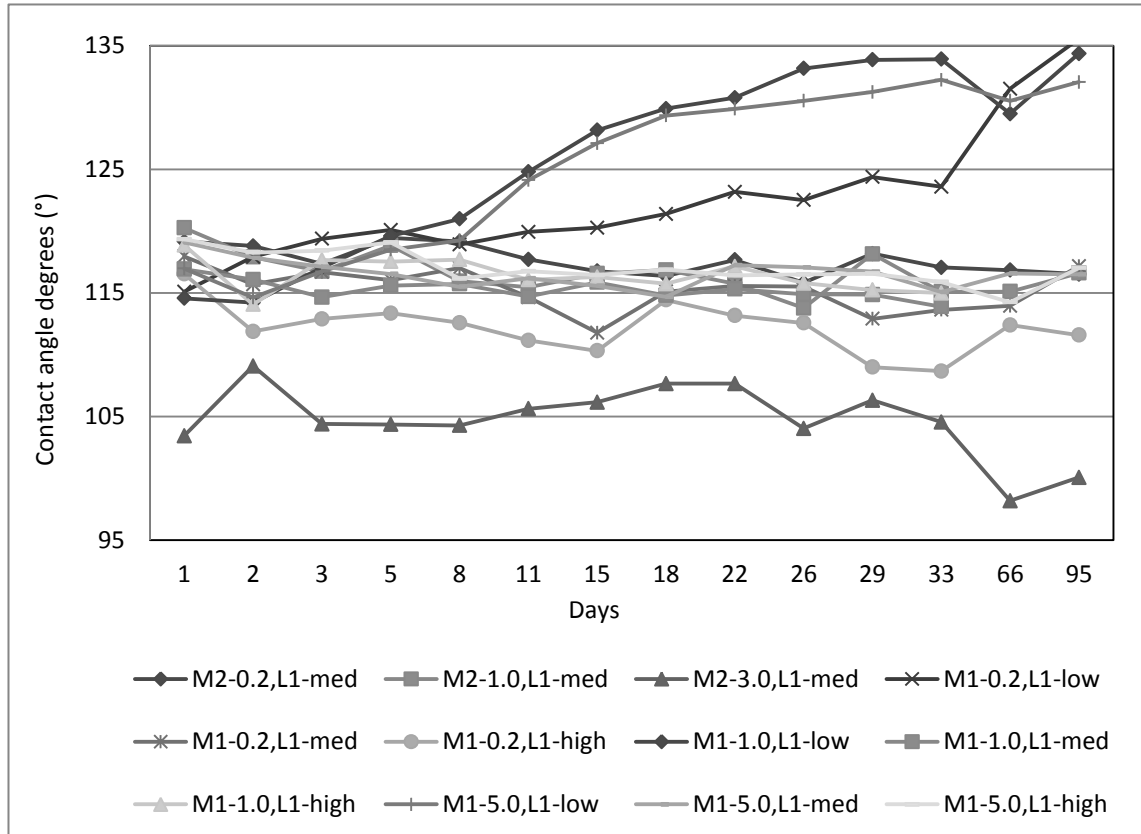

Figure 36. *Contact angles of L1 lubricant impregnated PTFE –membranes as a function of time, 95 days.*

As depicted in Figure 37, the L2's lubricant contained SLIPS samples had quite low and steady water contact angles throughout the tested time, 95 days. There were only small variations between the measurement points, fewer than 5 degrees within a sample. Also the lowest L2's oil impregnated sample, M1-1.0 with L2-low lubricant, had static water contact angle of 97.5° as the highest sample, M1-0.2 with L2-low lubricant, was only around 10° degrees higher, contact angle being 108.4°. Therefore, when investigating supplier L2's impregnated samples by static water contact angle, no significant dissimilarity can be found neither between the different viscous lubricants nor with the membrane pore sizes.
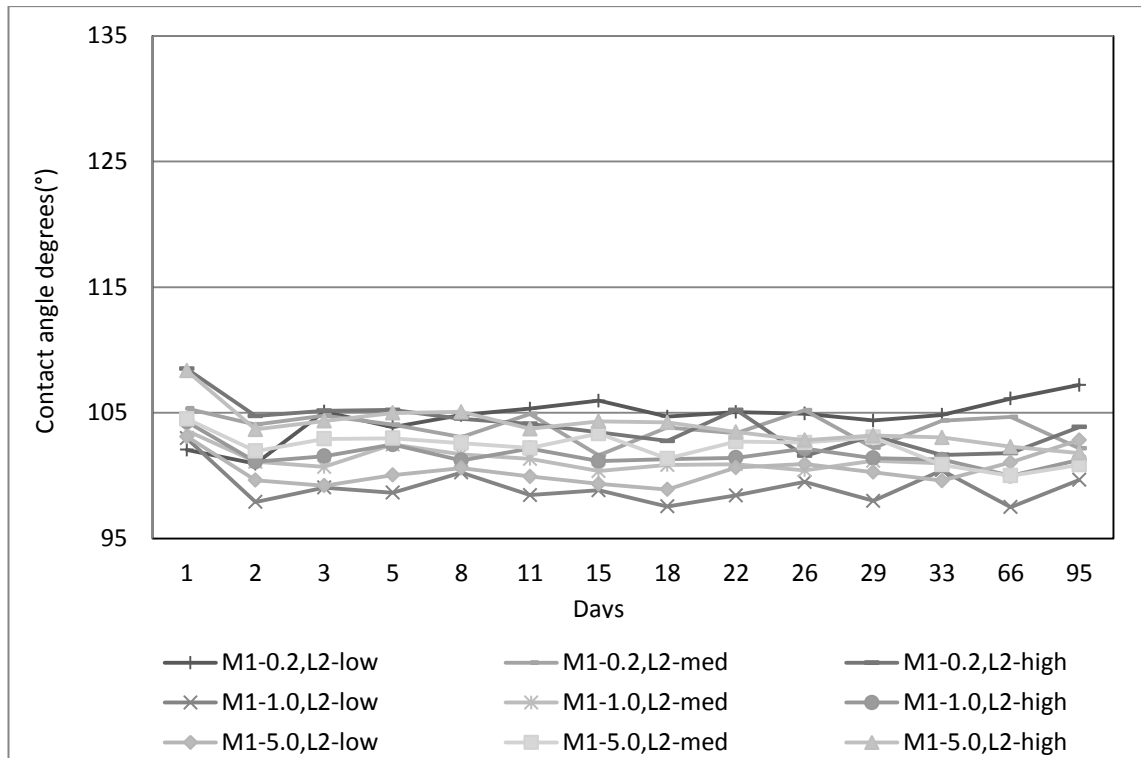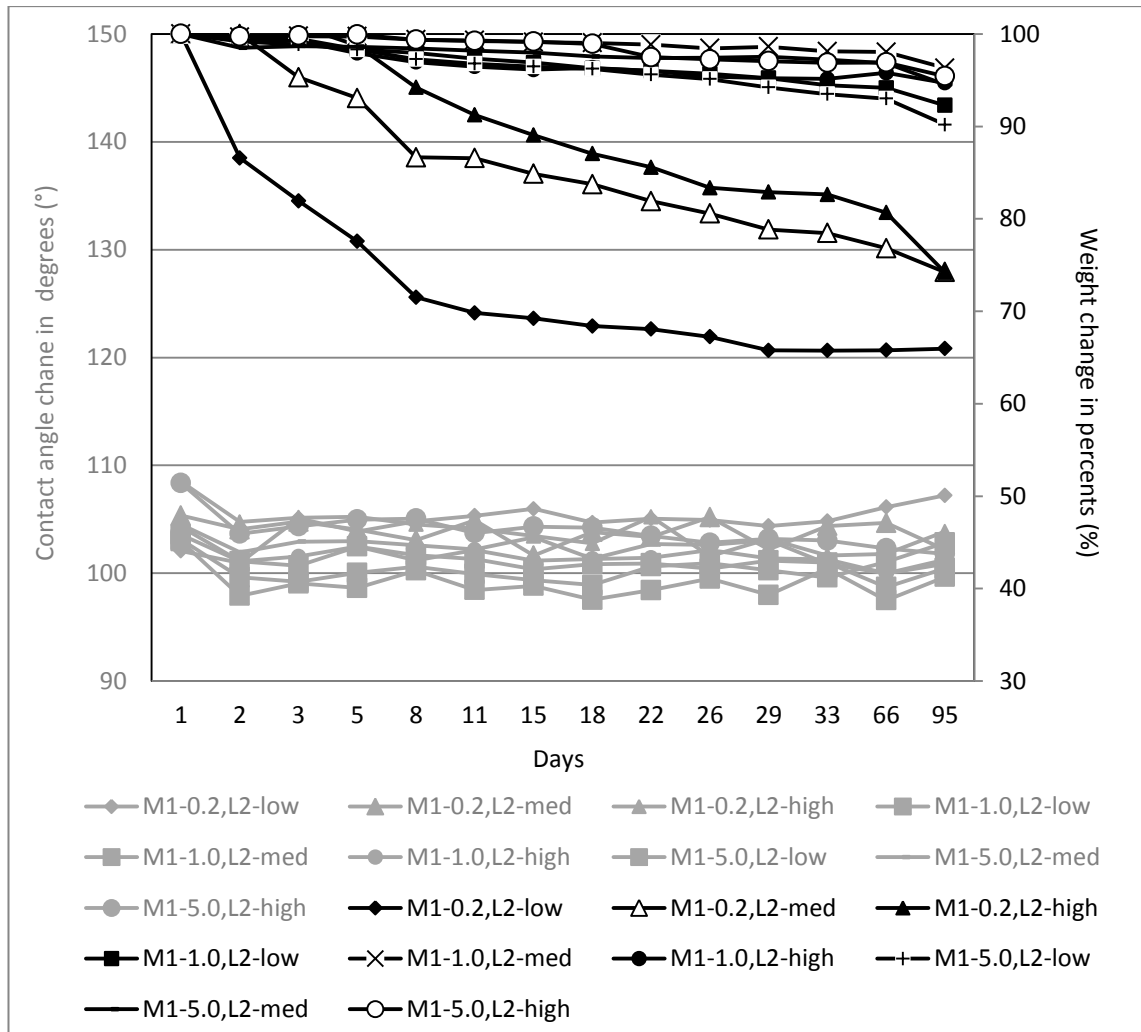
Figure 37. *The contact angle values of L2's lubricants as a function of time, 95 days.*

In Figure 38, it is illustrated how significant relevance the evaporization had towards altering water contact angle. As the L1-low lubricant had the most elevated evaporization, the contact angles started to arise. This could be explained by lubricant evaporization – as the lubricant vanished from the SLIPS, the water contact angle started to shift towards the water contact angle of totally dry membrane's value, collected to Table 8. These three samples, M1's membranes with L1-low lubricant, were the most dissipated combinations. Hence, the usage of L1-low lubricant is needed to take into consideration as the lubricant evaporates in the normal room temperature quite rapidly – after two weeks of period, almost 10% of the lubricant was lost. The viscous lubricant seems to vaporize more gradually from the M1-0.2 membrane, yet, this membrane was also the thinnest of all the studied membranes. The thinness of the membrane might be one reason to cause the lubricant to evaporate from the structure more easily and rapidly.
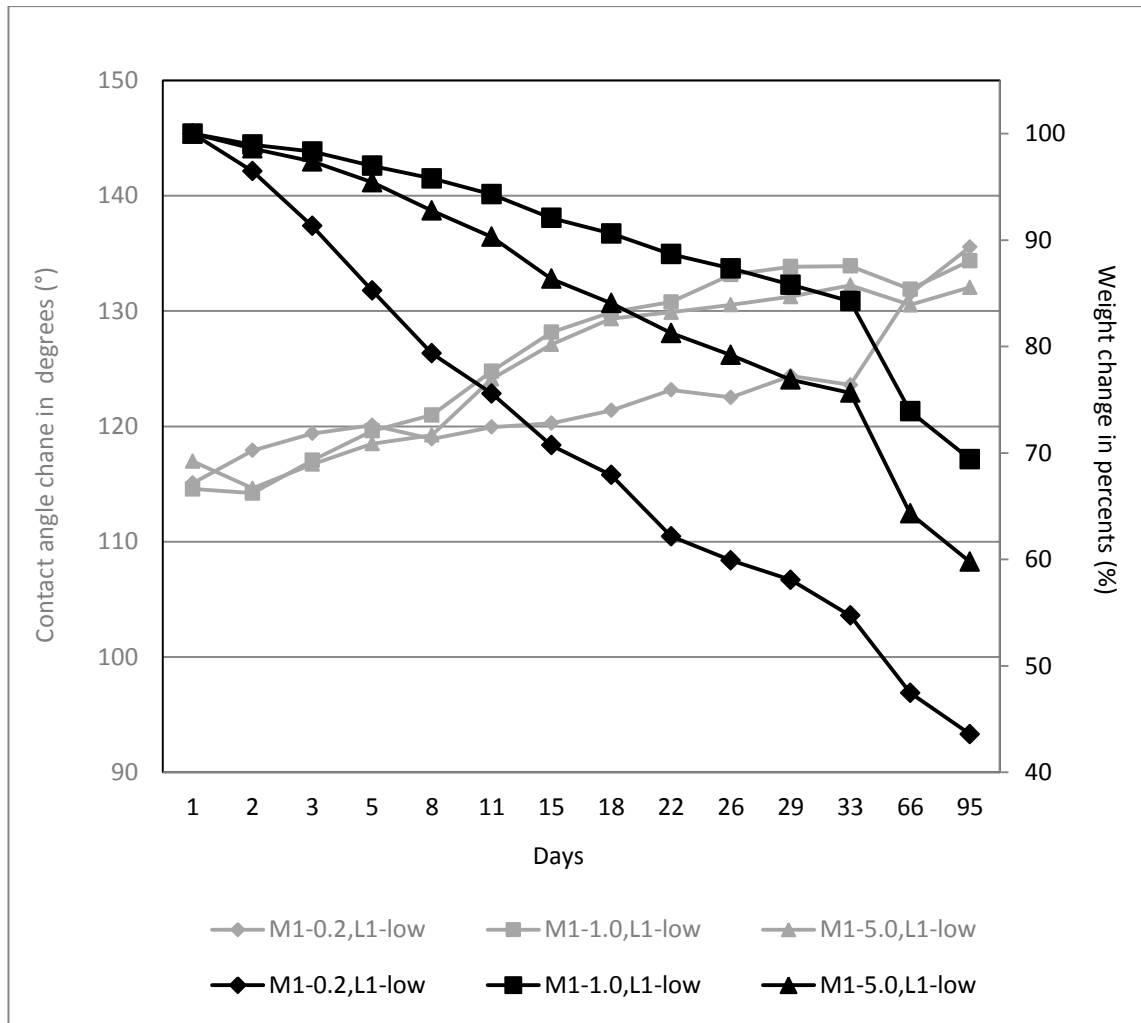
Figure 38. *The contact angle values (grey dots) fitted with evaporation rates (black dots) in percents. L1-low lubricants showing relatively fast evaporation and contact angle increase.*

Figure 39 illustrates the L2 impregnated membranes water contact angle and evaporation as a function of the three months' time. From the Figure 39, it is somewhat clear that the evaporation did not have major effects on the contact angle alterations. The three samples, which showed decline in contact angles', most likely lost their lubricant from the structure due to poor affinity towards the membrane. For some reason, the L2's oils did not perform well in the M1-0.2 porous membranes. L1-low lubricant impregnated SLIPS lost their mass as did the L2's oil infused samples in the M1-0.2 membrane.

Figure 39. *The contact angle values (grey dots) fitted with evaporation rates (black dots) in percents. Supplier L2's lubricant impregnated SLIPS samples showing some amount of lubricant loss but yet steady contact angle values.*

Hysteresis was experimented not only to depict wetting, but also to cyclic icing tests for correlation examination as hysteresis can have some effects on ice adhesion. It has been proposed that low hysteresis of the surface might yield low ice adhesion due to low solid-ice contact area (Kim et al., 2012; Kulinich & Farzaneh, 2009a) This would indicate that only a small amount of force is needed to get the droplet slide off or detach from the SLIPS. The contact angle hysteresis results have been divided between the lubricants into two figures, Figure 40 and 41, moreover, from the Appendix A all the samples and their hysteresis results can be seen in one figure.

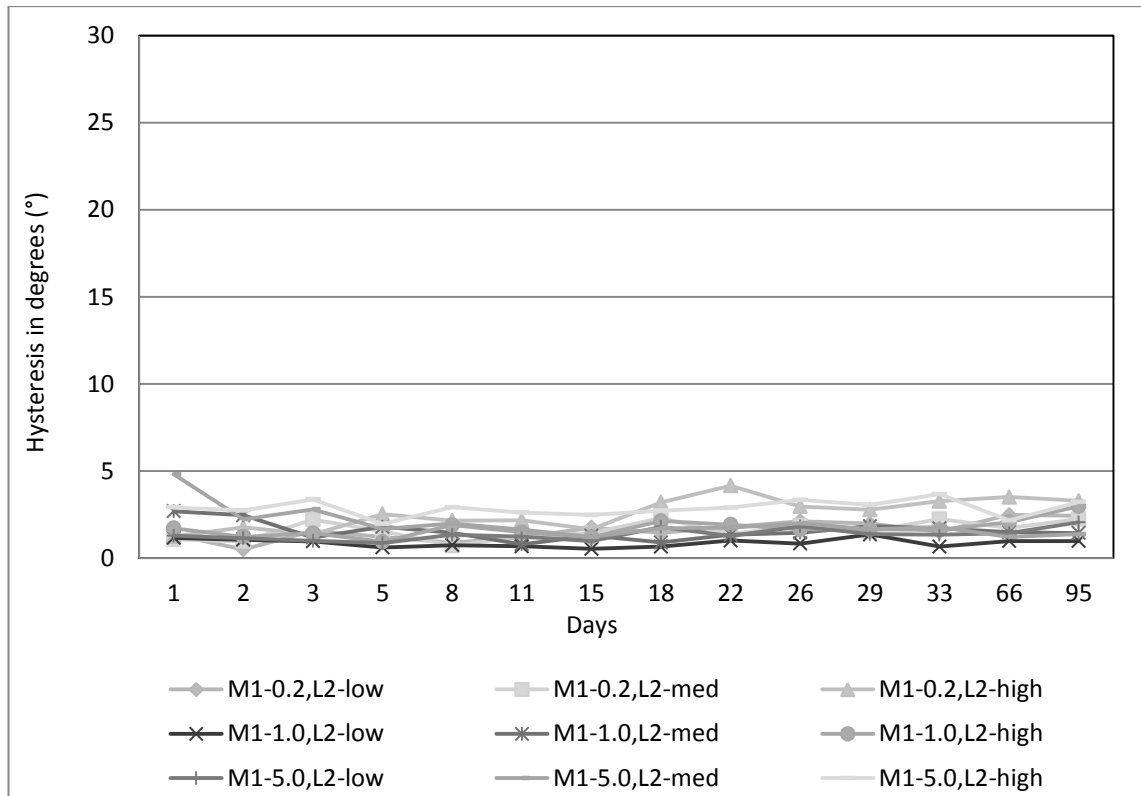The supplier L1's lubricant impregnated SLIPS samples had relatively low hysteresis throughout the tested three months' period showing the hysteresis of 5 degrees or less. For the three considerably differing samples, which arise clearly after two or three weeks, the hysteresis increased. These are the same three samples whose water contact angle also arose due to lubricant lost, L1-low lubricant impregnated samples. For the

same reason, lubricant lost due to evaporation, the hysteresis also upgraded, as seen in Figure 40. The records for L1-low lubricant impregnated samples stop after 33 days as the hysteresis increased beyond measurement range. In the case of hysteresis, the membrane pore size showed no importance to the matter. Likewise, the are no clear differences between medium viscosity lubricants and high viscosity lubricants.
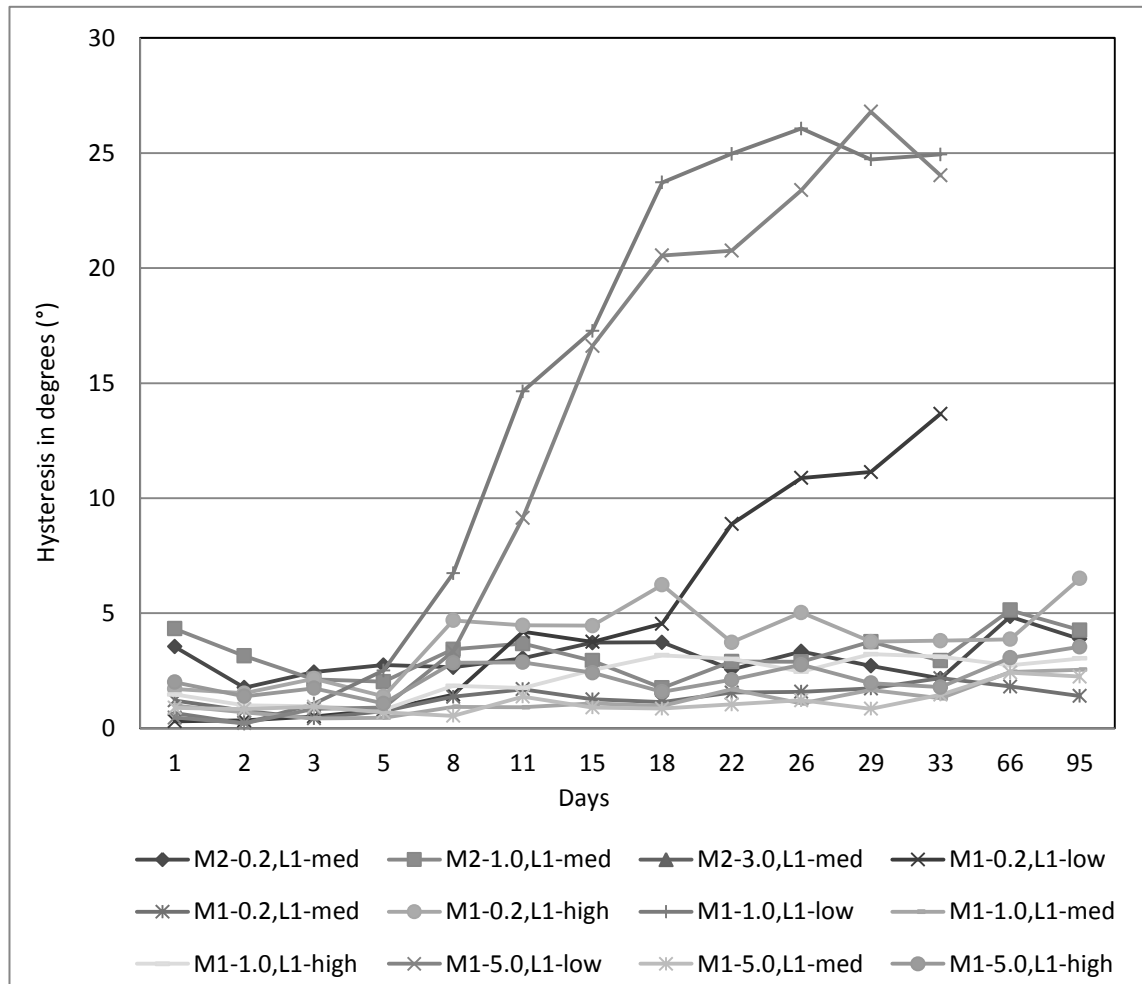
Figure 40. *The contact angle hysteresis of supplier L1's lubricant impregnated samples.*

It was an encouraging result that in the tests, supplier L2's oils impregnated SLIPS had as low hysteresis as the supplier L1's lubricants, since different lubricant are ought to be used in various of end-products. In some cases the hysteresis of L2 lubricant infused membranes seems to be even a few degrees lower than in L1 lubricants. Altogether, the hysteresis results gained from both lubricants are relatively low, showing no correlation to membrane pore sizes.

Figure 41. *The contact angle hysteresis of supplier L2's lubricant impregnated PTFE -membranes.*

Sliding angle depicts the droplets ability to slide off from the surface as the sliding angle is the smallest degree in which the droplet starts to move on the surface (Callies & Quéré, 2005). In all the tested samples, the sliding angles arose from the freshly fabricated SLIPS' sliding angle. The increase in sliding angle over time is consequence of few factors: the vaporization of the lubricant but also the contamination of the surfaces. The surfaces were kept in an ambient temperature room, nonetheless, there are dust and dirt present in the room. It was observed after some period of time, the dust and fibers were present on the SLIPS hence altering the surface chemistry and offering pinning sites for the droplets. These are the challenges needed to tackle, as represented in chapter 4.3.

Yet again the SLIPS samples with L1-low lubricant started to differ from the mainstream of other samples, showed in Figure 42. As the lubricant evaporated from these three, there were more pinning sites in the porous surface to drops to stick. By the tilting component used, it was not possible to detect sliding angles over 40 degrees hence there are no recordings of L1-low lubricant impregnated samples as to in sliding angle or hysteresis after a month. The data shows no clear correlation between sliding angle and pore sizes studied in the thesis.
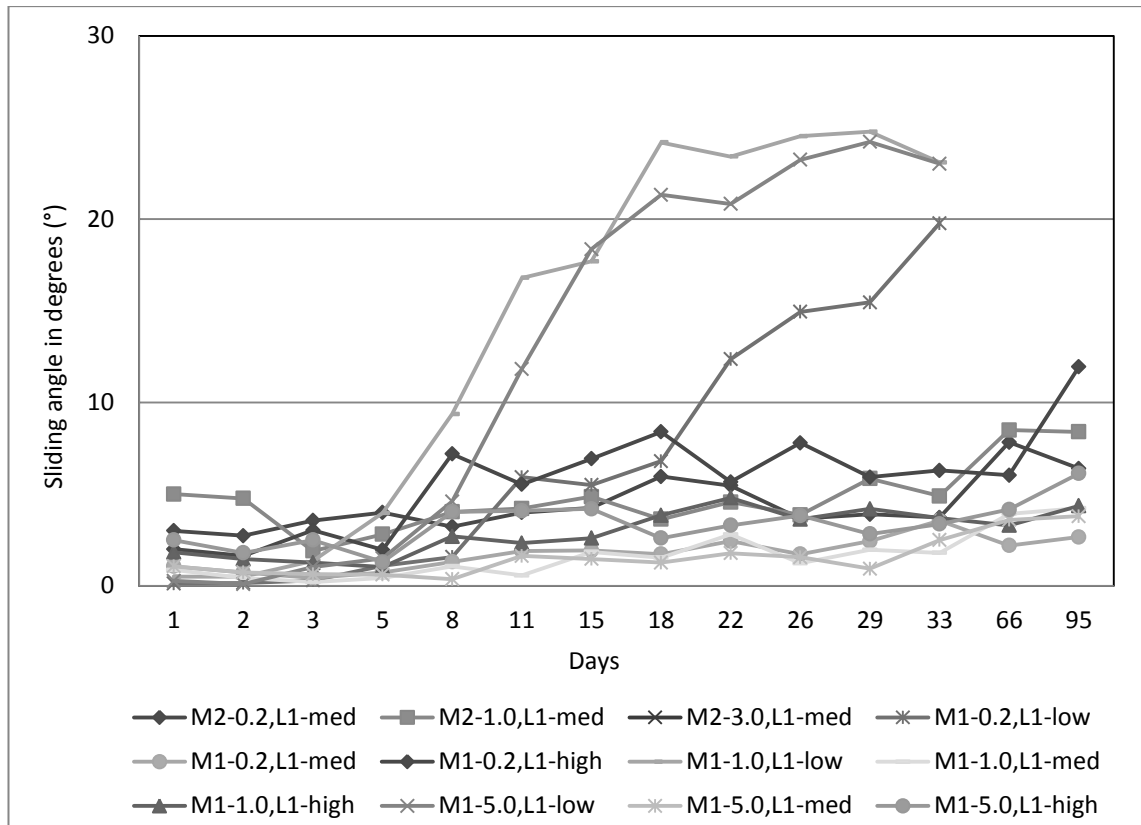
Figure 42. *The sliding angle of supplier L1's lubricants impregnated PTFE – membranes.*

As the hysteresis of supplier L2's oil SLIPS, the sliding angle was also rather steady and relatively low, as seen in Figure 43. Some increase in the sliding angle might be seen during the three months but the elevation of few degrees could also be explained by standard deviation. Though, the pinning effect of droplets is to be expected as the surfaces tend to gather some dust on them not forgetting the effect of evaporation to pinning sites. Supplier L2's oil SLIPS had sliding angle under 6° throughout the test. Same kind of low hysteresis results (ca. 2°) have been acknowledged elsewhere for other liquid infused surfaces as well (Manna & Lynn, 2015).
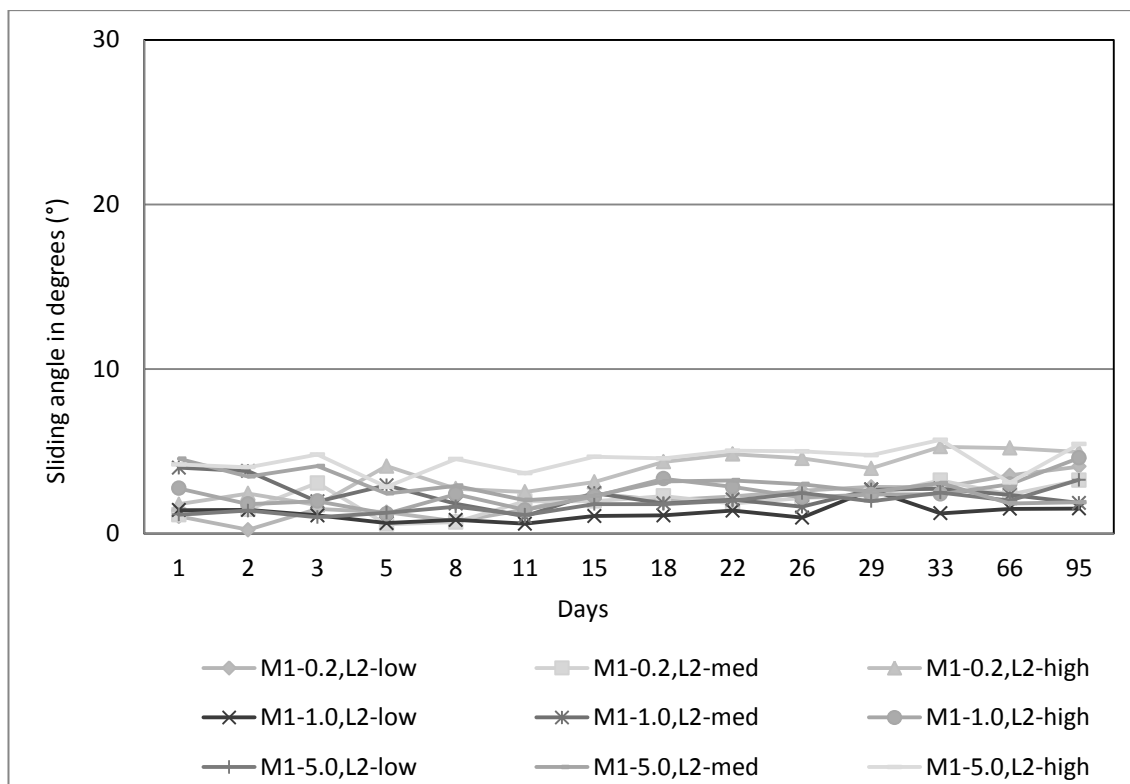
Figure 43. *The siding angle of L2 lubricants infused membranes.*

Only L1-low SLIPS samples also lost thoroughly their surface properties as to the somewhat radical increase in wettability parameters: water contact angle, contact angle hysteresis and in sliding angle. Interestingly, L2's oil infused M-0.2 SLIPS, the weight loss did not affect the surface properties dramatically. This might be due to the fact that L1-low evaporates from the surface of the M's 0.2 µm membrane hence altering the surface properties. In comparison, the oil of supplier L2's in M 0.2 µm pore size membrane might leak from the membrane-glass interface away – that is, L2's oil could have greater affinity to the glass substrate than M's lubricants. Supplier L2's oil impregnated SLIPS performed well since the surface properties stayed relatively constant throughout the testing.

8.2 Cyclic ice adhesion test

By examining and reviewing the wettability and vaporization tests' results, the SLIPS samples for the cyclic ice adhesion tests were chosen. The membranes with small pore sizes seemed to have moderately high contact angles but low hysteresis and sliding angle. The L1-med and L2-med results were steady throughout the tests thus these lubricants were tested more comprehensively. It was also interesting to see how the low viscosity L1-low would perform in below zero temperatures. Moreover, the characteristics of more rigid L1-high were intriguing to examine. From all the

membranes, also the no oil infused membrane samples were tested in the cyclic ice adhesion test to have a better comprehension on the lubricant effects on ice releasement in SLIPS. The selected sample matrix for icing tests is seen in Table 10. After every ice adhesion measurement, the wettability of the samples was tested.

Table 10.   *The test matrix for the cyclic ice adhesion tests.*

	No oil	L1-low	L1-med	L1-high	L2-med
M2-0.2	x		x		x
M1-0.2	x	x	x	x	x
M1-1.0	x	x	x	x	x
M1-5.0	x		x		

For the ice adhesion testing, Teflon tape from 3M was used as a reference sample. The samples were cycled for four times as after every cycle the wettability was examined by static contact angle and sliding angle measurements. The results are presented in a bar diagram in Figure 44.

Within the first cycle, six out of fifteen SLIPS samples showed extremely low ice adhesion with ice adhesion strength under 20 kPa. These low ice adhesion samples were all constituted from small pore size membranes, 0.2 µm being the average pore size. These small pore size membranes from both suppliers, M1 and M2, showed equally low ice adhesion strength. Additionally, the results were in total fairly promising as the highest recorded ice adhesion strength for SLIPS was only 70 kPa in the first cycle. For bare aluminum, mirror-polished and tested with the centrifugal ice adhesion machinery, the ice adhesion results are around 360 kPa (Farhadi et al., 2011; Kulinich et al., 2011) Conversely, it is need to be pointed out that aluminum cannot be considered as suitable material choice for icephobic solutions since its surface energy value is rather high and aluminum is hydrophilic by its nature (Minford, 1993). The standard deviation in the performed cyclic icing test was around 10 kPa on average for the SLIPS samples, altering from 2 to 15 kPa between the samples, as in Figure 44.
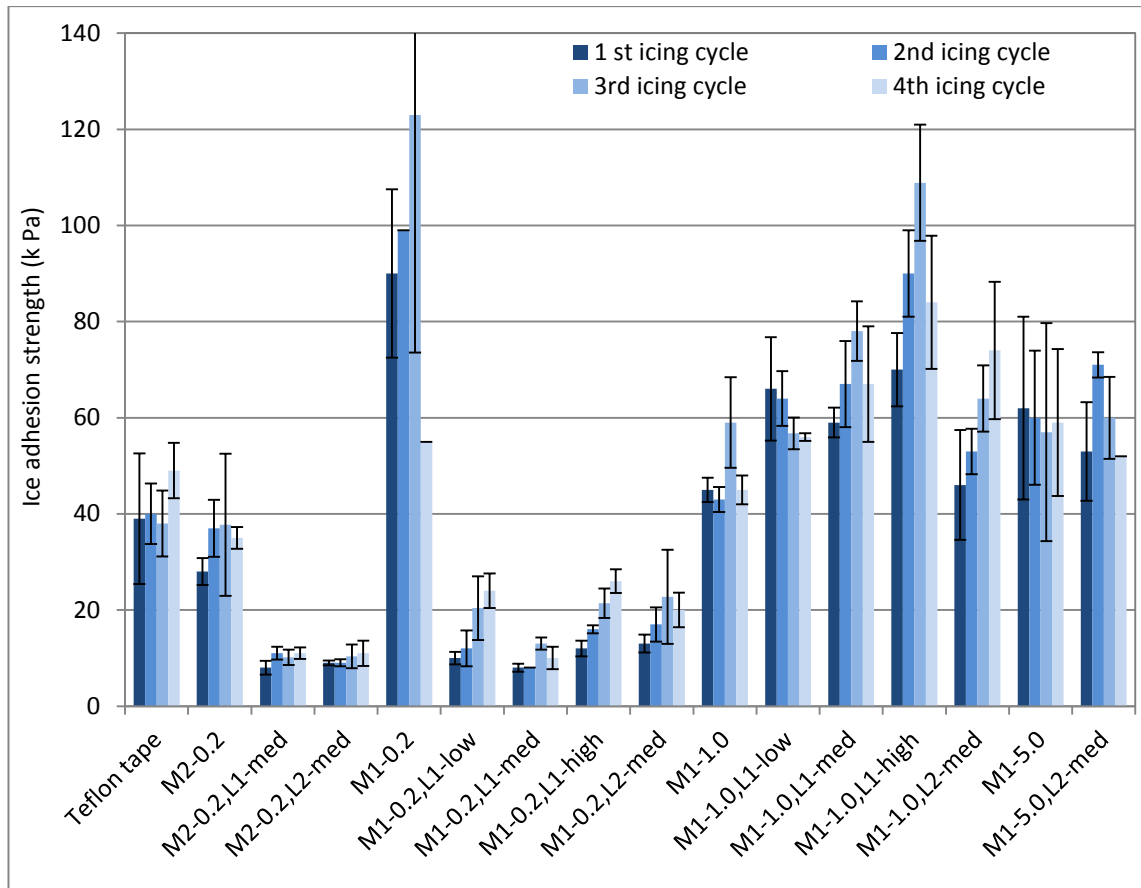
Figure 44.   *Ice adhesion results of SLIPS. Teflon tape was used as a reference sample.*

In M2's 0.2 µm pore size membrane, there was a supporting matrix behind every PTFE –film. This supporting matrix might be beneficial to ice releasement as the ice adhesion results for unimpregnated M2-0.2 samples were relatively low, only 30-35 kPa within the cycles. The supporting texture was transformed into the accreted ice from the surface, as proven in Figure 45.

Dry membrane of M1 0.2 µm pore size did not have such a low ice adhesion as the force needed to detach the ice was 90 kPa in the first cycle. By this result, the supporting matrix in the m membrane attracts interest. It was observed from the detached ice that in the M2-0.2 membrane, without any lubricant, the ice had surface texture from the supporting membrane as well, depicted in Figure 45. By this observation, the possible benefits of surface structure and supporting structure under the surface ought to be tested in the future.

Figure 45. *Supplier M2's membrane of 0.2 µm pore size had a supporting matrix behind the structure. This resulted in the same texture to accreted ice pieces contacting the PTFE –membrane. The texture was seen in both, lubricant infused samples and in plain membrane samples which had no lubricant impregnated into.*

When the M2's 0.2 µm pore size membrane was introduced to lubricants, L1-med and L2-med, the ice adhesion dropped to 10 kPa, as seen in the figure 44. By comparing these values to the literature, it could be stated that the gained ice adhesion results are fairly low.

After examining the Figure 44 and the ice adhesion results, a correlation between small pore size and low ice adhesion can be seen. In both PTFE –membranes, in M1 as in M2, the ice adhesion of the 0.2 µm pore size membranes was noticeably the lowest. There are also other recordings stating that greater surface texture might result in higher ice adhesion in results (Chen et al., 2012). Different type of lubricants, obtained from different suppliers, or viscosities did not have such an effect as membrane pore size had. The only exception is the M1's 0.2 µm pore size membrane without any lubricant, hence the membrane's ice adhesion was the highest ca. 90 kPa. This proves the concept of infusing small pore sizes membranes with lubricating oil. The pore sizes of 1.0 and 5.0 µm did not have significant differences between.

In Figures 46 and 47 the static contact angle and contact angle hysteresis results within the cyclic ice adhesion tests are viewed. In the contact angle hysteresis illustration in Figure 47, there are no plain membranes without the lubricant since the sliding angle was above measurable range (~40°). M2-0.2 with L2-med SLIPS sample have no recordings before the cyclic ice adhesion testing, since it was not obtained to the original testing matrix, in Table 8. Hence, the sample recordings start from the first icing cycle in both, Figure 46 and Figure 47.

In some cases the static contact angles seem to decline after the cycles, as expected since the wind, ice accretion and ice releasement will ease the lubricant deprivation from the surface. Moreover, it was detected that the surface had tears and wears in the ice adhesion measurements. This alters the surface morphology providing greater voids

to where the water droplets will stick and pin into. The static contact angles of the L1 lubricant impregnated SLIPS show decrease or stay relatively static. The same phenomena occurs in the L2 oil infused SLIPS, as to more icing cycles are needed to obtain more data for the impacts of icing and de-icing cycles in the longer time period. No obvious conclusions can be drawn between the two lubricants nor between the different pore sizes in the effects of icing cycles to the static contact angle.
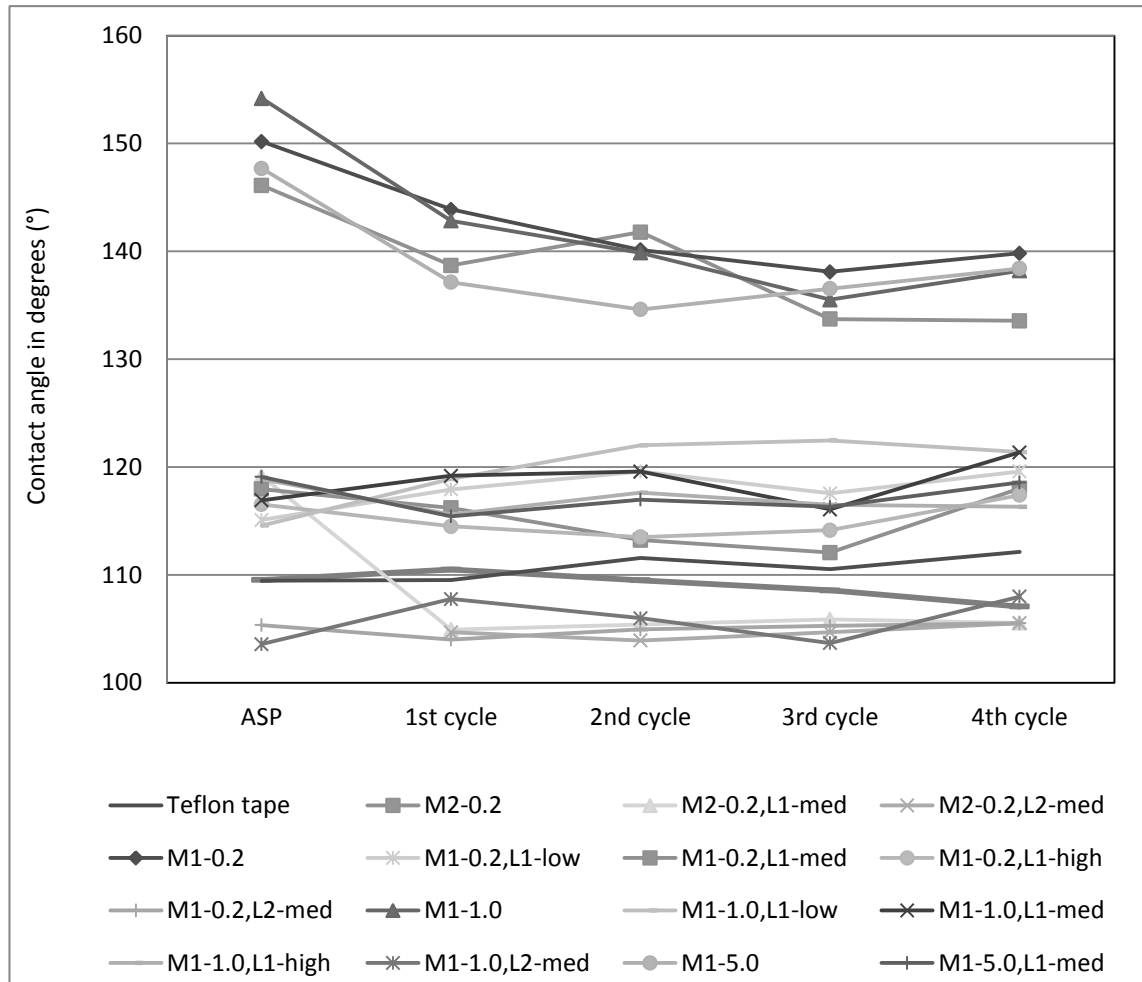
Figure 46. *The static contact angle results from the SLIPS taken after every icing cycle. ASP refers to "after sample preparation".*

The contact angle hysteresis show more explicit and anticipated behavior within the icing cycles. For the same reasons as in the static contact angle diminish, the somewhat abrasion like conditions in the tests change the surface and increase the contact angle hysteresis. All of the tested SLIPS show increase in the contact angle hysteresis, but the most obvious graduation can be seen in the M1's 0.2 µm pore size membrane with L1-low lubricant. The lubricant was lost presumably due to many factors, such as evaporation, wind and ice detachment. Moreover, the M1's 0.2 µm pore size membrane was the thinnest of the membranes which makes it vulnerable towards lubricant loss. The membrane also accumulated dents and cuts within the cycles, which were observed

with the naked eye. Overall, the hysteresis of the rest of the SLIPS samples in the cyclic ice adhesion test stayed moderately satisfactory, as the hysteresis stayed under 5° in the four icing cycles.
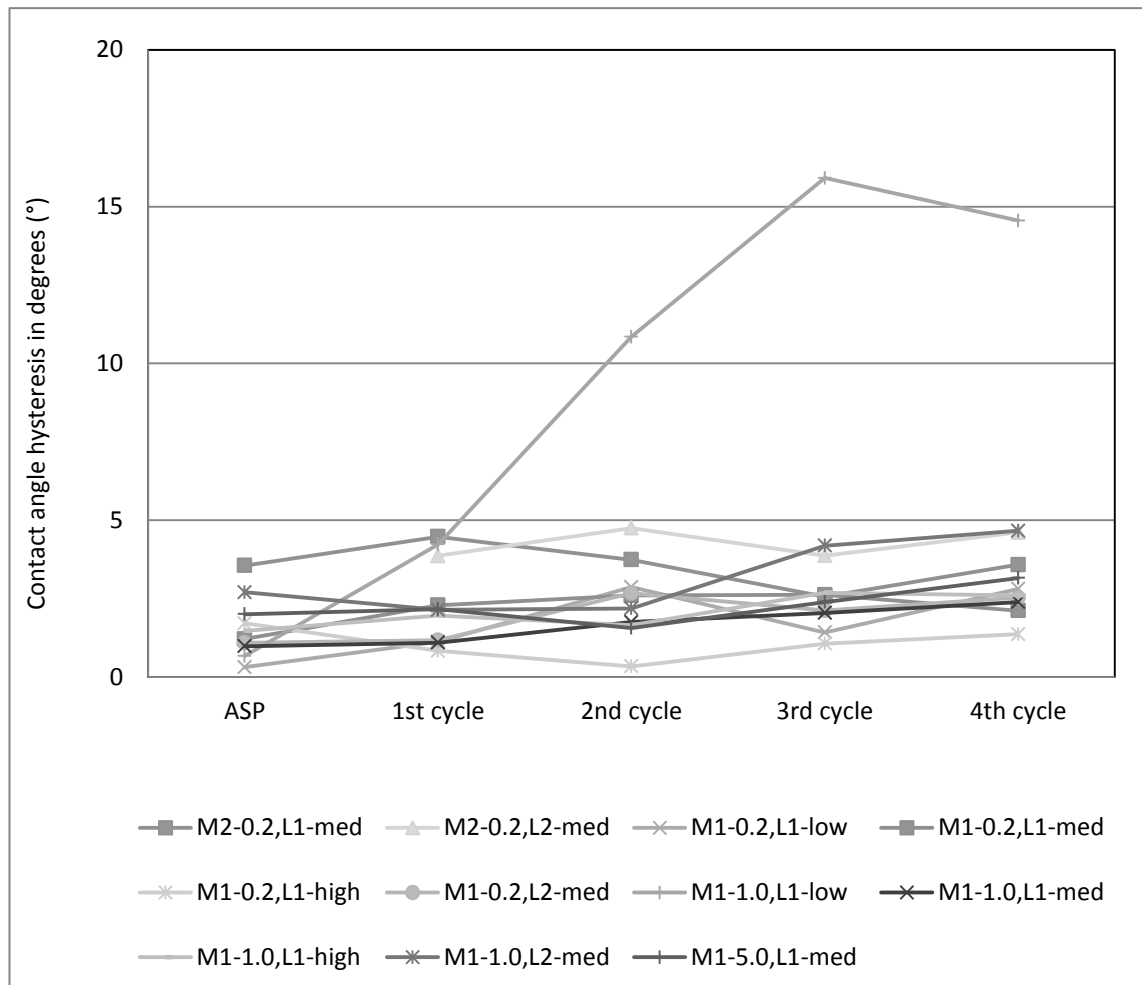

Figure 47. *The contact angle hysteresis results from the SLIPS taken after every icing cycle. ASP refers to "after sample preparation".*

By the results of these experiments, it would seem that when it comes to ice adhesion, the SLIPS porous solid's pore size has a major impact on the ice detachment. Most likely, other parameters also will affect to ice adhesion, such as fiber diameter, surface roughness and porosity (fraction of air vs. solid in the structure) in the membrane. These parameters would need more testing. When observing the bars in the Figure 44, the ice adhesion results of M1's 0.2 μm pore size membrane with any tested lubricant, are indeed somewhat similar and positively low. Also, moderately low ice adhesion can be observed in M1's 5.0 μm pore size membrane SLIPS and to some extent in the M1's 1.0 μm pore size membrane SLIPS. More testing and prolonged ice cycles are needed to perform in order to definitely make any assumptions concerning the proper viscosity lubricant for SLIPS and long-term durability of the surfaces. By reviewing these tests

results, no clear assumption can be drawn on this prospect, as all of the tested lubricants performed well in the cyclic ice adhesion tests.

The optical transparency has been recorded for a variety of SLIPS (Chen et al., 2014; Okada & Shiratori, 2014; Wong et al., 2011). Additionally, the SLIPS fabricated in this thesis also proved to have moderately good transparency as depicted in Figure 48. All of the six tested membranes were shown to be transparent with lubricating liquid L1-med, despite of the altering thicknesses or supporting matrixes. The thickness has some effects on the transparency as it would seem that the thicker samples are more opaque than the thinner ones.
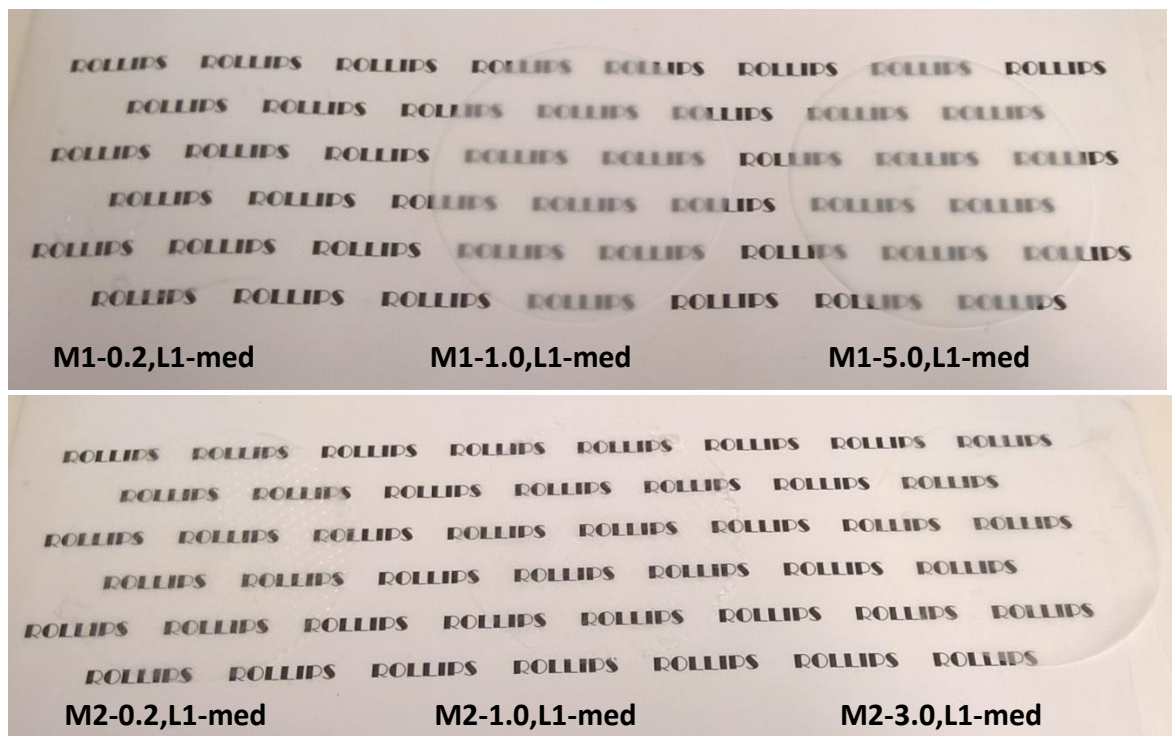
Figure 48. *The optical transparency of the fabricated SLIPS. All of the porous membranes exhibited good transparency with L1-med lubricant.*

9. GENERAL CONCLUSIONS

From the results obtained from the evaporation testing, it is clear that the lubricants with low viscosity, especially L1-low, will vaporize significantly after few weeks of time. The medium viscosity lubricants, L1-med and L2-med, the evaporation was moderately low as it was in high viscosity lubricants L1-high and L2-high. The test provides information on choosing the right viscosity lubricant to suitable SLIPS –applications.

The wettability tests show that evaporation of lubricant is likely to result in droplet pinning and elevated hysteresis on surfaces. As to this, poorly chosen lubricant/porous solid pairs might result in sticking of water and frost on surface which can deteoriate the surface even more by lubricant loss. Clear evidence on the lubricant type cannot be stated as the L1 oils and L2 oils performed well in the wettability tests. In the future, it is important to focus on lubricants which are durable in the structure as to environmental friendly. Definite correlation on the effect of membrane pore sizes and other dimensions on wettability are also under deliberation. It would need more systematic testing to specify the effects of all the surface parameters of SLIPS in wettability measurements.

The cyclic ice adhesion testing might give some ideas where to focus the future experiments. In the icing tests, the smallest pore size used, 0.2 µm, was seen as the best choice of the tested pore sizes. The lubricant type or the viscosity did not have a major effects on ice adhesion on these tests. However, more cycles are needed to reveal the long term effects of accreted and detached ice on the surfaces. The performance of the more viscous lubricants would also be interesting to find out in the below zero temperatures.

Another interesting detail, observed in the cyclic ice adhesion testing, was the supporting matrix behind one PTFE –membrane type. The supporting matrix created a texture to the detached ice but also yielded moderately low ice adhesion when compared to membranes without the supporting matrix. This phenomenon likewise needs to be examined further.

Especially in SLIPS, there are some challenges which might limit their usage in wide applications. As tested in a large scale, their performance in extreme conditions is questioned regarding shear and abrasion forces and long-term stability which might be depreciated as a result of evaporation of the lubricating fluid from the porous structure or its depletion with the removed water and ice. Moreover, it remains uncertain how to efficiently fabricate SLIPS to all of the desired end-products and how to maintain the surface in perfect condition, to name few technical challenges. These issues are needed to overcome and to be solved in near future.

Moreover, it needs to be taken into consideration that the membranes used in the experiment were not designed for the surface applications. Due to this, the membranes were not manufactured to serve for the purposes as tested in this work. In the future, it could be possible to alter or modify the membranes towards more robust anti-ice or ice-repellent characteristics.

10. SUGGESTIONS FOR FUTURE WORK

Practical future work consists of studying the structure of the SLIPS in more detailed way. To do this, more closer and detailed look needs to be taken to the membranes as investigating their structures with imaging and resolving the proper thickness for the surface membrane as to its best functional pore size. The studies are ought to be turned towards environmental friendly materials, without sacrificing performance and low costs.

Introduction of novel, innovative and effective fabrication methods are required to accomplish and meet the challenges which are relevant in SLIPS, currently. New application areas arise, as the research and understanding within the research community grows. This means that more fundamental studies on wetting, condensation and icing as a phenomenon are needed in the field of SLIPS on a different substrates and lubricants. Also, elemental studies on the effect of nanoscale structures and their hierarchy are welcome, on lubricant stability and evaporation as current solutions rely on microstructured surfaces. That is, to secure long-term operation of SLIPS it is needed to develop solid-lubricant pairs to prevent lubricant depletion from the surface. The affinity between the lubricant and the porous solid material is one crucial element to take into consideration as to surface chemistry and texture. Moreover, the operating life of SLIPS could be improved by investigating the degradation of porous solid materials and lubricant. As to ultra violet radiation and multiple freezing and melting cycles the information gained will help to improve the SLIPS to function in harsh conditions and alternating environments.

More studies on anti-icing performance needs to be gathered when it comes to different lubricants and their evaporation rate in a much wider temperature rate, ranging from freezing temperatures to even more elevated temperatures than room temperature. This could be performed by cyclic icing tests, where the amount of cycles is sufficient. Evaporation testing could also be conducted in below zero temperatures, or in outdoor environment mimicking the real-life conditions.

Especially the knowledge on materials performance in the Arctic conditions would be crucial to know. This should be done to support the preparation of legislations, standardizations and instructions as also to prove reliability of safety and efficiency in the Arctic environment.

By doing discipline and pioneering research work on the matter, Finland's position in maritime, logistics and industrial operations could be strengthened via new innovations. By examining the possibilities of slippery liquid infused surfaces both, water and ice-

repellency, could be improved and engineered but also a step towards easy emptying, self-cleaning and self-healing materials and surfaces could be taken.

REFERENCES

Anand, S., Paxson, A. T., Dhiman, R., Smith, J. D., & Varanasi, K. K. (2012). Enhanced Condensation on Lubricant- Impregnated Nanotextured Surfaces, Vol. 6(11), pp.10122–10129. Available: http://doi.org/10.1021/nn303867y

Andersson, M., & Torikian, J. (2000). De-icing Methods for Rail Vehicles. *TRITA-FKT*, (38). Available: http://trid.trb.org/view.aspx?id=675873

Antonini, C. (2011). Superhydrophobicity as a strategy against icing: Analysis of the water/surface dynamic interaction for icing mitigation. Università degli studi di Bergamo, 2011, pp. 238. Available: https://aisberg.unibg.it/bitstream/10446/881/1/phd_thesis_Antonini.pdf

Arclio. (2015). Northern Sea Route Information Office. Webpage. Accessed 5.11.2015. Available: http://www.arctic-lio.com/

Aytug, T., Paranthaman, M. P., Simpson, J. T., & Bogorin, D. F. (2014). Superhydrophobic films and methods for making superhydrophobic films. Patent: US 20140065368 A1. Available: http://www.google.com/patents/US20140065368

Azimi, G., Dhiman, R., Kwon, H.-M., Paxson, A. T., & Varanasi, K. K. (2013). Hydrophobicity of rare-earth oxide ceramics. *Nature Materials*, *12*(4), pp.315–20. Available: http://doi.org/10.1038/nmat3545

Bartell, F. E., & Shepard, J. W. (1953). Surface roughness as related to hysteresis of contact angles. I. The system paraffin-water-air. *The Journal of Physical Chemistry*, *57*(2), pp.211–215. Available: http://doi.org/DOI 10.1021/la063572r

Barthlott, W., & Neinhuis, C. (1997a). Characterization and distribution of water repellent, self-cleaning plant surfaces. *Annals of Botany*, *79*, pp.667–677.

Barthlott, W., & Neinhuis, C. (1997b). Purity of the sacred lotus, or escape from contamination in biological surfaces. *Planta*, *202*(1), pp.1–8. Available: http://doi.org/10.1007/s004250050096

Bechert, D. W., Bruse, M., & Hage, W. (2000). Experiments with three-dimensional riblets as an idealized model of shark skin. *Experiments in Fluids*, *28*, pp.403–412. Available: http://doi.org/10.1007/s003480050400

Bharathidasan, T., Kumar, S. V., Bobji, M. S., Chakradhar, R. P. S., & Basu, B. J. (2014). Effect of wettability and surface roughness on ice-adhesion strength of hydrophilic, hydrophobic and superhydrophobic surfaces. *Applied Surface Science*, *314*, pp.241–250. Available: http://doi.org/10.1016/j.apsusc.2014.06.101

Bhushan, B. (2009). Biomimetics: lessons from nature--an overview. *Philosophical Transactions. Series A, Mathematical, Physical, and Engineering Sciences*, *367*(1893), pp.1445–1486. Available: http://doi.org/10.1098/rsta.2009.0011

Bhushan, B., Jung, Y. C., & Koch, K. (2009a). Micro-, nano- and hierarchical structures for superhydrophobicity, self-cleaning and low adhesion. *Philosophical Transactions. Series A, Mathematical, Physical, and Engineering Sciences*, *367*(1894), pp.1631–1672. Available: http://doi.org/10.1098/rsta.2009.0014

Bhushan, B., Jung, Y. C., & Koch, K. (2009b). Self-cleaning efficiency of artificial superhydrophobic surfaces. *Langmuir : The ACS Journal of Surfaces and Colloids*, *25*(5), pp.3240–3248. Available: http://doi.org/10.1021/la803860d

Bird, J. C., Dhiman, R., Kwon, H. M., & Varanasi, K. K. (2013). Reducing the contact time of a bouncing drop. *Nature*, *503*, pp.385–388. Available: http://doi.org/10.1038/nature12740

Blossey, R., & Scientifique, C. (2003). Self-cleaning surfaces — virtual realities, *Nature Materials*, 2, pp.301–306.

Bohn, H. F., & Federle, W. (2004). Insect aquaplaning: Nepenthes pitcher plants capture prey with the peristome, a fully wettable water-lubricated anisotropic surface. *Proceedings of the National Academy of Sciences of the United States of America*, *101*(39), pp.14138–14143. Available: http://doi.org/10.1073/pnas.0405885101

Borenstein, S. W. (1994). *Microbiologically Influenced Corrosion Handbook*. Woodhead Publishing. Available: https://books.google.com/books?id=9UZf04XAFyoC&pgis=1

Boreyko, J. B., & Collier, C. P. (2013). Delayed frost growth on jumping-drop superhydrophobic surfaces. *ACS Nano*, *7*(2), pp.1618–27. Available: http://doi.org/10.1021/nn3055048

Boreyko, J. B., Polizos, G., Datskos, P. G., Sarles, S. a, & Collier, C. P. (2014). Air-stable droplet interface bilayers on oil-infused surfaces. *Proceedings of the National Academy of Sciences of the United States of America*, *111*(21), pp.7588–93. Available: http://doi.org/10.1073/pnas.1400381111

Burton, Z., & Bhushan, B. (2006). Surface characterization and adhesion and friction properties of hydrophobic leaf surfaces. *Ultramicroscopy*, *106*, pp.709–719. Available: http://doi.org/10.1016/j.ultramic.2005.10.007

Callies, M., Chen, Y., Marty, F., Pépin, A., & Quéré, D. (2005). Microfabricated textured surfaces for super-hydrophobicity investigations. *Microelectronic Engineering*, *78-79*, pp.100–105. http://doi.org/10.1016/j.mee.2004.12.093

Callies, M., & Quéré, D. (2005). On water repellency. *Soft Matter*, *1*, pp.55-61. Available: http://doi.org/10.1039/b501657f

Callow, J. A., & Callow, M. E. (2011). Trends in the development of environmentally friendly fouling-resistant marine coatings. *Nature Communications*, *2*. Available: http://doi.org/10.1038/ncomms1251

Cao, L., Jones, A. K., Sikka, V. K., Wu, J., & Gao, D. (2009). Anti-Icing superhydrophobic coatings. *Langmuir*, *25*(21), pp.12444–12448. Available: http://doi.org/10.1021/la902882b

Cassie, B. D. (1944). Wettability of porous surfaces, *Trans. Faraday Soc.*,40, pp.546-551. Available: http://pubs.rsc.org/en/content/articlelanding/1944/tf/tf9444000546/unauth#!divAbstract

Charpentier, T. V. J., Neville, A., Baudin, S., Smith, M. J., Euvrard, M., Bell, A., … Barker, R. (2015). Liquid infused porous surfaces for mineral fouling mitigation. *Journal of Colloid and Interface Science*, *444*, pp.81–86. Available: http://doi.org/10.1016/j.jcis.2014.12.043

Charpentier, T. V. J., Neville, A., Millner, P., Hewson, R., & Morina, A. (2013). An Investigation of Freezing of Supercooled Water on Anti-Freeze Protein Modified Surfaces. *Journal of Bionic Engineering*, *10*(2), pp.139–147. Available: http://doi.org/10.1016/S1672-6529(13)60208-5

Chau, T. T. (2009). A review of techniques for measurement of contact angles and their applicability on mineral surfaces. *Minerals Engineering*, *22*(3), pp.213–219. Available: http://doi.org/10.1016/j.mineng.2008.07.009

Chau, T. T., Bruckard, W. J., Koh, P. T. L., & Nguyen, A. V. (2009). A review of factors that affect contact angle and implications for flotation practice. *Advances in Colloid and Interface Science*, *150*(2), pp.106–115. Available: http://doi.org/10.1016/j.cis.2009.07.003

Chen, J., Dou, R., Cui, D., Zhang, Q., Zhang, Y., Xu, F., Jiang, L. (2013). Robust prototypical anti-icing coatings with a self-lubricating liquid water layer between ice and substrate. *ACS Applied Materials and Interfaces*, *5*, pp.4026–4030. Available: http://doi.org/10.1021/am401004t

Chen, J., Liu, J., He, M., Li, K., Cui, D., Zhang, Q., Song, Y. (2012). Superhydrophobic surfaces cannot reduce ice adhesion. *Applied Physics Letters*, *101*(11), pp.111603. Available: http://doi.org/10.1063/1.4752436

Chen, L., Geissler, A., Bonaccurso, E., & Zhang, K. (2014). Transparent slippery surfaces made with sustainable porous cellulose lauroyl ester films. *ACS Applied Materials and Interfaces*, *6*, pp.6969–6976. Available: http://doi.org/10.1021/am5020343

Chen, X., Ma, R., Zhou, H., Zhou, X., Che, L., Yao, S., & Wang, Z. (2013). Activating the microscale edge effect in a hierarchical surface for frosting suppression and defrosting promotion. *Scientific Reports*, *3*, pp.2515. Available: http://doi.org/10.1038/srep02515

Choi, H., Boccazzi, P., Laibinis, P. E., Sinskey, A. J., & Jensen, K. F. (2003). Poly (ethylene glycol) (peg) - modified poly (dimethylsiloxane) (pdms) for protein- and cell-resistant surf ' aces in microbioreactor, pp.1105–1108.

Congdon, T., Dean, B. T., Kasperczak-Wright, J., Biggs, C. I., Notman, R., & Gibson, M. I. (2015). Probing the Biomimetic Ice Nucleation Inhibition Activity of Poly(vinyl alcohol) and Comparison to Synthetic and Biological Polymers. *Biomacromolecules*, *16*(9), pp.2820–2826. Available: http://doi.org/10.1021/acs.biomac.5b00774

Congdon, T., Notman, R., & Gibson, M. I. (2013). Antifreeze (Glyco)protein mimetic behavior of poly(vinyl alcohol): Detailed structure ice recrystallization inhibition activity study. *Biomacromolecules*, *14*(5), pp.1578–1586. Available: http://doi.org/10.1021/bm400217j

Cordier, P., Tournilhac, F., Soulié-Ziakovic, C., & Leibler, L. (2008). Self-healing and thermoreversible rubber from supramolecular assembly. *Nature*, *451*(7181), pp.977–80. Available: http://doi.org/10.1038/nature06669

Dalili, N., Edrisy, a., & Carriveau, R. (2009). A review of surface engineering issues critical to wind turbine performance. *Renewable and Sustainable Energy Reviews*, *13*(2), pp.428–438. Available: http://doi.org/10.1016/j.rser.2007.11.009

Daniel, D., Mankin, M. N., Belisle, R. a., Wong, T. S., & Aizenberg, J. (2013). Lubricant-infused micro/nano-structured surfaces with tunable dynamic omniphobicity at high temperatures. *Applied Physics Letters*, *102*(2013). Available: http://doi.org/10.1063/1.4810907

Dehghani-sanij, A., Muzychka, Y. S., & Naterer, G. F. (2015). Analysis of Ice Accretion on Vertical Surfaces of Marine Vessels and Structures in Arctic Conditions. *Ocean Engineering*, *7*. Available: http://doi.org/10.1115/OMAE2015-41306

Della-Bona, A. (2005). Characterizing ceramics and the interfacial adhesion to resin: II- the relationship of surface treatment, bond strength, interfacial toughness and fractography. *Journal of Applied Oral Science*, *13*(2), pp.101–109. Available: http://doi.org/10.1590/S1678-77572005000200002

DNV GL AS. (2015). Safer Smarter Greener, DNVGL.com. Webpage. Accessed: 4.11.2015. Available: https://www.dnvgl.com/

Duman, J. G. (2001). Antifreeze and ice nucleator proteins in terrestrial arthropods. *Annu Rev Physiol.*63. pp.327-57. http://10.1146/annurev.physiol.63.1.327

DuPont. (2011). *DuPont Performance Lubricants*. Product overview. Accessed: 3.11.2015. Available: http://www.tmcindustries.com/PDF%20Files/Krytox_Overview_LowRes-TMC.pdf

DuPont. (2015). Teflon® Fluoropolymer Resins | DuPont USA. Webpage. Accessed: 24.10.2015, Available: http://www.dupont.com/products-and-services/plastics-polymers-resins/fluoropolymers/brands/teflon-fluoropolymer-resin.html

Ebert, D., & Bhushan, B. (2012). Durable Lotus-effect surfaces with hierarchical structure using micro- and nanosized hydrophobic silica particles. *Journal of Colloid and Interface Science*, *368*(1), pp.584–591. Available: http://doi.org/10.1016/j.jcis.2011.09.049

Emelyanenko, L. B. B. and A. M., & A. (2013). Anti-icing potential of superhydrophobic coatings. *Mendeleev Communications*, *23*, pp.74–75. Available: http://doi.org/10.1016/j.mencom.2013.

Epstein, A. K., Wong, T.-S., Belisle, R. a., Boggs, E. M., & Aizenberg, J. (2012). From the Cover: Liquid-infused structured surfaces with exceptional anti-biofouling performance. *Proceedings of the National Academy of Sciences*, *109*(33), pp.13182–13187. Available: http://doi.org/10.1073/pnas.1201973109

Esser-Kahn, A. P., Trang, V., & Francis, M. B. (2010). Incorporation of antifreeze proteins into polymer coatings using site-selective bioconjugation. *Journal of the American Chemical Society*, *132*(38), pp.13264–13269. Available: http://doi.org/10.1021/ja103038p

Farhadi, S., Farzaneh, M., & Kulinich, S. A. a. (2011). Anti-icing performance of superhydrophobic surfaces. *Applied Surface Science*, *257*(14), pp.6264–6269. Available: http://doi.org/10.1016/j.apsusc.2011.02.057

Farzaneh, M. (2008). *Atmospheric icinc of power networks*. Springer, London, United Kingdom, 2008, pp.381.

Feng, X., Feng, L., Jin, M., Zhai, J., Jiang, L., & Zhu, D. (2004). Reversible super-hydrophobicity to super-hydrophilicity transition of aligned ZnO nanorod films. *Journal of the American Chemical Society*, *126*(1), pp.62–63. Available: http://doi.org/10.1021/ja038636o

Ferrick, M. G., Mulherin, N. D., Haehnel, R. B., Coutermarsh, B. A., Durell, G. D., Tantillo, T. J., … Martinez, E. C. (2008). Evaluation of ice release coatings at cryogenic temperature for the space shuttle. *Cold Regions Science and Technology*, *52*(2), pp.224–243. Available: http://doi.org/10.1016/j.coldregions.2007.03.002

Finland's Prime Minister's Office. (2013). *Finland's Strategy for the Arctic Region 2013. Government resolution on 23 August 2013*. Accessed: 29.9.2015. Available: http://vnk.fi/en/publication?pubid=2411

Franssila, S. (2010). *Introduction to Microfabrication* (1st ed.). John Wiley & Sons. Available: https://books.google.com/books?id=cvoR9vmDJIQC&pgis=1

Fu, Q., Rao, G. V. R., Basame, S. B., Keller, D. J., Artyushkova, K., Fulghum, J. E., & López, G. P. (2004). Reversible control of free energy and topography of nanostructured surfaces. *Journal of the American Chemical Society*, *126*(29), pp.8904–8905. Available: http://doi.org/10.1021/ja047895q

Gao, L., & McCarthy, T. J. (2006). The "lotus effect" explained: two reasons why two length scales of topography are important. *Langmuir : The ACS Journal of*

Surfaces and Colloids, *22*(7), pp.2966–2967. Available: http://doi.org/10.1021/la0532149

Gao, L., & McCarthy, T. J. (2007). How Wenzel and Cassie were wrong. *Langmuir*, *23*(7), pp.3762–3765. Available: http://doi.org/10.1021/la062634a

Gao, X., & Jiang, L. (2004). Biophysics: water-repellent legs of water striders. *Nature*, *432*(November), 36. Available: http://doi.org/10.1038/432036a

Genzer, J., & Efimenko, K. (2006). Recent developments in superhydrophobic surfaces and their relevance to marine fouling: a review. *Biofouling*, *22*(5), pp.339–360. Available: http://doi.org/10.1080/08927010600980223

Glavan, A. C., Martinez, R. V., Subramaniam, A. B., Yoon, H. J., Nunes, R. M. D., Lange, H., … Whitesides, G. M. (2014). Omniphobic "rF paper" produced by silanization of paper with fluoroalkyltrichlorosilanes. *Advanced Functional Materials*, *24*, pp.60–70. Available: http://doi.org/10.1002/adfm.201300780

Heinrich, A., Ross, R., Zumwalt, G., Provorse, J., Padmanabhan, V., Thompson, J., & Riley, J. (1991). *Aircraft Icing Handbook, Volume 1 of 3*. U.S Department of Transportation.

Hejazi, V., Sobolev, K., & Nosonovsky, M. (2013). From superhydrophobicity to icephobicity: forces and interaction analysis. *Scientific Reports*, *3*, 2194. Available: http://doi.org/10.1038/srep02194

Hou, X., Zhou, F., Yu, B., & Liu, W. (2007). Superhydrophobic zinc oxide surface by differential etching and hydrophobic modification. *Materials Science and Engineering: A*, *452-453*, pp.732–736. Available: http://doi.org/10.1016/j.msea.2006.11.057

Howell, C., Vu, T. L., Lin, J. J., Kolle, S., Juthani, N., Watson, E., … Aizenberg, J. (2014). Self-Replenishing Vascularized Fouling-Release Surfaces. *ACS Appl Mater Interfaces*. 6(15):pp.13299-307.

Hsieh, C.-T., Lai, M.-H., & Cheng, Y.-S. (2009). Fabrication and superhydrophobicity of fluorinated titanium dioxide nanocoatings. *Journal of Colloid and Interface Science*, *340*(2), pp.237–42. Available: http://doi.org/10.1016/j.jcis.2009.08.029

Hu, J., Xu, K., Wu, Y., Lan, B., Jiang, X., & Shu, L. (2014). The freezing process of continuously sprayed water droplets on the superhydrophobic silicone acrylate resin coating surface. *Applied Surface Science*, *317*, pp.534–544. Available: http://doi.org/10.1016/j.apsusc.2014.08.145

Ishizaki, T., & Saito, N. (2010). Rapid formation of a superhydrophobic surface on a magnesium alloy coated with a cerium oxide film by a simple immersion process at room temperature and its chemical stability. *Langmuir : The ACS Journal of Surfaces and Colloids*, *26*(12), pp.9749–55. Available: http://doi.org/10.1021/la100474x

IWAIS. (2009). 13th International Workshop on Atmospheric Icing of Structures. Webpage. Accessed: 4.11.2015. Available: http://www.iwais2009.ch/index.php%3Fid=44.html

Jianyong Lv, Yanlin Song, Lei Jiang, and J. W. (2014). Bio-Inspired Strategies for Anti-Icing. *ACS Nano*, 8(4), pp 3152–3169, Available: http://pubs.acs.org/doi/pdf/10.1021/nn406522n

Jin, M., Feng, X., Xi, J., Zhai, J., Cho, K., Feng, L., & Jiang, L. (2005). Super-Hydrophobic PDMS Surface with Ultra-Low Adhesive Force. *Macromolecular Rapid Communications*, *26*(22), pp.1805–1809. Available: http://doi.org/10.1002/marc.200500458

Jung, S., Dorrestijn, M., Raps, D., Das, A., Megaridis, C. M., & Poulikakos, D. (2011). Are Superhydrophobic Surfaces Best for Icephobicity, pp.3059–3066. Available: http://doi.org/10.1021/la104762g

Jung, Y. C., & Bhushan, B. (2006). Contact angle, adhesion and friction properties of micro-and nanopatterned polymers for superhydrophobicity. *Nanotechnology*, *17*(19), pp.4970–4980. Available: http://doi.org/10.1088/0957-4484/17/19/033

Kako, T., Nakajima, a., Irie, H., Kato, Z., Uematsu, K., Watanabe, T., & Hashimoto, K. (2004). Adhesion and sliding of wet snow on a super-hydrophobic surface with hydrophilic channels. *Journal of Materials Science*, *39*(2), pp.547–555. Available: http://doi.org/10.1023/B:JMSC.0000011510.92644.3f

Kenisarin, M., & Mahkamov, K. (2007). Solar energy storage using phase change materials. *Renewable and Sustainable Energy Reviews*, *11*(9), pp.1913–1965. Available: http://doi.org/10.1016/j.rser.2006.05.005

Ketelson, H., Perry, S., Sawyer, G., & Jean, J. (2011). Exploring the Science and Technology of Contact Lens Comfort. Accessed: 3.11.2015. Available: http://www.clspectrum.com/articleviewer.aspx?articleID=106075

Khorasani, M. T., Mirzadeh, H., & Kermani, Z. (2005). Wettability of porous polydimethylsiloxane surface: morphology study. *Applied Surface Science*, *242*(3-4), pp.339–345. Available: http://doi.org/10.1016/j.apsusc.2004.08.035

Kim, P., Adorno-Martinez, W. E., Khan, M., & Aizenberg, J. (2012). Enriching libraries of high-aspect-ratio micro- or nanostructures by rapid, low-cost, benchtop nanofabrication. *Nature Protocols*, *7*(2), pp.311–27. Available: http://doi.org/10.1038/nprot.2012.003

Kim, P., Kreder, M. J., Alvarenga, J., & Aizenberg, J. (2008). Hierarchical or Not? Effect of the Length Scale and Hierarchy of the Surface Roughness on Omniphobicity of Lubricant-Infused Substrates. *Nano Lett*. 13(4), pp.1793-9 Available: http://doi.org/dx.doi.org/10.1021/nl4003969

Kim, P., Kreder, M., & Wong, T.-S. (2011). Slippery icephobic materials. Webpage. Accessed: 4.11.2015. Available:

http://aizenberglab.seas.harvard.edu/index.php?show=research_project&proj=71&wh=1280x927x1280x1024

Kim, P., Wong, T. S., Alvarenga, J., Kreder, M. J., Adorno-Martinez, W. E., & Aizenberg, J. (2012). Liquid-infused nanostructured surfaces with extreme anti-ice and anti-frost performance. *ACS Nano*, *6*(8), pp.6569–6577. Available: http://doi.org/10.1021/nn302310q

Kim, S. H. (2008). Fabricating superhydrophobic surfaces. *Journal of Adhesion Science and Technology*, *22*(3-4), pp.235–250. Available: http://doi.org/10.1163/156856108X305156

Koch, K., Bhushan, B., & Barthlott, W. (2009). Multifunctional surface structures of plants: An inspiration for biomimetics. *Progress in Materials Science*, *54*(2), pp.137–178. Available: http://doi.org/10.1016/j.pmatsci.2008.07.003

Koch, K., Bhushan, B., Ensikat, H.-J., & Barthlott, W. (2009). Self-healing of voids in the wax coating on plant surfaces. *Philosophical Transactions. Series A, Mathematical, Physical, and Engineering Sciences*, *367*(1894), pp.1673–1688. Available: http://doi.org/10.1098/rsta.2009.0015

Koch, K., Bhushan, B., Jung, Y. C., & Barthlott, W. (2009). Fabrication of artificial Lotus leaves and significance of hierarchical structure for superhydrophobicity and low adhesion. *Soft Matter*, *5*(7), 1386. Available: http://doi.org/10.1039/b818940d

Kondo, H. (2012). How a Fungi-derived Antifreeze Protein Works: Elucidation of Molecular Structure and Antifreeze Mechanism (Press Release). Accessed: 5.11.2015. Available: http://www.spring8.or.jp/en/news_publications/press_release/2012/120529/

Kourounis, G. (2007). Winter Ascent of Mount Washington. Webpage. Accessed 4.11.2015. Available: http://www.stormchaser.ca/Mount_Washington/Mount_Washington_2007/Mount_Washington_Climb.html

Krog, J. O., Zachariassen, K. E., Larsen, B., & Smidsrød, O. (1979). Thermal buffering in Afro-alpine plants due to nucleating agent-induced water freezing. *Nature*, *282*(5736), pp.300–301. Available: http://doi.org/10.1038/282300a0

Kulinich, S. A., Farhadi, S., Nose, K., & Du, X. W. (2011). Superhydrophobic surfaces: Are they really ice-repellent? *Langmuir*, *27*(1), pp.25–29. Available: http://doi.org/10.1021/la104277q

Kulinich, S. A., & Farzaneh, M. (2004). Alkylsilane self-assembled monolayers: modeling their wetting characteristics. *Applied Surface Science*, *230*(1-4), pp.232–240. Available: http://doi.org/10.1016/j.apsusc.2004.02.031

Kulinich, S. A., & Farzaneh, M. (2009a). How wetting hysteresis influences ice adhesion strength on superhydrophobic surfaces. *Langmuir*, *25*(16), pp.8854–8856. Available: http://doi.org/10.1021/la901439c

Kulinich, S. A., & Farzaneh, M. (2009b). Ice adhesion on super-hydrophobic surfaces. *Applied Surface Science*, *255*(18), pp.8153–8157. Available: http://doi.org/10.1016/j.apsusc.2009.05.033

Kulinich, S. A., & Farzaneh, M. (2011). On ice-releasing properties of rough hydrophobic coatings. *Cold Regions Science and Technology*, *65*(1), pp.60–64. Available: http://doi.org/10.1016/j.coldregions.2010.01.001

Kumar, G., & Prabhu, K. N. (2007). Review of non-reactive and reactive wetting of liquids on surfaces. *Advances in Colloid and Interface Science*, *133*(2), pp.61–89. Available: http://doi.org/10.1016/j.cis.2007.04.009

Kwok, D. Y., Lam, C. N. C., Li, a., Leung, a., Wu, R., Mok, E., & Neumann, a. W. (1998). Measuring and interpreting contact angles: A complex issue. *Colloids and Surfaces A: Physicochemical and Engineering Aspects*, *142*(D), pp.219–235. Available: http://doi.org/10.1016/S0927-7757(98)00354-9

Kwon, Y., Choi, S., Anantharaju, N., Lee, J., Panchagnula, M. V., & Patankar, N. a. (2010). Is the Cassie-Baxter formula relevant? *Langmuir*, *26*(22), pp.17528–17531. Available: http://doi.org/10.1021/la102981e

Laforte, C., & Beisswenger, a. (2005). Icephobic Material Centrifuge Adhesion Test. *Proceedings of the International Workshop on Atmospheric Icing of Structures (IWAIS XI)*, (June), 1–5. Available: http://www.mendeley.com/research/icephobic-material-centrifuge-adhesion-test/

Laforte, J., Allaire, M., & Laforte, C. (2005). Demonstration of the Feasibility of a New Mechanical Method of Cable De-Icing. Proceedings 11th International Workshop on Atmospheric Icing of Structures, Montreal, pp.347-352.

Laforte, J. L., Allaire, M. a., & Laflamme, J. (1998). State-of-the-art on power line de-icing. *Atmospheric Research*, *46*(1-2), pp.143–158. http://doi.org/10.1016/S0169-8095(97)00057-4

Lafuma, A., & Quéré, D. (2011). Slippery pre-suffused surfaces. *EPL (Europhysics Letters)*, *96*(5), 56001. Available: http://doi.org/10.1209/0295-5075/96/56001

Lai, L., & Irene, E. A. (1999). Area evaluation of microscopically rough surfaces. *Journal of Vacuum Science & Technology B: Microelectronics and Nanometer Structures*, *17*(1), 33. Available: http://doi.org/10.1116/1.590513

Lalia, B. S., Anand, S., Varanasi, K. K., & Hashaikeh, R. (2013). Fog-harvesting potential of lubricant-impregnated electrospun nanomats. *Langmuir*, *29*(42), pp.13081–13088. Available: http://doi.org/10.1021/la403021q

LG Electronics Inc. (2015). LG G Flex 2 Curved Display Phone | LG Self Healing Phone. Webpage. Accessed: 22.9.2015. Available: http://www.lg.com/uk/mobiles/g-flex2/flex2-curved-smartphone.html

Li, J., Kleintschek, T., Rieder, A., Cheng, Y., Baumbach, T., Obst, U., … Levkin, P. a. (2013). Hydrophobic liquid-infused porous polymer surfaces for antibacterial applications. *ACS Applied Materials and Interfaces*, *5*, pp.6704–6711. Available: http://doi.org/10.1021/am401532z

Li, Y., Li, L., & Sun, J. (2010). Bioinspired Self-Healing Superhydrophobic Coatings. *Angewandte Chemie*, *122*(35), pp.6265–6269. Available: http://doi.org/10.1002/ange.201001258

Liang, J., Hu, Y., Fan, Y., & Chen, H. (2013). Formation of superhydrophobic cerium oxide surfaces on aluminum substrate and its corrosion resistance properties. *Surface and Interface Analysis*, *45*(8), pp.1211–1216. Available: http://doi.org/10.1002/sia.5255

Lindstrom, A. B., Strynar, M. J., & Libelo, E. L. (2011). Polyfluorinated compounds: past, present, and future. *Environmental Science & Technology*, *45*(19), pp.7954–61. Available: http://doi.org/10.1021/es2011622

Liu, Y., Chen, X., & Xin, J. H. (2008). Hydrophobic duck feathers and their simulation on textile substrates for water repellent treatment. *Bioinspiration & Biomimetics*, *3*, 46007. Available: http://doi.org/10.1088/1748-3182/3/4/046007

Lu, X., Zhang, C., & Han, Y. (2004). Low-Density Polyethylene Superhydrophobic Surface by Control of Its Crystallization Behavior. *Macromolecular Rapid Communications*, *25*(18), pp.1606–1610. Available: http://doi.org/10.1002/marc.200400256

Manabe, K., Nishizawa, S., Kyung, K., & Shiratori, S. (2014). Optical Phenomena and Anti-Frosting Property on Biomimetics Slippery Fluid-Infused Antireflective Films via Layer-by-Layer by Comparing with Superhydrophobic and Antireflective Films. *ACS Applied Materials & Interfaces*. 6(16). pp.13985-93 Available: http://doi.org/10.1021/am503352x

Manna, U., & Lynn, D. M. (2015). Fabrication of Liquid-Infused Surfaces Using Reactive Polymer Multilayers: Principles for Manipulating the Behaviors and Mobilities of Aqueous Fluids on Slippery Liquid Interfaces. *Advanced Materials*, 27(19). pp.3007-3012. Available: http://doi.org/10.1002/adma.201500893

Mara, K., Kelk, G., Etkin, D., Burton, I., & Kalhok, S. (1999). Glazed over: Canada copes with the ice storm of 1998. *Environment*, pp. 6–11. Available: http://search.proquest.com/docview/224017573?pq-origsite=gscholar

Mastenbroek Aeroskill. (2015). TKS Anti-Ice Systems. Webpage. Accessed: 4.11.2015. Available: http://www.aeroskill.nl/dealership/tks

Mata, A., & Fleischman, A. J. (2005). Characterization of Polydimethylsiloxane (PDMS). *Biomed Microdevices*.7(4). pp.281-93.

McHale, G. (2007). Cassie and Wenzel: Were they really so wrong? *Langmuir*, *23*(15), pp.8200–8205. Available: http://doi.org/10.1021/la7011167

McKeen, L. W. (2006). *Fluorinated Coatings and Finishes Handbook: The Definitive User's Guide*. William Andrew. Available: https://books.google.com/books?id=eBOKppTWZd0C&pgis=1

Meister, K., Ebbinghaus, S., Xu, Y., Duman, J. G., DeVries, A., Gruebele, M., … Havenith, M. (2013). Long-range protein-water dynamics in hyperactive insect antifreeze proteins. *Proceedings of the National Academy of Sciences of the United States of America*, *110*(5), pp.1617–22. Available: http://doi.org/10.1073/pnas.1214911110

Menini, R., & Farzaneh, M. (2009). Elaboration of Al2O3/PTFE icephobic coatings for protecting aluminum surfaces. *Surface and Coatings Technology*, *203*(14), pp.1941–1946. Available: http://doi.org/10.1016/j.surfcoat.2009.01.030

Met Office. (2015). Aircraft de-icing forecast service. Webpage. Accessed: 4.11.2015. Available: http://www.metoffice.gov.uk/aviation/deicing

Meyers, A. (2008). Surface allows self-cleaning: sacred lotus. Webpage. Accessed: 4.11.2015. Available: http://www.asknature.org/strategy/714e970954253ace485abf1cee376ad8

Michael, N., & Bhushan, B. (2007). Hierarchical roughness makes superhydrophobic states stable. *Microelectronic Engineering*, *84*, pp.382–386. Available: http://doi.org/10.1016/j.mee.2006.10.054

Minford, J. D. (1993). *Handbook of Aluminum Bonding Technology and Data*. CRC Press. Available: https://books.google.com/books?id=dSQ8cS5WXpcC&pgis=1

Moretto, H.-H., Schulze, M., & Wagner, G. (2000, June 15). Silicones. *Ullmann's Encyclopedia of Industrial Chemistry*, pp.1–38. Available: http://doi.org/10.1002/14356007.a24_057

Morra, M., Occhiello, E., & Garbassi, F. (1989). Contact angle hysteresis on oxygen plasma treated polypropylene surfaces. *Journal of Colloid and Interface Science*, *132*(2), pp.504–508. Available: http://doi.org/10.1016/0021-9797(89)90264-6

Nakagami, M. (2007). Verification on the Effects of PTFE Tapes on Reducing Snow Accretion on Overhead Power Transmission Lines. In *IWAIS XII*. Available: http://iwais.compusult.net/html/IWAIS_Proceedings/IWAIS_2007/Category7 De-icing and Anti-icing Techiniques/Lecture/Nakagami.pdf

Nakajima, A. (2011). Design of hydrophobic surfaces for liquid droplet control. *NPG Asia Materials*, *3*(5), pp.49–56. Available: http://doi.org/10.1038/asiamat.2011.55

Nakajima, A., Fujishima, A., Hashimoto, K., & Watanabe, T. (1999). Preparation of Transparent Superhydrophobic Boehmite and Silica Films by Sublimation of Aluminum Acetylacetonate. *Advanced Materials*, *11*(16), pp.1365–1368. Available: http://doi.org/10.1002/(SICI)1521-4095(199911)11:16<1365::AID-ADMA1365>3.0.CO;2-F

Nakajima, A., Hashimoto, K., Watanabe, T., Takai, K., Yamauchi, G., & Fujishima, A. (2000). Transparent superhydrophobic thin films with self-cleaning properties. *Langmuir*, *16*(17), pp.7044–7047. Available: http://doi.org/10.1021/la000155k

National Transportation Safety Board. (1988). Aviation Accident Report AAR-88-09: Continental Airlines, Inc., Flight 1713 McDonnell Douglas DC-9-14, N626TX. Webpage. Accessed: 4.11.2015. Available: http://www.ntsb.gov/investigations/AccidentReports/Pages/AAR8809.aspx

National Transportation Safety Board. (1996). Aviation Accident Report AAR-96-01: In-flight Icing Encounter and Loss of Control Simmons Airlines, d.b.a. American Eagle Flight 4184 Avions de Transport Regional (ATR) Model 72-212, N401AM. Webpage. Accessed: 4.11.2015. Available: http://www.ntsb.gov/investigations/AccidentReports/Pages/AAR9601.aspx

Neinhuis, C., Koch, K., & Barthlott, W. (2001). Movement and regeneration of epicuticular waxes through plant cuticles. *Planta*, *213*(3), pp.427–434. Available: http://doi.org/10.1007/s004250100530

Norton, F. J. (1945, October 9). Waterproofing treatment of materials. Patent: US 2386259 A   Available: http://www.google.com/patents/US2386259

Nosonovsky, M. (2011). Materials science: Slippery when wetted. *Nature*, *477*, pp.412–413. Available: http://doi.org/10.1038/477412a

Nosonovsky, M., & Bhushan, B. (2005). Roughness optimization for biomimetic superhydrophobic surfaces. *Microsystem Technologies*, *11*(7), pp.535–549. Available: http://doi.org/10.1007/s00542-005-0602-9

Nosonovsky, M., & Bhushan, B. (2008). *Multiscale Dissipative Mechanisms and Hierarchical Surfaces: Friction, Superhydrophobicity, and Biomimetics*. Springer Science & Business Media. Available: https://books.google.com/books?hl=fi&lr=&id=FxOUH_ST9xEC&pgis=1

Nosonovsky, M., & Hejazi, V. (2012). Why superhydrophobic surfaces are not always icephobic. *ACS Nano*, *6*(10), pp.8488–8491. Available: http://doi.org/10.1021/nn302138r

Nosonovsky, M., & Rohatgi, P. K. (2011). *Biomimetics in Materials Science: Self-Healing, Self-Lubricating, and Self-Cleaning Materials*. Available: https://books.google.com/books?hl=fi&lr=&id=cmmQBsZvxp4C&pgis=1

Oberli, L., Caruso, D., Hall, C., Fabretto, M., Murphy, P. J., & Evans, D. (2014). Condensation and freezing of droplets on superhydrophobic surfaces. *Advances in Colloid and Interface Science*, *210*, pp.47–57. Available: http://doi.org/10.1016/j.cis.2013.10.018

Ocean. (2012). De-icing a cargo boat − Achievements. Webpage. Accessed: 4.11.2015. Available: https://www.groupocean.com/en/achievements/view/21

Okada, I., & Shiratori, S. (2014). High-transparency, self-standable Gel-SLIPS fabricated by a facile nanoscale phase separation. *ACS Applied Materials and Interfaces*, *6*, pp.1502–1508. Available: http://doi.org/10.1021/am404077h

Onda, T., Shibuichi, S., Satoh, N., & Tsujii, K. (1996). Super-water-repellent fractal surfaces. *Langmuir*, *12*(9), pp.2125–2127. Available: http://doi.org/Doi 10.1021/La950418o

Pan, Y., Bhushan, B., & Zhao, X. (2014). The study of surface wetting, nanobubbles and boundary slip with an applied voltage: A review. *Beilstein Journal of Nanotechnology*, *5*(1), pp.1042–65. Available: http://doi.org/10.3762/bjnano.5.117

Parent, O., & Ilinca, A. (2011). Anti-icing and de-icing techniques for wind turbines: Critical review. *Cold Regions Science and Technology*, *65*(1), pp.88–96. Available: http://doi.org/10.1016/j.coldregions.2010.01.005

Parker, a R., & Lawrence, C. R. (2001). Water capture by a desert beetle. *Nature*, *414*(November), pp.33–34. Available: http://doi.org/10.1038/35102108

Patankar, N. a. (2004). Mimicking the lotus effect: Influence of double roughness structures and slender pillars. *Langmuir*, *20*(19), pp.8209–8213. Available: http://doi.org/10.1021/la048629t

Peltier, R., Brimble, M. a., Wojnar, J. M., Williams, D. E., Evans, C. W., & DeVries, A. L. (2010). Synthesis and antifreeze activity of fish antifreeze glycoproteins and their analogues. *Chemical Science*, *1*(5), 538. Available: http://doi.org/10.1039/c0sc00194e

Peng, C., Xing, S., Yuan, Z., Xiao, J., Wang, C., & Zeng, J. (2012). Preparation and anti-icing of superhydrophobic PVDF coating on a wind turbine blade. *Applied Surface Science*, *259*, pp.764–768. Available: http://doi.org/10.1016/j.apsusc.2012.07.118

Perkins, P. J. (1978). Aircraft Icing. Available: http://doi.org/10.1175/1520-

Prestidge, C. A., & Ralston, J. (1996). Contact angle studies of particulate sulphide minerals, *Minerals Engineering 9*(1), pp.85–102.

Qiu, R., Zhang, Q., Wang, P., Jiang, L., Hou, J., Guo, W., & Zhang, H. (2014). Fabrication of slippery liquid-infused porous surface based on carbon fiber with enhanced corrosion inhibition property. *Colloids and Surfaces A: Physicochemical and Engineering Aspects*, *453*, pp.132–141. Available: http://doi.org/10.1016/j.colsurfa.2014.04.035

Quéré, D. (2005). Non-sticking drops. *Reports on Progress in Physics*, *68*, pp.2495–2532. Available: http://doi.org/10.1088/0034-4885/68/11/R01

Richard, D., & Quéré, D. (2007). Viscous drops rolling on a tilted non-wettable solid. *Europhysics Letters (EPL)*, *48*(3), pp.286–291. Available: http://doi.org/10.1209/epl/i1999-00479-1

Roach, P., Shirtcliffe, N. J., & Newton, M. I. (2008). Progess in superhydrophobic surface development. *Soft Matter*, *4*(2), pp.224–240. Available: http://doi.org/10.1039/B712575P

Rolith Inc. (2015). Self-Cleaning / Superhydrophobic Surfaces. Webpage. Accessed: 4.11.2015. Available: http://www.rolith.com/applications/self-cleaning

Rulon E. Johnson, & Robert H. Dettre. (1964). *Contact Angle, Wettability, and Adhesion*. (F. M. Fowkes, Ed.), 43. Washington, D.C.: American Chemical Society. Available: http://doi.org/10.1021/ba-1964-0043

Ruohomaa, R. (2014). *Icephobic surfaces – Development of icing test equipment and of superhydrophobic coating prepared with solution precursor flame spray*. Tampere University of Technology, unpublished thesis.

Rutter, M. P. (2011). Plant offers slick strategy. Webpage. Accessed: 12.11.2015. Available: http://news.harvard.edu/gazette/story/2011/09/plant-offers-slick-strategy/

Ryerson, C. C. (2008). Assessment of Superstructure Ice Protection as Applied to Offshore Oil Operations Safety, (April), 156. U.S. Department of Defense, US Army Research.

Ryerson, C. C. (2011). Ice protection of offshore platforms. *Cold Regions Science and Technology*, *65*(1), pp.97–110. Available: http://doi.org/10.1016/j.coldregions.2010.02.006

Rykaczewski, K., Anand, S., Subramanyam, S. B., & Varanasi, K. K. (2013). Mechanism of frost formation on lubricant-impregnated surfaces. *Langmuir*, *29*(17), pp.5230–5238. Available: http://doi.org/10.1021/la400801s

Saito, H., & Takai, K. (1997). Water- and Ice-Repellent Coatings, *997*(4), pp.4–7.

Saito, H., Takai, K., & Goro, Y. (1997). A study on coating water-repellent, *3*(3), pp.185–189.

Samaha, M. a., Tafreshi, H. V., & Gad-El-Hak, M. (2012). Influence of flow on longevity of superhydrophobic coatings. *Langmuir*, *28*(25), pp.9759–9766. Available: http://doi.org/10.1021/la301299e

Sellinger, A., Weiss, P. M., Nguyen, A., Lu, Y., Assink, R. A., Gong, W., & Brinker, C. J. (1998). Continuous self-assembly of organic-inorganic nanocomposite coatings that mimic nacre, *394*(6690), pp.256–260. Available: http://doi.org/10.1038/28354

Shibuichi, S., Onda, T., Satoh, N., & Tsujii, K. (1997). Super Water-repellent Surfaces Resulting from Fractal Structure. II. *Journal of Japan Oil Chemists' Society*, *46*(6), pp.649–659,713. Available: http://doi.org/10.5650/jos1996.46.649

Shillingford, C., MacCallum, N., Wong, T.-S., Kim, P., & Aizenberg, J. (2014). Fabrics coated with lubricated nanostructures display robust omniphobicity.

Nanotechnology, *25*, 014019. Available: http://doi.org/10.1088/0957-4484/25/1/014019

Shiu, J.-Y., Kuo, C.-W., & Chen, P. (2004). Fabrication of tunable superhydrophobic surfaces. In A. R. Wilson (Ed.), *Smart Materials, Nano-, and Micro-Smart Systems* pp. 325–332. International Society for Optics and Photonics. Available: http://doi.org/10.1117/12.582312

Sigma-Aldrich Co. (2015). Silicone oils - Silicones. Webpage. Accessed: 29.10.2015. Available: http://www.sigmaaldrich.com/materials-science/material-science-products.html?TablePage=20204397

Sim, D. (2014). Amazing Scenes as Severe Storm Encases Slovenian Town in Ice. *IBTimes*. Webpage. Accessed: 29.10.2015. Available: http://www.ibtimes.co.uk/amazing-scenes-severe-storm-encases-slovenian-town-ice-1434997

Sivas, S. L., Riegler, B., Thomaier, R., & Hoover, K. (2013). A Silicone-Based Ice-Phobic Coating for Aircraft. *Scientific Reports*, 3, 2194 . Available: http://doi.org/10.1038/srep02194

Spori, D. M., Drobek, T., Zürcher, S., Ochsner, M., Sprecher, C., Mühlebach, A., & Spencer, N. D. (2008). Beyond the lotus effect: Roughness influences on wetting over a wide surface-energy range. *Langmuir*, *24*(10), pp.5411–5417. Available: http://doi.org/10.1021/la800215r

Starov, V. M., Velarde, M. G., & Radke, C. J. (2007). *Wetting and Spreading Dynamics*. Available: https://books.google.com/books?hl=fi&lr=&id=NT6KPxETpPMC&pgis=1

Stenroos, C. (2015). Properties of icephobic surfaces in different icing conditions. Tampere University of Technology. Ms Thesis. Available: http://dspace.cc.tut.fi/dpub/handle/123456789/23364

Subrahmanyam, T. V., Prestidge, C. A., & Ralston, J. (1996). Contact angle and surface analysis studies of sphaerite particles, *9*(7), pp.727–741.

Subramanyam, S. B., Rykaczewski, K., & Varanasi, K. K. (2013). Ice adhesion on lubricant-impregnated textured surfaces. *Langmuir*, *29*, pp.13414–13418. Available: http://doi.org/10.1021/la402456c

Sun, T., & Qing, G. (2011). Biomimetic smart interface materials for biological applications. *Advanced Materials*, *23*(12), pp.57–77. Available: http://doi.org/10.1002/adma.201004326

SWZ Maritime. (2014). Arctic Design: Sea Spray Icing Models to Be Improved | SWZ Maritime. Webpage. Accessed: 4.11.2015, Available: http://www.swzonline.nl/news/4492/arctic-design-sea-spray-icing-models-be-improved

Tokic, A. (2015). Volkswagen Banishes Frost With Anti-Fog and Anti-Icing Windshield. Webpage. Accessed: 4.11.2015, Available: http://www.autoguide.com/auto-news/2010/11/volkswagen-banishes-frost-with-anti-fog-and-anti-icing-windshield.html

Tuteja, A., Choi, W., Ma, M., Mabry, J. M., Mazzella, S. a, Rutledge, G. C., … Cohen, R. E. (2007). Designing superoleophobic surfaces. *Science (New York, N.Y.)*, *318*(0704), pp.1618–1622. Available: http://doi.org/10.1126/science.1148326

Ulusoy, U., & Yekeler, M. (2005). Correlation of the surface roughness of some industrial minerals with their wettability parameters. *Chemical Engineering and Processing: Process Intensification*, *44*(5), pp.555–563. Available: http://doi.org/10.1016/j.cep.2004.08.001

Wang, H., He, G., & Tian, Q. (2012). Effects of nano-fluorocarbon coating on icing. *Applied Surface Science*, *258*(18), pp.7219–7224. Available: http://doi.org/10.1016/j.apsusc.2012.04.043

Wang, H., Xue, Y., Ding, J., Feng, L., Wang, X., & Lin, T. (2011). Durable, Self-Healing Superhydrophobic and Superoleophobic Surfaces from Fluorinated-Decyl Polyhedral Oligomeric Silsesquioxane and Hydrolyzed Fluorinated Alkyl Silane. *Angewandte Chemie International Edition*, *50*(48), pp.11433–11436. Available: http://doi.org/10.1002/anie.201105069

Wang, P., Lu, Z., & Zhang, D. (2015). Slippery liquid-infused porous surfaces fabricated on aluminum as a barrier to corrosion induced by sulfate reducing bacteria. *Corrosion Science*, *93*, pp.1–8. Available: http://doi.org/10.1016/j.corsci.2015.01.015

Wang, X., Liu, X., Zhou, F., & Liu, W. (2011). Self-healing superamphiphobicity. *Chem. Commun.*, *47*(8), pp.2324–2326. Available: http://doi.org/10.1039/C0CC04066E

Varanasi, K. K., Deng, T., Smith, J. D., Hsu, M., & Bhate, N. (2010). Frost formation and ice adhesion on superhydrophobic surfaces. *Applied Physics Letters*, *97*(23). Available: http://doi.org/10.1063/1.3524513

Veeramasuneni, S., Drelich, J., Miller, J. ., & Yamauchi, G. (1997). Hydrophobicity of ion-plated PTFE coatings. *Progress in Organic Coatings*, *31*(3), pp.265–270. Available: http://doi.org/10.1016/S0300-9440(97)00085-4

Wenzel, R. N. (1936). Resistance of Solid Surfaces. *Ind. Eng. Chem.*, *28*, pp.988–994. Available: http://doi.org/10.1021/ie50320a024

Verho, T., Bower, C., Andrew, P., Franssila, S., Ikkala, O., & Ras, R. H. A. (2011). Mechanically durable superhydrophobic surfaces. *Advanced Materials (Deerfield Beach, Fla.)*, *23*(5), pp.673–8. Available: http://doi.org/10.1002/adma.201003129

White, S. R., Sottos, N. R., Geubelle, P. H., Moore, J. S., Kessler, M. R., Sriram, S. R., … Viswanathan, S. (2001). Autonomic healing of polymer composites. *Nature*, *409*(6822), pp.794–7. Available: http://doi.org/10.1038/35057232

Wilson, P. W., Lu, W., Xu, H., Kim, P., Kreder, M. J., Alvarenga, J., & Aizenberg, J. (2013). Inhibition of ice nucleation by slippery liquid-infused porous surfaces (SLIPS). *Physical Chemistry Chemical Physics : PCCP*, *15*, pp.581–5. Available: http://doi.org/10.1039/c2cp43586a

Vincentz Network GmbH & Co. KG. (2011). Corrosion resistance of an epoxy-polyamide coating evaluated. Webpage. Accessed: 4.11.2015 Available: http://www.european-coatings.com/Raw-materials-technologies/Raw-materials/Coatings-pigments/Corrosion-resistance-of-an-epoxy-polyamide-coating-evaluated

Wong, T.-S., Kang, S. H., Tang, S. K. Y., Smythe, E. J., Hatton, B. D., Grinthal, A., & Aizenberg, J. (2011). Bioinspired self-repairing slippery surfaces with pressure-stable omniphobicity. *Nature*, *477*(7365), pp.443–447. Available: http://doi.org/10.1038/nature10447

Xiao, L., Li, J., Mieszkin, S., Fino, A. Di, Clare, A. S., Callow, M. E., … Levkin, P. a. (2013). Liquid-infused slippery surfaces show marine anti-biofouling properties. *ACS Applied Materials & Interfaces*, *under revi*.

Xiao, R., Miljkovic, N., Enright, R., & Wang, E. N. (2013). Immersion condensation on oil-infused heterogeneous surfaces for enhanced heat transfer. *Scientific Reports*, *3*, 1988. Available: http://doi.org/10.1038/srep01988

Xiu, Y., Liu, Y., Hess, D. W., & Wong, C. P. (2010). Mechanically robust superhydrophobicity on hierarchically structured Si surfaces. *Nanotechnology*, *21*(15), 155705. Available: http://doi.org/10.1088/0957-4484/21/15/155705

Yabu, H., & Shimomura, M. (2005). Single-step fabrication of transparent superhydrophobic porous polymer films. *Chemistry of Materials*, *17*(21), pp.5231–5234. Available: http://doi.org/10.1021/cm051281i

Yao, X., Song, Y., & Jiang, L. (2011). Applications of bio-inspired special wettable surfaces. *Advanced Materials*, *23*(6), pp.719–734. Available: http://doi.org/10.1002/adma.201002689

Yinhe Wind Power Co. Ltd. (2012). Non-stop innovation: Anti-icing. Webpage. Accessed: 29.10.2015 Available: http://www.yinhe-windpower.com/en/Technological.aspx?Id=7

Young, T. (1805). An Essay on the Cohesion of Fluids. *Philosophical Transactions of the Royal Society of London*, *95*(January), pp.65–87. Available: http://doi.org/10.1098/rstl.1805.0005

Youngblood, J. P., & McCarthy, T. J. (1999). Ultrahydrophobic Polymer Surfaces Prepared by Simultaneous Ablation of Polypropylene and Sputtering of

Poly(tetrafluoroethylene) Using Radio Frequency Plasma. *Macromolecules*, *32*(20), pp.6800–6806. Available: http://doi.org/10.1021/ma9903456

Zaggia, A., & Ameduri, B. (2012). Recent advances on synthesis of potentially non-bioaccumulable fluorinated surfactants. *Current Opinion in Colloid & Interface Science*, *17*(4), pp.188–195. Available: http://doi.org/10.1016/j.cocis.2012.04.001

Zhang, J., Li, J., & Han, Y. (2004). Superhydrophobic PTFE surfaces by extension. *Macromolecular Rapid Communications*, *25*(11), pp.1105–1108. Available: http://doi.org/10.1002/marc.200400065

Zhang, X., Guo, Y., Zhang, Z., & Zhang, P. (2013). Self-cleaning superhydrophobic surface based on titanium dioxide nanowires combined with polydimethylsiloxane. *Applied Surface Science*, *284*, pp.319–323. Available: http://doi.org/10.1016/j.apsusc.2013.07.100

Zheng, Q., Lv, C., Hao, P., & Sheridan, J. (2010). Small is beautiful, and dry. *Science China Physics, Mechanics and Astronomy*, *53*(12), pp.2245–2259. Available: http://doi.org/10.1007/s11433-010-4172-1

Zhou, H., Wang, H., Niu, H., Gestos, A., Wang, X., & Lin, T. (2012). Fluoroalkyl silane modified silicone rubber/nanoparticle composite: a super durable, robust superhydrophobic fabric coating. *Advanced Materials (Deerfield Beach, Fla.)*, *24*(18), pp.2409–12. Available: http://doi.org/10.1002/adma.201200184

Zhu, L., Xue, J., Wang, Y., Chen, Q., Ding, J., & Wang, Q. (2013). Ice-phobic Coatings Based on Silicon-Oil-Infused Polydimethylsiloxane. *ACS Applied Materials & Interfaces*, *5*, pp.4053–4062.

Zielecka, M., & Bujnowska, E. (2006). Silicone-containing polymer matrices as protective coatings: Properties and applications. *Progress in Organic Coatings*, *55*(2), pp.160–167. Available: http://doi.org/10.1016/j.porgcoat.2005.09.012

Zimmermann, J., Reifler, F. A., Schrade, U., Artus, G. R. J., & Seeger, S. (2007). Long term environmental durability of a superhydrophobic silicone nanofilament coating. *Colloids and Surfaces A: Physicochemical and Engineering Aspects*, *302*(1-3), pp.234–240. Available: http://doi.org/10.1016/j.colsurfa.2007.02.033

Zou, L., Xiang, X., Fan, J., & Li, F. (2007). Single-Source Precursor to Complex Metal Oxide Monoliths with Tunable Microstructures and Properties: The Case of Mg-Containing Materials. *Chemistry of Materials*, *19*(26), pp.6518–6527. Available: http://doi.org/10.1021/cm702309e

Zushi, Y., Hogarh, J. N., & Masunaga, S. (2011). Progress and perspective of perfluorinated compound risk assessment and management in various countries and institutes. *Clean Technologies and Environmental Policy*, *14*(1), pp.9–20. Available: http://doi.org/10.1007/s10098-011-0375-z

APPENDIX A: THE CONTACT ANGLE HYSTERESIS RESULTS FOR ALL SLIPS SAMPLES
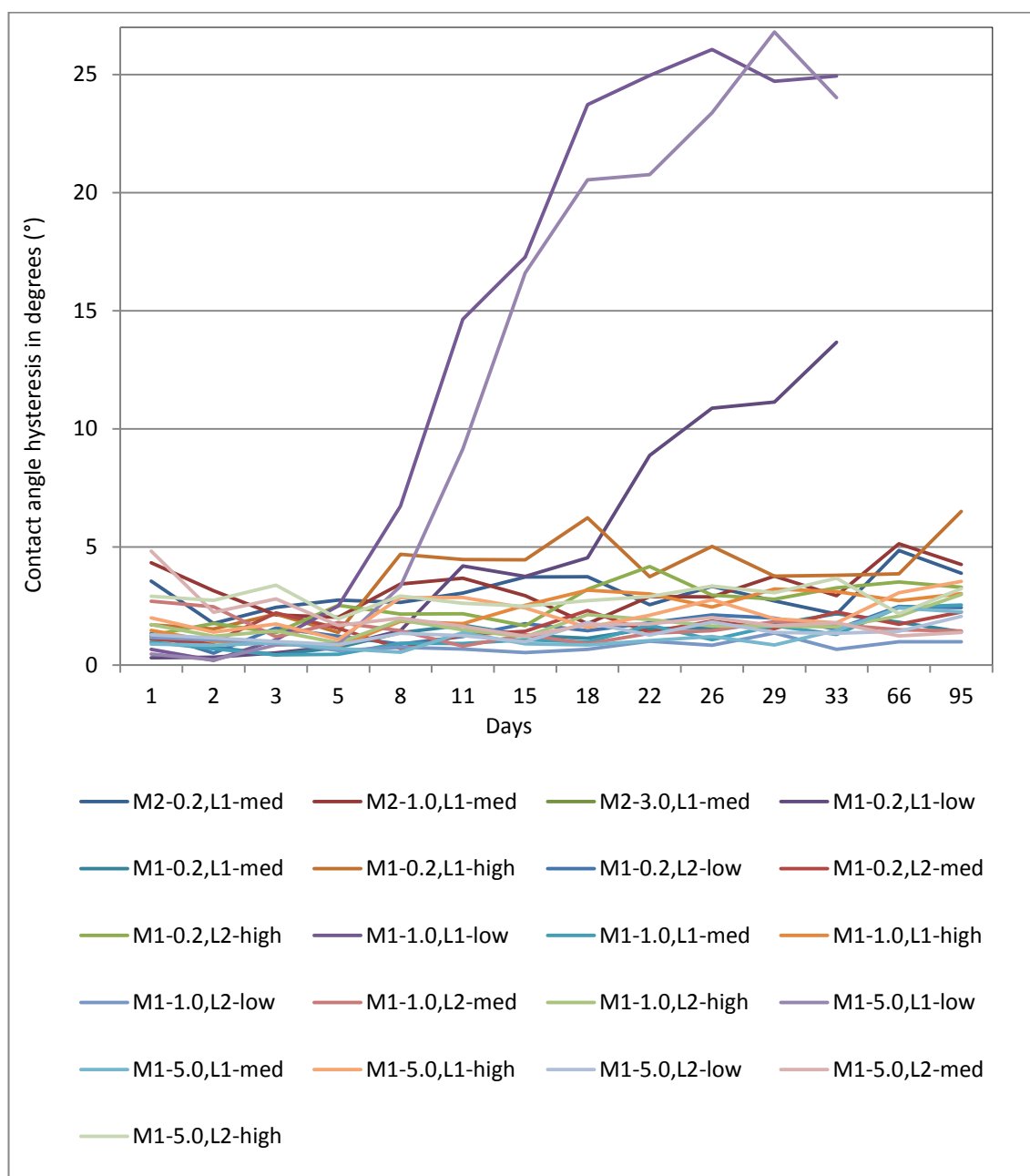
Figure 49. *The contact angle hysteresis' of all the studied samples.*